Charles University in Prague, Faculty of Science
Department of macromolecular and physical chemistry

Ph.D. study program: Physical chemistry

RNDr. Magdalena Michlová

Vývoj a optimalizace systémů pro SERS na úrovni jedné molekuly

Development and optimization of systems for SERS on single molecule level

PhD Thesis

Supervisor: Prof. RNDr. Blanka Vlčková, CSc.

Prague, 2012

This work was elaborated at the Department of Physical and Macromolecular Chemistry, Charles University in Prague, under the supervision of Prof. RNDr. Blanka Vlčková, CSc.

I guarantee that the work is original and only the literature listed in references was used.

Prague, July 10, 2012

……..

ACKNOWLEDGEMENTS

Especially, I would like to thank to Prof. RNDr. Blanka Vlčková, CSc. for invaluable guidance, for pedagogical access, for inexhaustible patience and for all the assistance during my PhD study.

Further, I thank to Doc. RNDr. Peter Mojzeš, CSc. for all the assistance with measurement Raman spectra and for his help with the interpretation of the results.

I also thank to RNDr. Miroslavu Šlouf, PhD. and Jiřina Hromádková for their assistance in obtaining and interpreting the TEM and SEM micrographs.

I thank to my colleagues RNDr. Karolína Šišková, PhD., RNDr. Petr Šmejkal, PhD. and Mgr. Markéta Kokošková for great and inspiring working environment, for stimulating discussions and for help with technical problems.

Last but not least, I thank to my family for patience, assistance and moral support during my study and finalization of PhD Thesis.

CONTENT

ABSTRACT

Dimers and small aggregates as well as compact aggregates of Ag nanoparticles (NPs) were assembled and chemically anchored to supporting surfaces. The supporting surfaces were either glass slides or SiO_x – coated Cu or Au grids for TEM, both chemically functionalized by 3-aminopropyltrimethoxysilane (APTMS). Compact aggregates of Ag NPs incorporating protoporphyrin IX (PPIX) molecules were prepared by adsorption of chlorides in the presence of PPIX. Dimers and small aggregates of Ag NPs were assembled by selected molecular linkers: 4,4'-diaminoazobenzene (DAAB), 4,4'-diaminoterphenyl (DATP) and 5,10,15,20-tetrakis(4-aminophenyl)porphine (TAPP). The most efficient strategy of dimers and small aggregates preparation has been their assembling by a three – step procedure involving (i) attachment of isolated Ag NPs to the NH2 groups of APTMS functionalized TEM grid, (ii) attachment of molecular linker (with two functional NH2 groups in para position) to Ag NPs by a one terminal NH2 group, and (iii) attachment of Ag NPs to the second, free terminal NH2 group of the linker. In this procedure, the control over the perpendicular orientation of the bifunctional linker and its attachment by one terminal group to Ag NP surface has been accomplished by functionalization of Ag NPs by adsorbed citrate which acted as the adsorbate pre – orienting matrix. The control over the resulting dimer (small aggregate) separation from other dimers and small aggregates has been achieved by a sufficiently wide spacing of Ag NPs in the first step (i) of the three – step procedure. Furthermore, the strategy for obtaining SERS signal of molecular linker from a particular, selected single dimer and/or small aggregate of Ag NPs visualized by TEM has been developed. An unequivocal correspondence between the TEM – imaged dimer (and/or small aggregate) and the SERS signal obtained from it has been accomplished by employment of SiO2 coated Au finder grids for TEM. An accurate establishment of the positional coordinates of the nanoobject (dimer or aggregate) with respect to the marks (letter or number) on the finder grid enabled to find the same nanoobject both in TEM (for its visualisation) and in the optical microscope which focused exciting laser beam onto it and enabled to obtain SERS signal of the molecular linker from it. The SERS signal of molecular linkers exhibits temporal fluctuations associated with achievement of a single molecule level of detection. Stability of the molecular linkers in strong optical fields appears to be conditioned by the perpendicular orientation of the linker with respect to Ag NP surface, and is further affected by the actual structure of the linker as well as by the nanoobject morphology. Finally, the single molecularly – bridged Ag NP dimer was found to represent an optimal system in which the single molecule dynamics can be followed via time – evolution of the SERS signal of the molecular linker obtained from it. The advantage of a dimer over a small aggregate is, that the SERS signal of the dimer originates from a single hot spot, while, in case of a small aggregate, the SERS signal is a superposition of molecular dynamic events occurring in several hot spots. Furthermore, the molecularly – bridged Ag NP dimer is an exact experimental realization of a model system of Ag NP dimer with a single molecule located in a single hot spot at the interconnect between the two NPs. According to the theoretical model calculations, a dimer of Ag NPs with the molecule located between them is the most efficient light amplification system providing largest enhancement of SERS by the EM mechanism of SERS.

ABSTRAKT

Byly připraveny dimery, malé agregáty a kompaktní agregáty Ag nanočástic (NP), navázané chemicky na povrch pevných podložek. Těmito podložkami byly buď Cu či Au TEM síťky s vrstvou SiO_2 nebo sklíčka, obojí s povrchem funkcionalizovaným 3-aminopropyltrimethoxysilanem (APTMS). Kompaktní agregáty Ag NP obsahující protoporfyrin IX (PPIX) byly připraveny působením chloridů na Ag sol v přítomnosti PPIX. Dimery a malé agregáty Ag NP byly uspořádány s využitím vybraných molekulárních spojek: 4,4‘- diaminoazobenzen (DAAB), 4,4‘-diaminoterfenyl (DATP) a 5,10,15,20-tetrakis(4-aminofenyl)porfin (TAPP). Jako nejúčinnější postup jejich přípravy se ukázala třístupňová procedura sestávající z (i) navázání izolovaných Ag NP na povrch podložky prostřednictvím NH_2 skupin APTMS, (ii) adsorpce molekulární spojky přes jednu z jejích NH_2 skupin a (iii) připojení dalších Ag NP ke zbývající volné NH_2 skupině. Při této proceduře byla využita funkcionalizace Ag NP citrátovými anionty ke kontrole kolmé adsorpční geometrie molekulárních spojek, přičemž adsorbované citrátové ionty fungovaly jako účinná preorientační matrice. Vzdálenosti mezi jednotlivými dimery či malými agregáty byly určeny dostatečnou vzdáleností mezi izolovanými Ag NP v prvním kroku výše zmíněné třístupňové procedury. Byla také vyvinuta strategie pro měření SERS signálu molekulární spojky z vybraného jednotlivého dimeru či malého agregátu, jehož struktura byla zobrazena pomocí TEM. Jednoznačné korespondence mezi TEM snímkem daného dimeru (či malého agregátu) a změřeným SERS signálem bylo dosaženo použitím Cu nebo Au vyhledávacích TEM sítěk s vrstvou SiO_2, které pomocí polohových souřadnic umožnily nalezení téhož nanoobjektu jak v TEM, tak v Ramanově mikrospektrometru. SERS signál molekulárních spojek vytvářejících dimery a malé agregáty z Ag NP vykazuje časové fluktuace spojené s dosažením úrovně detekce jednotlivých molekul. Stabilita molekulárních spojek v silných optických polích souvisí s jejich kolmou orientací k povrchu Ag NP a je navíc závislá jak na konkrétní molekulární struktuře, tak na morfologii daného plazmonického nanoobjektu. Dimery Ag NP vázaných jedinou molekulou představují optimální systém pro studium dynamiky jednotlivých molekul sledováním časového vývoje SERS signálu dané molekulární spojky. Navíc jsou téměř dokonalou realizací teoretického modelu, který předpovídá přítomnost jediného hot spotu v mezeře mezi oběma Ag NP, takže molekulární spojka se nachází přesně v místě s nejvyšším zesílením SERS pomocí EM mechanismu. Oproti tomu SERS signál z malých agregátů může být superpozicí signálů odrážejících molekulárně-dynamické události probíhající současně v několika různých hot spotech.

1. INTRODUCTION

1.1. Surface enhanced Raman scattering (SERS)

1.1.1. Brief history of Raman scattering and SERS

In 1921 Indian physicists Chandrasekhara Venkata Raman and Kariamanikam Srinivasa Krishnan [1] discovered a new effect involving a change in wavelength of scattered monochromatic visible light. During the following eight years C. V. Raman with his collaborators published a series of findings. Since 1928 this effect has borne his name. The phenomenon had been predicted theoretically by Adolf Smekal [2] and the effect has been sometimes called the Smekal-Raman effect. Raman scattering was independently discovered by Grigory Landsberg and Leonid Mandelstam [3]. In 1930, C. V. Raman received a Nobel Prize for his work on the scattering of light.

In 1974, Martin Fleischman et al. [4] presented a study on Raman spectra of pyridine adsorbed on electro-chemical roughened Ag electrodes. Nowadays, this study is considered as the first observation of the SERS effect. Nevertheless, the study itself attributed observation of Raman signal from a monolayer of pyridine molecules to an increase in the effective surface area occasioned by the roughening of the electrodes. In 1977, two groups independently noted that the observed signal levels could not be explained only by means of an increased surface area. Jeanmaire and Van Duyne [5] published and described a charge-transfer effect, while Albrecht and Creighton [6] proposed an electromagnetic effect.

1.1.2. Mechanism of SERS

SERS originates from coupled optical responses of plasmonic metal (such as Ag and Au) nanostructures (nanoparticles, nanowires etc.) and of molecules located on (or in a close proximity of) their surfaces (Fig.1.1). In such coupled system, both the incident light and the light inelastically (Raman) scattered by adsorbed molecules are enhanced by resonance Mie scattering of light by the plasmonic metal nanostructures. This, in a nutshell, is the electromagnetic (EM) mechanism of SERS. The EM mechanism of SERS is the principal mechanism of SERS and operates

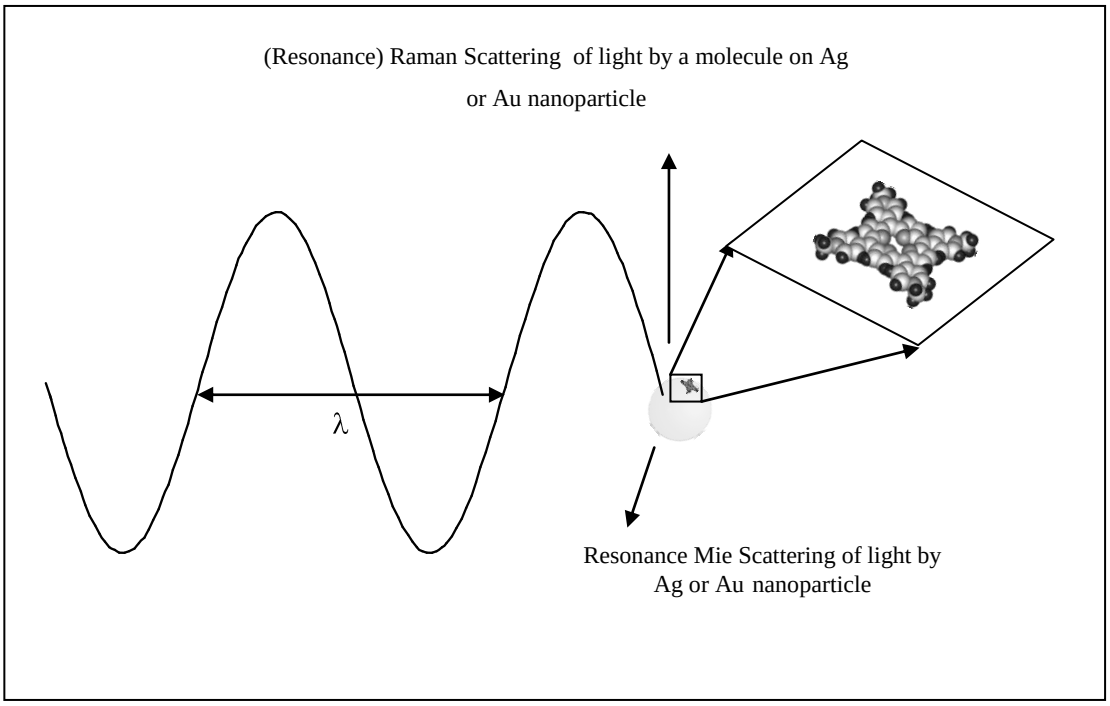

Fig. 1.1.: Schematic depiction of surface-enhanced Raman scattering.

independently on the nature of the target molecular species. Explanation of the phenomenon of SERS on the basis of the light amplification by free-electron-like (plasmonic) metal nanostructures has been published [7] just one year after its discovery [5]. Provided that the wavelength of incident light obeys simultaneously with the EM resonance condition also a molecular resonance condition, molecular resonances contribute to the overall enhancement of Raman scattering. The mechanisms and applications of SERS have been the subject of several seminal review and feature articles [8 – 18].

The best SERS signals are obtained from molecules absorbed on roughened surfaces (5 - 200 nm) of free-electron-like metals – Ag, Au, Cu and alkali metals.
SERS active surfaces used for measurements are:

1. Electrochemically roughened electrodes – preparation of electrodes is based on an oxidation- reduction cycle or a repetitive anodization e.g. of silver electrodes in the presence of an electrolyte, e.g. KCl [5]. Advantages of the electrochemically roughened electrodes are a possibility to control their potential and a possibility to be used in a non-aqueous ambient, however the enhancement factors do not amount a value like another substrates.
2. Metal island films – the surfaces made up from irregular arrays of metal particles. The particles have extensive size distribution, usually 150 – 600 nm in

diameter [19]. Metal films are usually distributed on a glass or quartz by evaporation of metal under ultra high vacuum.

3. Metal hydrosols (colloids) are dispersions of metal nanoparticles in aqueous or organic solution. The metal nanoparticle size distribution is usually 3 – 200 nm. Metal hydrosols can be prepared by a number of ways – chemical, photochemical or radiolytical reduction of a metal salt, laser ablation etc. The most frequent preparation of metal nanoparticles is a chemical reduction of a metal salt by a suitable reducing agent at defined conditions in an aqueous ambient. The commonly used reduction agents are sodium borohydride [20, 21] and sodium citrate [22]. Preparation of metal nanoparticles in aqueous ambient by reduction is a rather simple method and metal nanoparticles are stabilized by the electric double-layer surrounding the nanoparticles. Metal hydrosol prepared in an organic ambient are usually stabilized by adding a stabilizing agent.

This work is focused on systems with Ag nanoparticles (NPs). Ag NPs are usually polyhedral single crystals (such as dodecahedrons or icosaedrons), however, for simple theoretical treatments, they are approximated by spheres. Let us first briefly explain how and when an Ag NP operates as a light amplifier. When a small Ag NP (approximated by a sphere) is illuminated by light of a particular wavelength at which (or close to which) Mie resonance condition is fulfilled, the conduction electrons within the particle are caused to oscillate with the same frequency as that of the incident light, and an oscillating dipole is created. The resonance excitation of this dipole is also dubbed a dipolar surface plasmon excitation. In a simple quasistatic approximation, the dipole is described by dipole moment $\boldsymbol{P}$,

$$\boldsymbol{P} = g \cdot r^3 \cdot \boldsymbol{E_0} \tag{1}$$

where $\boldsymbol{E_0}$ is the intensity of the electric field of the incident light, r is the nanoparticle radius and g is a factor, in which the material (as well as the optical) characteristics of the system are interrelated:

$$g = \frac{\varepsilon(\lambda) - \varepsilon_m}{\varepsilon(\lambda) + 2\varepsilon_m} \tag{2}$$

where $\varepsilon(\lambda)$ is the relative complex permitivity (dielectric function) of a metal (which, in our case, is Ag) and ε_m is the relative permitivity (dielectric constant) of the medium (usually water or air) surrounding the Ag NPs.

The material characteristics of the metal (Ag) and of the ambient are related to their optical characteristics, in particular to the complex refractive index of the metal $N(\lambda) = n + ik$ (where n is the refraction index and k is the index of absorption) and to the refractive index of the medium n_m (which is assumed to be non-absorbing throughout the visible spectral region and hence $k_m = 0$) by relations:

$$\varepsilon(\lambda) = N^2(\lambda) \qquad \varepsilon_m = (n_m)^2 \tag{3}$$

The factor g and the dipole moment $\boldsymbol{P}$ maximize when the resonance condition is fulfilled, i.e. when

$$\mathrm{Re}\,\varepsilon(\lambda) = -2\varepsilon_m \tag{4}$$

and $I_m\, \varepsilon\, (\lambda)$ (which represents the resonance damping) is very small.

The resonance wavelength at which the resonance condition is fulfilled for isolated Ag spheres in water is ~ 390 nm, and the real system, which fits this description is an Ag NP hydrosol.

The most important point is that the oscillating dipole re-radiates light, the intensity of which is proportional to the square modulus of the dipole moment:

$$I \approx \left(\frac{1}{\lambda}\right)^4 |\boldsymbol{P}|^2 \tag{5}$$

Hence at (or close to) the resonance wavelength, Ag nanoparticles work as light amplifiers [23]. In the EM mechanism of SERS, both the incident and the Raman scattered light are enhanced, and the final enhancement of Raman scattering of a molecule adsorbed on an isolated Ag NP is about 4 orders of magnitude.

Nevertheless, assemblies of closely spaced Ag NP are far better amplifiers than those of the isolated ones. For closely spaced nanoparticles, the particles

mutually interact by dipole-dipole interaction with several consequences. In most cases, a red shift and broadening of the resonance wavelength region is observed. In some of the assemblies, the strong optical fields excited by the incident laser light are non-uniformly distributed and spacially localized. The nanoscale regions in which the strong EM fields are localized are dubbed hot spots. Existence of hot spots has been predicted theoretically and proved experimentally both in large fractal aggregates of Ag NPs and in dimers and very small aggregates of these NPs [24 – 30]. The EM mechanism enhancement factors can range between 4 and 11 orders of magnitude, in dependence on the morphology of Ag NP assembly, localization of a molecule within the assembly and the excitation wavelength and light polarization selected for the SERS experiment. Theory of the EM mechanism of SERS has been explained in detail for in several review articles [8, 9, 16].

Molecular resonance contributes to the overall enhancement of Raman scattering provided that their resonance condition is fulfilled simultaneously with the EM resonance. Molecular resonances are somewhat similar to resonance Raman scattering which occurs when the wavelength of the incident light matches that of an allowed electronic transition within a molecule. However, in SERS, one has always to evaluate possible alternations of the geometric as well as electronic structure of the target molecule caused by the molecule-Ag surface interaction. It became a custom in SERS literature to consider two types of molecular resonance contributions. In the case of surface enhancement resonance Raman scattering (SERRS), a molecule itself is a chromophore with respect to excitation wavelength used for SERS experiment. Nevertheless, when the molecular resonance contribution is evaluated for a given target molecule, its actual structure in the particular SERS-active system has to be considered. For example, free-base porphyrins adsorbed directly onto the Ag NP surface are frequently converted into Ag metalloporphyrins (Fig. 1.2).

Such a conversion manifests itself clearly in the SERRS spectral pattern [21, 31,32]. In that case, one has to evaluate the resonance contribution for an Ag metalloporhyrin. A theoretical treatment of SERRS has been published e.g. in ref. 7. Another possibility is that the molecule is non-chromophoric with respect to the excitation wavelength, but forms a chromophoric surface complex. An example of such molecule is 2,2’-bipyridine (BPY) which, under specific conditions, forms an Ag-BPY surface complex [33]. In that case, molecular resonance contribution stems from the match between the excitation wavelength and the wavelength of a photo-

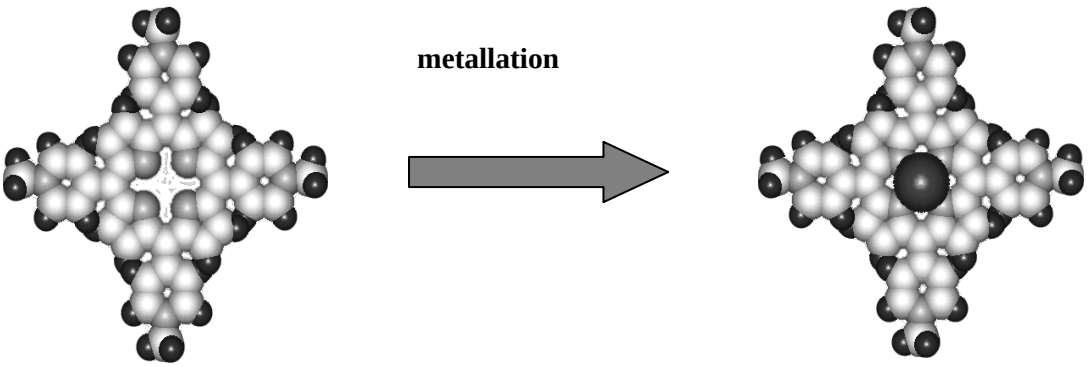

Fig. 1.2.: Metallation of a free base porphyrin directly adsorbed on Ag NP surface

induced charge transfer transition within the Ag-adsorbate (e.g. Ag-BPY) surface complex (Fig. 1.3), and is usually dubbed the chemical mechanism of SERS. Theoretical treatment and experimental evidence for the chemical mechanism of SERS can be found in refs. [10, 13].

While routine SERS spectral measurements of target molecules in systems with Ag NP can be performed with conventional Raman spectrometers, for single molecule SERS, the benefits of Raman microspectroscopy (stemming from coupling of a confocal optical microscope to a Raman spectrometer) are required.

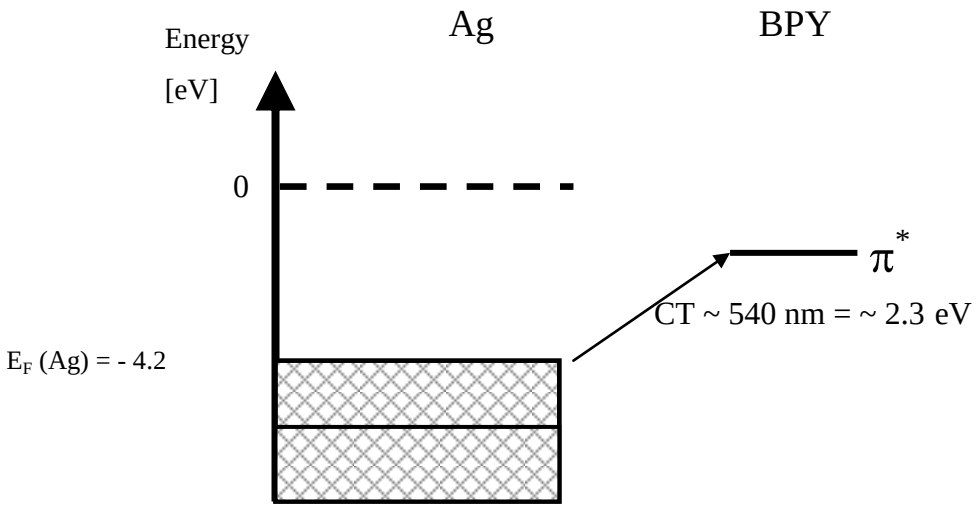

Fig. 1.3.: Proposed electronic structure of Ag-2,2'-bipyridine surface complex

1.2. Single-molecule surface enhanced Raman spectroscopy (SM-SERS)

SM-SERS has been reported about fifteen years ago [34, 35].The growing interest in SM-SERS [14, 16, 30, 36-39] is a part of a resurgence of interest in SERS generally which has emerged from several contributing causes, among them the unique physical and chemical properties of nanostructures [40] and the development of the field of plasmonics [41].

SM-SERS has been reported for the first time by Kneipp et al. [34]. In their Raman microspectroscopic measurements of very small volumes of a highly diluted hydrosol of small Ag NP aggregates containing cresyl violet in $1x10^{-14}$ M concentration, there was on average 0.6 molecules in the probed volume. SERS signal obtained from this system in 1 s intervals showed temporal fluctuations. A histogram of signal intensities for a particular Raman band showed, instead of a Gaussian profile obtained for more concentrated systems, a Poisson distribution of signal intensities, which was attributed to acquisition of the signal from 0, 1, 2 or 3 molecules. Kneipp's results immediately evoked a question whether single molecule SERS and SERRS are explicable by a combination of the EM and molecular resonance mechanisms. The answer was provided chiefly through calculations of Kall and coworkers [26 – 28], which have shown that, indeed, for a molecule located in a hot spot between two Ag NPs and excited by light polarized parallel to the dimer axis, the EM mechanism enhancement can be of $1x10^{11}$, and when combined with another three orders of magnitude provided by a molecular resonance, it can achieve the $1x10^{14}$ enhancement [16] observed experimentally. In addition to that, observation of temporal fluctuations of the SERS signal (so called ''blinking'') has been interpreted as manifestation of a dynamic behavior of a single, or of very few molecules [17, 29, 32, 34, 39].

EM and molecular resonance contributions can account for the highest observed SERS enhancement on the order of $1x10^{14}$. Theoretical estimates show that in principle, two kinds of plasmonic nanoparticle morphologies can account for the hot spots providing giant electromagnetic SERS enhancement:

a) dimers and small aggregates formed from silver and gold NPs [26, 42, 43], where strong field enhancement exists particularly at the intersection between two nanoparticles, and

b) fractal types of nanostructures, which are comprised of aggregates and clusters formed by the self-assembling of NPs [24, 44, 45]. EM effects in fractal structures can result in enhancement factors up to $1x10^{11}$.

The extent of the electromagnetic enhancement contribution to SM-SERS remains a subject of discussion [46], but there is strong evidence that SM – SERS spectroscopy is primarily a phenomenon associated with the enhanced local optical fields in the vicinity of metal nanostructures. The high local optical fields in the hot spots of silver and gold aggregates structures can be considered the key effect in SERS at an extremely high enhancement level [15, 17].

1.3. Characteristics of selected adsorbates

SM-SERS is enabled by localized surface plasmon resonance occurring on nanostructured metal surfaces and inducing large electromagnetic field intensification in certain points or areas of the surface. The most effective locations for extremely high enhancements are interstitial sites of nanometre-scale between NPs, named hot spots [47 - 49]. An ideal situation for building interparticle hot spot is the use of bifunctional molecules which act as NPs linkers. Moskovits et al. demonstrated [48, 49], that dithiol-containing adsorbates can act as linker molecules, leading to the chemically driven production of SERS active systems consisting of assemblies of strongly interacting NPs. However, thiol linkers usually form very tight self-assembled monolayer due to the strong intermolecular interactions between aliphatic chains [50].

In this thesis, another type of molecules, namely those with two amino groups in para-position, have been selected and tested as prospective linkers of Ag NPs. Examples of such linkers are 4,4´-diaminoterphenyl (DATP) and 4,4´-diaminoazobenzene (DAAB).

1.3.1. Protoporphyrin IX (PPIX) and its previous spectral studies

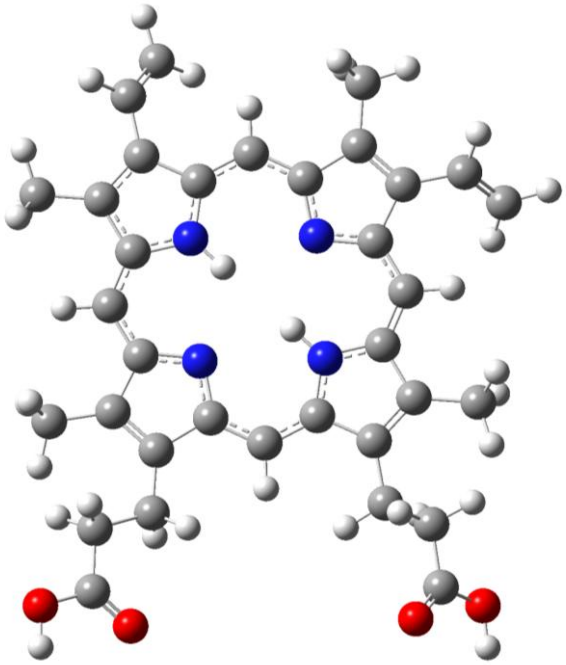

Figure 1.4: Protoporphyrin IX

PPIX (Figure 1.4) is a biochemically widely used carrier molecule for divalent cations. Together with iron (Fe 2+) the body of the heme group of hemoglobin, myoglobin and many other heme-containing enzymes like cytochrome c and catalase are formed. Complexed with magnesium ions (Mg 2+) the main part of the Chlorophylls are formed. Complexed with zinc-ions (Zn 2+) it forms Zinc protoporphyrin. The number (e.g. IX) indicates the position of different side chains, but historically, as the nomenclature has grown, it has done so systematically only in parts. PPIX as a direct precursor of heme is accumulated by patients of erythropoietic protoporphyria, which is one of the genetic disorders of the biosynthesis of the heme -pathway. It causes a severe photosensivity against visible light. The sensitivity of protoporphyrin IX against light is also used as a therapy against different forms of cancer (photodynamic therapy, PDT) [51]. It was shown to be a suitable adsorbate for evaluation of the effect of the morphological changes induced in Ag NPs by adsorbed chlorides on the EM mechanism contribution to the SERRS enhancement [52].

Electronic absorption spectra of PPIX (free base) in aqueous ambient as a function of pH were thoroughly investigated and formation of porphyrin aggregates (both H- and J-type) at pH>3 was reported, while monomeric PPIX was identified in some non-aqueous solvents [53, 54]. Resonance Raman spectra and SERRS spectra of PPIX (excited at 514.5 nm) in systems with Ag NP hydrosols were reported in ref. [55] and an assignment of the resonance Raman scattering (RRS) and SERRS spectral bands has not been provided in ref. [52].

1.3.2. 5,10,15,20-tetrakis(4-aminophenyl)porphine (TAPP)

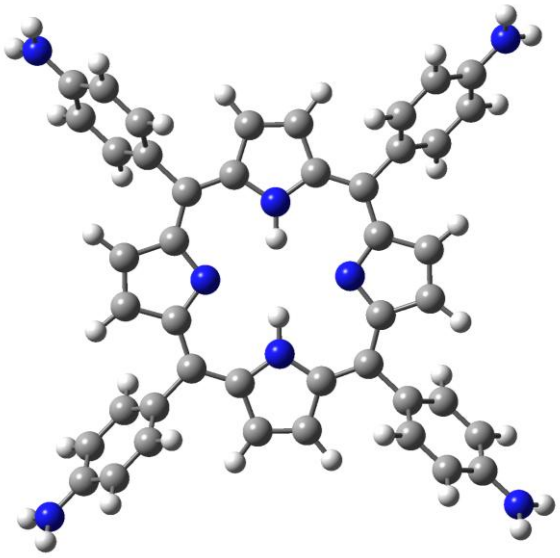

Figure 1.5: 5,10,15,20-tetrakis(4-aminophenyl) porphine

TAPP (Figure 1.5) was selected as a linker since it possesses strongly argentophilic amine groups containing lone pairs on nitrogen atoms. The amine group of the aminophenyl substituent can rotate and thus achieve a lone pair orientation favorable for bonding to the Ag NP surface. In a study reported by Šišková et al. [56], it was shown that this porphyrin can be bond to Ag NP surface by all four lone pairs on aminophenyl-group nitrogen atoms adopting thus immediately upon adsorption the parallel orientation with respect to the surface required for the porphyrin metallation

On the other hand, for fulfillment of its function as a linker, TAPP will have to be adsorbed in a perperdicular orientation with respect to Ag NP surface.

1.3.3. 4,4´- diaminoterphenyl (DATP)

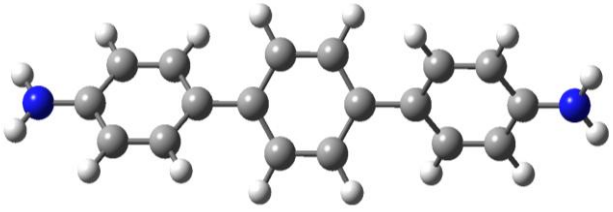

Figure 1.6: 4,4´- diaminoterphenyl

Both DATP and the following 4,4´-diaminoazobenzene (DAAB) are bifunctional molecules with two primary amino- groups. Due to the position and the affinity of the amino-groups to noble metals these molecules can act as a molecular linker between two noble metal surfaces. This was demonstrated for both DATP and DAAB in the study of conductivity of single molecule connecting two gold electrodes [57]. In contrast to DAAB, DATP is a rigid rod shaped molecule

ca. 1.4 nm long. The planes of the benzene rings are tilted to each other in consequence of the ortho hydrogens repulsion.

1.3.4. 4,4´-diaminoazobenzene (DAAB)

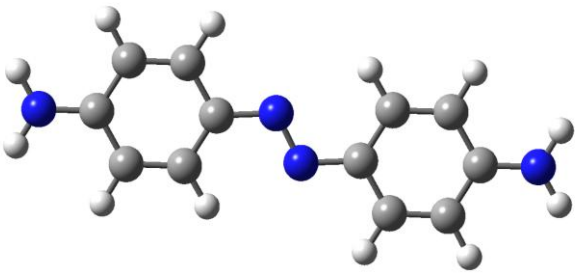

Figure 1.7: 4,4´-diaminoazobenzene

DAAB (Figure 1.7) is an interesting molecule because of its reversible trans/cis photoisomerisation. Although it has been known for a long time, the excitation mechanism and optical properties of the azobenzene chromophore are still under investigation [58, 59].The azobenzene group is isomerised from the more stable trans to the cis ground state by UV light of 366 nm and back to the trans conformer with 436 nm radiation [60]. The photoswitchable azobenzene moiety has been utilised in the past for controlling the properties of functional polymeric materials [61] and for novel applications such as data storage [62, 63] and self-assembling systems [64]. The presence of two amino groups in para-position indicates, that this molecule can become a prospective Ag NP linker, provided that it is adsorbed in a perpendicular orientation to Ag NP surface.

2. OBJECTIVES

1. Experimental realization, i.e. design, preparation and characterization of Ag nanoparticle assemblies for which the presence of hot spots (i.e. strong optical fields after an appropriate optical excitation) has been predicted theoretically in accurate or simplified models previously published.

2. Designing and testing approaches to localization of molecules into the hot spots and obtaining of SERS or SERRS signal of these molecules, and, whenever possible, also its time-evolution.

3. Interpretation of the SERS and/or SERRS spectra and their temporal evolutions in terms of dynamics of molecules incorporated into a particular Ag nanoparticle assembly, with an ultimate goal to approach single molecule level of detection, and, consequently, a possibility to follow single molecule dynamics within a particular Ag nanoparticle assembly.

4. Pinpointing of the factors which are important for a successful localization of molecules into hot spots in various Ag nanoparticle assemblies and of the factors which affect the stability of the testing molecules in strong optical fields.

3. EXPERIMENTAL

3.1. Materials

3-aminoprophyltrimethoxysilane – APTMS (Aldrich), 97%

4,4´-diaminoazobenzene – DAAB (Lancaster), 95%

4,4´-diaminoterphenyl – DATP (Lancaster), 95%

5,10,15,20-tetrakis(4-aminophenyl)porphine - H_2TAPP (Porphyrin Products, inc.)

sodium citrate – $Na_3C_6H_5O_7 \cdot 2H_2O$ (Aldrich), p.a.

doubly distilled, deionized water

silver nitrate – $AgNO_3$ (Aldrich), p.a.

chloroform – $CHCl_3$ (Merck), Uvasol

ethanol - EtOH (Merck), Uvasol

glycerine – $C_3H_5(OH)_3$ (Lachema), p.a.

sodium chloride – NaCl (Aldrich), p.a.

nitric acid – HNO_3 (Lachema), p.a.

hydrochloric acid – HCl (Lachema), p.a.

sulphuric acid – H_2SO_4 (Lachema), p.a.

penthylamine – $C_8H_{11}N$ (Aldrich)

protoporphyrin IX – PPIX – disodium salt (Porphyrin Products, inc.)

sodium borohydride - $NaBH_4$ (Merk), p.a.

tetraoctylammonium bromide – $[(C_8H_{17})_4N]^+Br^-$ (Aldrich)

3.2. Instrumentation

3.2.1. Electronic absorption spectra

Electronic absorption spectra were measured with a Perkin Elmer Lambda 12 UV-Vis spectrometer.

3.2.2. Electron microscopy

Transmission electron microscopy (TEM) images of the samples were obtained with a JEOL JEM 200 CV transmission electron microscope. The instrumental magnification varied from 20 000 to 150 000.

Scanning electron microscopy (SEM) images of samples deposited on glass slides were obtained with a FESEM microscope (Quana 200 FEG, FEI).

3.2.3. SERS micro-Raman spectra

SERRS micro-Raman spectra of selected Ag NP aggregates attached to chemically derivatized TEM grids or glass slides were collected through a confocal optical microscope using a micro-Raman Labram-HR spectrometer (Jobin-Yvon/Horiba) operating in either the spectral or the imaging mode. Measurements were performed with the 514.5 nm Ar^+ laser excitation line with incident laser power of 10 mW and a laser spot size of ca. 0.7 μm. Spectral acquisition time was 2 s.

3.3. Preparation of Ag hydrosols

3.3.1. Preparation of Ag NP hydrosol by reduction of silver nitrate by sodium borohydride (H I)

Ag hydrosol was prepared by reduction of $AgNO_3$ by $NaBH_4$ in aqueous ambient, in particular by a modification [21] of the procedure originally reported in [20]. Briefly, 9 mL of 2.2 x 10^{-3} M aqueous solution of $AgNO_3$ were added dropwise to regularly stirred 75 mL of 1.1 x10^{-3} M aqueous solution of $NaBH_4$ at 2°C.

3.3.1.1. Effect of preparation conditions on particle size distribution in Ag NP hydrosol (H I)

The STEPDOS® microprocessor controlled diaphragm metering pump was used to control the rate of $AgNO_3$ aqueous solution addition, and its values of 200, 300, 400, 500 and 600 μL/min were applied to prepare different Ag hydrosol samples. The Ag hydrosol samples were characterized by TEM images - particle size and distributions are demonstrated in Fig. 3.1. – 3.5. The lowest polydispersity of the Ag NP hydrosol has been achieved at the slowest rate of the $AgNO_3$ solution addition, i.e. at 200 μL/min (Fig.1B), while the largest polydispersity has been encountered in the Ag NP hydrosol prepared at the addition rate of 600 μL/min (Fig. 3.5B). A low polydispersity of Ag NP hydrosols is required for applications involving Ag NP assembling, such as Ag NP dimer formation. In contrast to that, increasing polydispersity of Ag nanoparticle hydrosols has been shown to increase the SERS signals obtained from systems with fractal Ag NP aggregates and selected testing adsorbates [65]. A possibility to control polydispersity of Ag NP hydrosols by the rate of the reagent addition is thus important for their preparations targeted on a desired type of application.

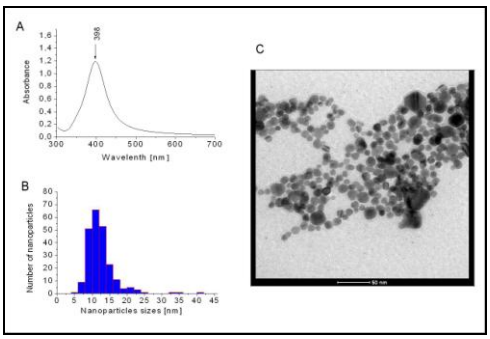

Figure. 3.1: Rate dropwise 200 μL/min

A) UV-Vis spectrum of Ag hydrosol
B) Particle size distribution of nanoparticles
C) TEM images of Ag nanoparticles

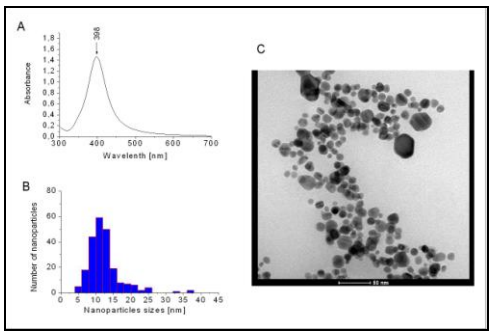

Figure. 3.2: Rate dropwise 300 μL/min

A) UV-Vis spectrum of Ag hydrosol
B) Particle size distribution of nanoparticles
C) TEM images of Ag nanoparticles

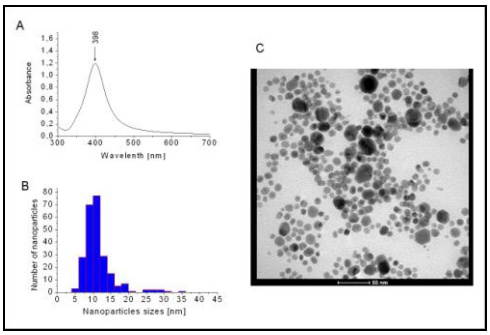

Figure. 3.3: Rate dropwise 400 µL/min

A) UV-Vis spectrum of Ag hydrosol

B) Particle size distribution of nanoparticles

C) TEM images of Ag nanoparticles

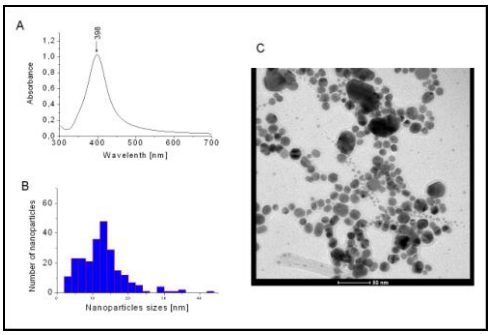

Figure. 3.4: Rate dropwise 500 µL/min

A) UV-Vis spectrum of Ag hydrosol

B) Particle size distribution of nanoparticles

C) TEM images of Ag nanoparticles

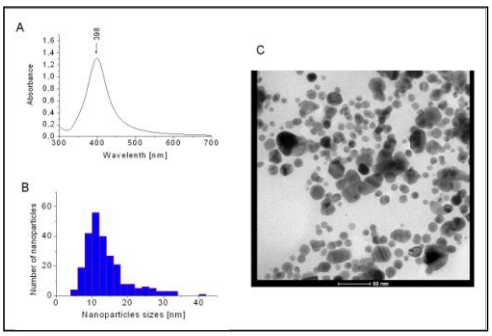

Figure. 3.5: Rate dropwise 600 µL/min

A) UV-Vis spectrum of Ag hydrosol

B) Particle size distribution of nanoparticles

C) TEM images of Ag nanoparticles

3.3.2. Preparation of Ag NP hydrosol by reduction of silver nitrate by sodium citrate (H II)

Ag hydrosol was prepared by reduction of silver nitrate ($AgNO_3$) by sodium citrate ($Na_3C_6H_5O_7 \cdot 2H_2O$) in aqueous ambient according to the procedure by Lee and Meisel [22].

In particular, 22.7 mg of $AgNO_3$ was disolved in 125 mL of deionized water. The solution was boiled in a glycerine bath heated to 107°C. An aliquot of 250 mg of $Na_3C_6H_5O_7 \cdot 2H_2O$ was disolved in 25 mL of deionized water and 2.5 mL of the aqueous solution of $Na_3C_6H_5O_7 \cdot 2H_2O$ were added to regularly stirred boiling aqueous solution of $AgNO_3$. Ag hydrosol was kept boiling and regularly stirring for 1 hour.

3.3.3. Preparation of Ag NP organosol

Organosols of Ag NPs were prepared by a two-phase synthesis. An aqueous solution of silver nitrate (30 mL, 0.03 M) was mixed with a solution of tetraoctylammonium bromide in chloroform (20.4 mL, 0.2M) and stirred for 1 h. Organic phase was separated, a solution of pentylamine in chloroform (100 L, containing 0.09 L of pentylamine) was added and the reaction mixture was stirred for 15 min. After that, 20.4 mL of 0.43 M aqueous solution of sodium borohydride (ice-cooled) was added, and the two phase system was stirred intensively for 12 h. The organic phase was separated, collected and washed with ultrapure water at least 5 x. Since the resulting Ag NP organosol was prone to oxidation by air, it was stored under nitrogen atmosphere.

3.4. Preparation of samples

3.4.1. Preparation of chemically modified supporting surfaces for TEM and micro-Raman measurements

SiO_x/formvar coated copper grids for TEM microscopy (Agar Scientific, Ltd.) were pre-treated by vapor-deposition of a thin carbon layer on their reverse sides. The outer SiO_x layer of the grids was derivatized by 3-aminopropyltrimethoxysilane (APTMS) through condensation of the reagent vapor onto the grids and removal of the excess reagent in vacuo.

3.4.2. Preparation of samples of Ag NP / PPIX systems

3.4.2.1. Preparation of Ag hydrosol/NaCl/PPIX systems containing PPIX incorporated in compact Ag NP aggregates

Samples were prepared by modification of Ag NPs by addition of 100 μl of 1M NaCl to 2 ml of Ag hydrosol, followed by addition of 10 μL of 10^{-4}M aqueous solution of PPIX.

3.4.2.2. Preparation of samples of PPIX incorporated in compact Ag NP aggregates for TEM and micro-Raman measurements

SiO_x/formvar coated copper grids for TEM microscopy (Agar Scientific, Ltd.) were derivatized according to the procedure described in Chapter 3.4.1. The derivatized grids were allowed to float on the surface of Ag hydrosol/NaCl/PPIX system for 3 h to enable the attachment of compact aggregates of Ag NPs to the amine-groups on the surface of the derivatized grids.

3.4.3. Preparation of samples of dimers and small aggregates in aqueous ambient by selected molecular linker

To enable for Raman spectral probing and TEM imaging of the same sample, the dimers and small aggregates were assembled on chemically derivatized SiOx/formvar coated copper finder grids for TEM microscopy (chemically modified according to the procedure described in Chapter 3.4.1.) by a three-step procedure involving:

(1) tethering the Ag NP to the grids with 3-aminopropyltrimethoxysilane during floating of the grids on Ag NP hydrosol surface

(2) attaching the linker molecules to the tethered Ag NP during immersion of the grids into solution of a molecular linker in ethanol

(3) exposing the grids to Ag NP hydrosol for a second time, during which additional NPs linked to the particles already tethered to the grid surface through the free amine groups of the linker molecules. The procedure is schematically depicted in Fig. 3.6. The appropriately wide spacing of aggregates (allowing for a single nano-object selection) was accomplished by optimalization of the preparation steps duration.

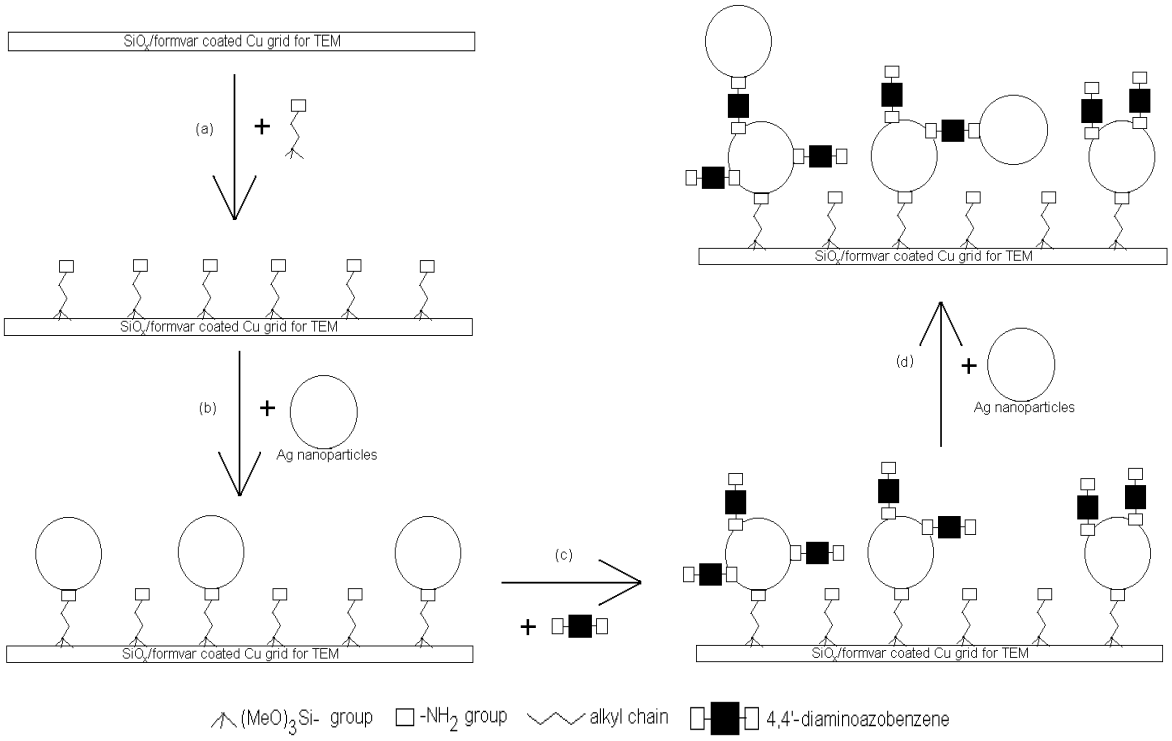

Figure 3.6: Three-step procedure for preparation dimers and small aggregates of Ag NP

3.4.4. Preparation of samples of Ag NP / H_2TAPP systems

3.4.4.1. Samples of TAPP-bridged Ag NP dimers and small aggregates originating from the organic ambient

Samples were prepared by mixing of chloroform solutions of TAPP with the organosol of pentylamine-capped Ag NPs under constant stirring. Glass slides were thoroughly cleaned and derivatized by immersion into neat APTMS for 3h. After rinsing with ethanol, the slides were immersed into the Ag organosol-TAPP system for 3 h.

3.4.4.2. Samples of TAPP-bridged Ag NP dimers and small aggregates originating from the aqueous ambient

Samples were prepared by assembling on chemically derivatized TEM grids (prepared by the procedure described in Chapter 3.4.1.) by a three-step procedure outlined in Chapter 3.4.3. In particular, the derivatized TEM grids were allowed to float on the surface of a Ag NP hydrosol for 1.5 h to allow Ag NPs to bond to the amine-groups on the surface of the derivatized grids. Subsequently, the grids were immersed in a 1 x 10^{-7} M solution of TAPP in ethanol for 4 h. Finally, the grids were allowed to float again on the surface of Ag NP hydrosol for 2 h

3.4.5. Preparation of samples of Ag NP / DATP systems

Samples were prepared by assembling on chemically derivatized TEM grids (prepared by the procedure described in Chapter 3.4.1.) by a three-step procedure outlined in Chapter 3.4.3. In particular, the derivatized TEM grids were allowed to float on the surface of Ag NP hydrosol for 1.5 h. Subsequently, the grids were immersed in a 1 x 10^{-7} M solution of DAPT in ethanol for 4 h. Finally, the grids were allowed to float again on the surface of Ag NP hydrosol for 2 h.

3.4.6. Preparation of samples of Ag NP / DAAB systems

Samples were prepared by assembling on chemically derivatized TEM grids (prepared by the procedure described in Chapter 3.4.1 by a three-step procedure (see Chapter 3.4.3). The derivatized grids were allowed to float on the surface of Ag nanoparticle hydrosol for 1.5 h. Subsequently, the grids were immersed in a 1 x 10^{-7} M solution of DAAB in ethanol for 4 h. Finally, the grids were allowed to float again on the surface of Ag NP hydrosol for 2 h.

4. RESULTS AND DISCUSSION

4.1. Compact Ag NP aggregates incorporating PP IX molecules

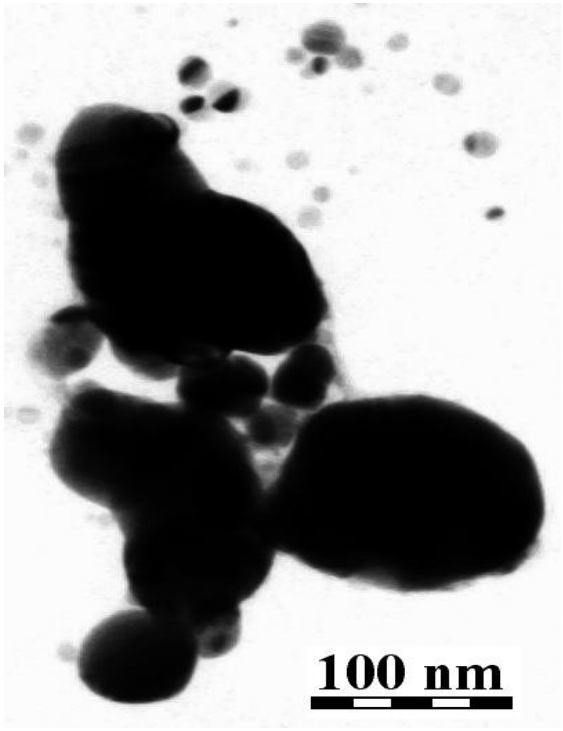

Figure 4.1: TEM image of a typical compact aggregate of interpenetrating, chloride modified Ag nanoparticles incorporating PPIX molecules.

TEM images as well as SERRS-micro-Raman spectra of single compact aggregates of chloride-modified Ag nanoparticles incorporating PPIX molecules were acquired from the same sample of the aggregates attached to the surface of APTMS derivatized, SiO_x coated TEM grid. TEM image of a typical single compact aggregate is shown in Figure 4.1. SERRS spectra from several single compact aggregates were acquired using 514.5 nm excitation. The SERRS signal showed large temporal fluctuations as well as variations from one aggregate to another. Nevertheless, within the signal fluctuations, SERRS spectra showing the characteristic bands of PPIX were obtained. An example of such a spectrum is shown in Figure 4.2. In this SERRS spectrum, some of the PPIX bands in the low wavenumbers region have their counterparts in SERRS spectra of PPIX measured in macrosampling setup and excited at 446.1 nm [52]: the 330 cm^{-1} band has its counterpart in the 329 cm^{-1} band of H_2PPIX, while the 377 cm^{-1} band corresponds to the 381 cm^{-1} band of AgPPIX. Their observation indicates that both the free-base and the Ag metalated PPIX species contribute to the fluctuating SERRS signal. In addition to those, spectral contributions of graphitic carbon and APTMS to the fluctuating signals were also identified. The number of PPIX molecules per a single compact aggregate was estimated to be ca 40 (or less) under the conditions of our experiment. Temporal fluctuations of the signal which are usually associated with a

single molecule level of detection indicated, that only a few of the overall amount of molecules per aggregate actually contribute to the detected signal.

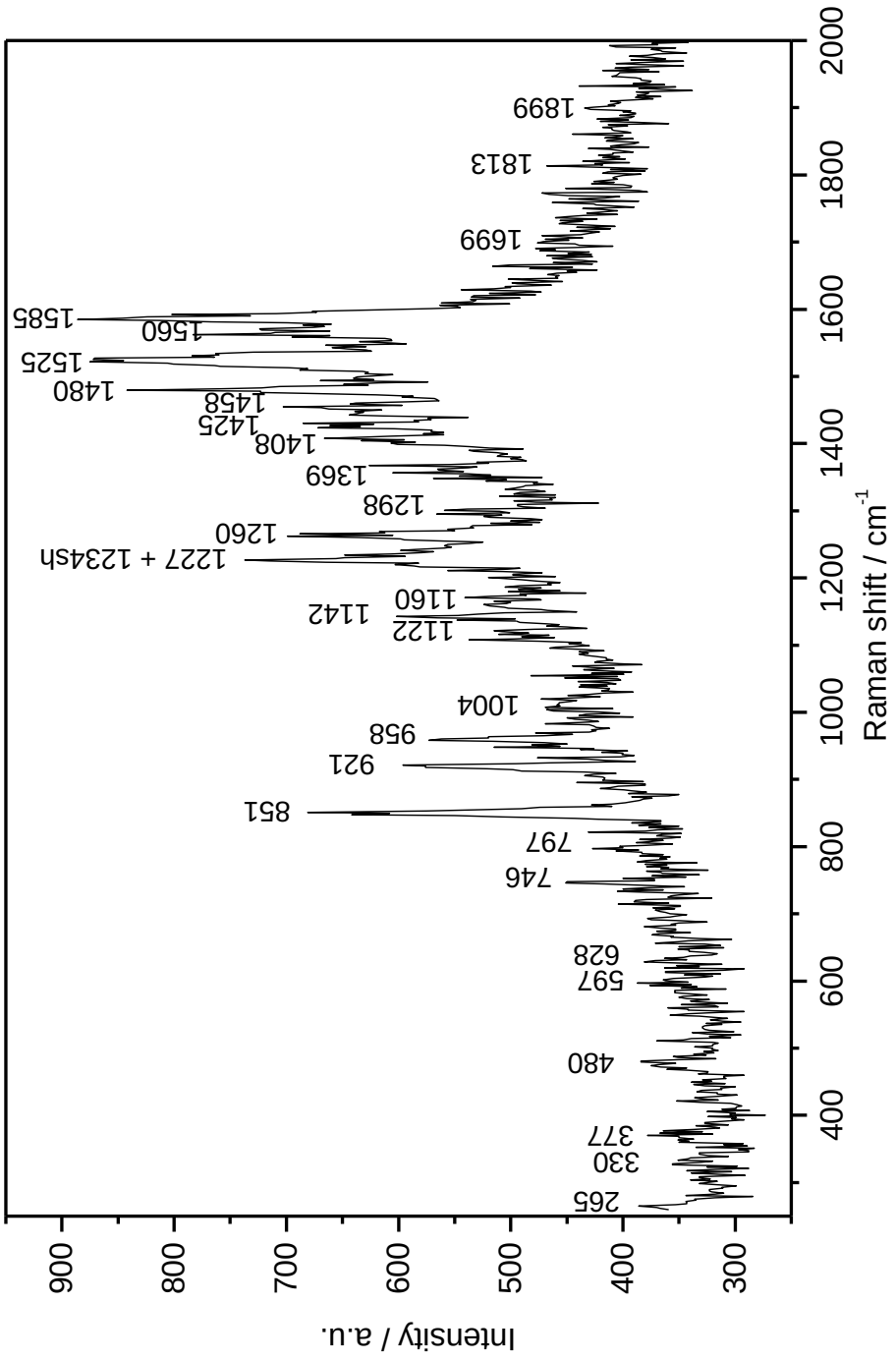

Figure 4.2: SERRS spectrum of PPIX obtained from a single aggregate of chloride-modified Ag nanoparticles incorporating PPIX molecules

4.2. TAPP-bridged Ag NP dimers and small aggregates

Dimers and small aggregates of Ag NPs bridged (linked) by TAPP were prepared both in organic (pentylamine-derivatized Ag nanoparticles) and in the aqueous ambient (citrate-derivatized Ag NPs) and assembled on glass slides and on TEM grids, respectively.

SEM image of a sample of TAPP-bridged, pentylamine capped Ag nanoparticles and TEM image of that of TAPP bridged, citrate capped Ag NPs are shown in Figure 4.3 A and B, respectively. Their comparison (Figure 4.3) indicates that, in both samples, monomers, dimers and small aggregates of Ag NP are present. SERS spectra obtained from the sample of TAPP-bridged, pentylamine capped Ag NPs are governed by the signal of graphitic carbon, which shows enormous temporal fluctuations of the signal intensity (Figure 4.4), and, in some of these spectra, a few narrow bands attributable to TAPP (an example of such spectrum is shown in Figure 4.5). The fluctuations of the graphitic carbon signal can possibly result from spacial oscilations of Ag NPs, which, after TAPP decomposition, remain tethered to the supporting surface, but are no longer fixed by the rigid porphyrin bridge. By contrast, SERS spectra obtained from the sample of TAPP bridged, citrate capped Ag NPs show temporal

A

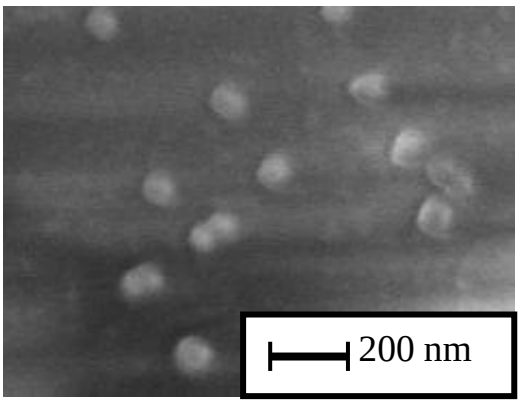

B

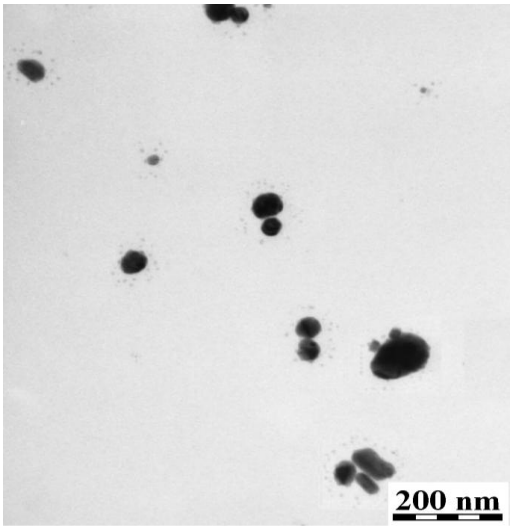

Figure 4.3:
A. SEM image of a sample of TAPP – bridged, pentylamine-capped Ag nanoparticles
B. TEM image of a sample of TAPP – citrate-capped Ag nanoparticles

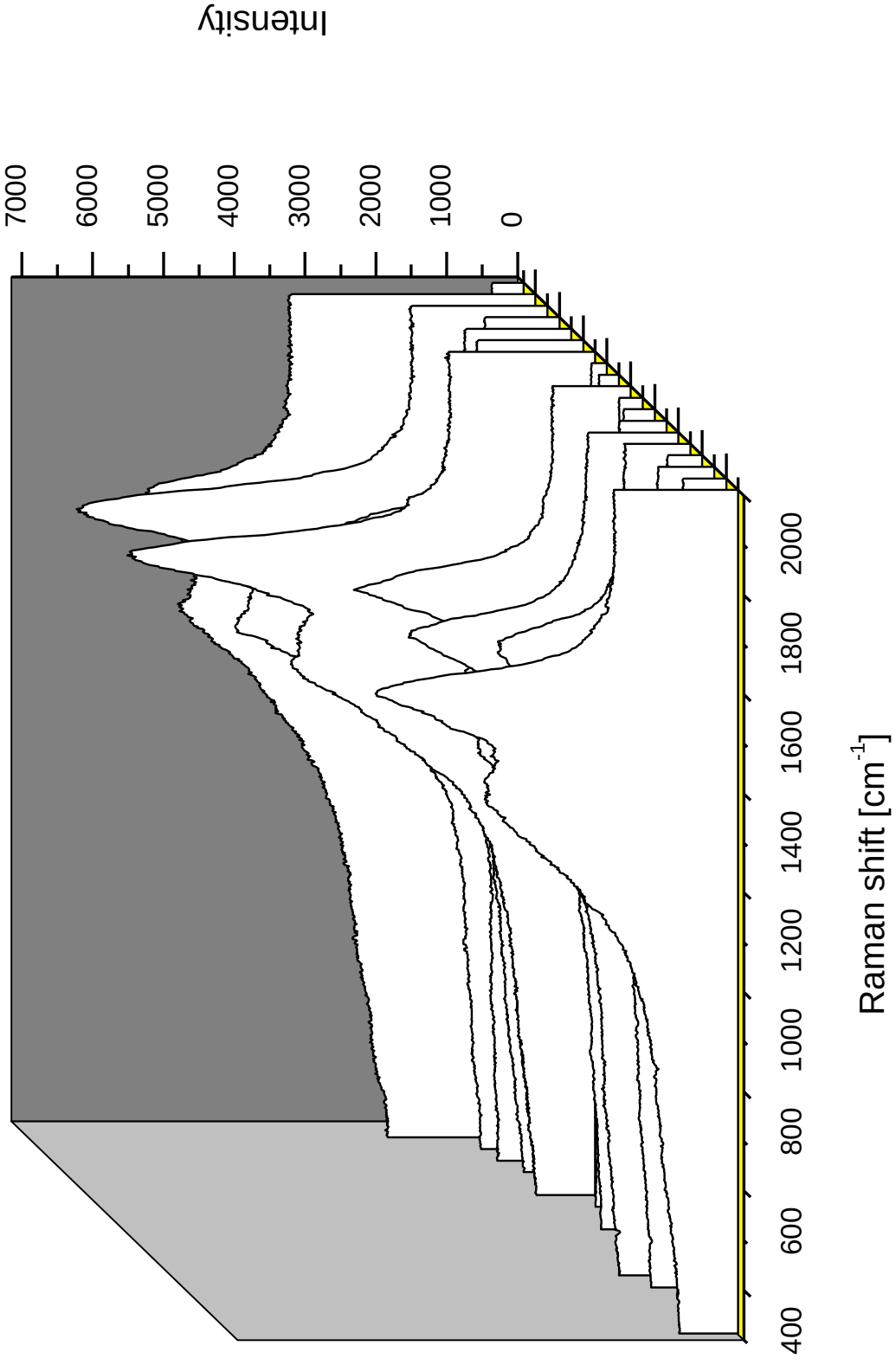

Fig. 4.4: Time-evolution of SERS spectra obtained from the samples shown in Fig. 4.3 A

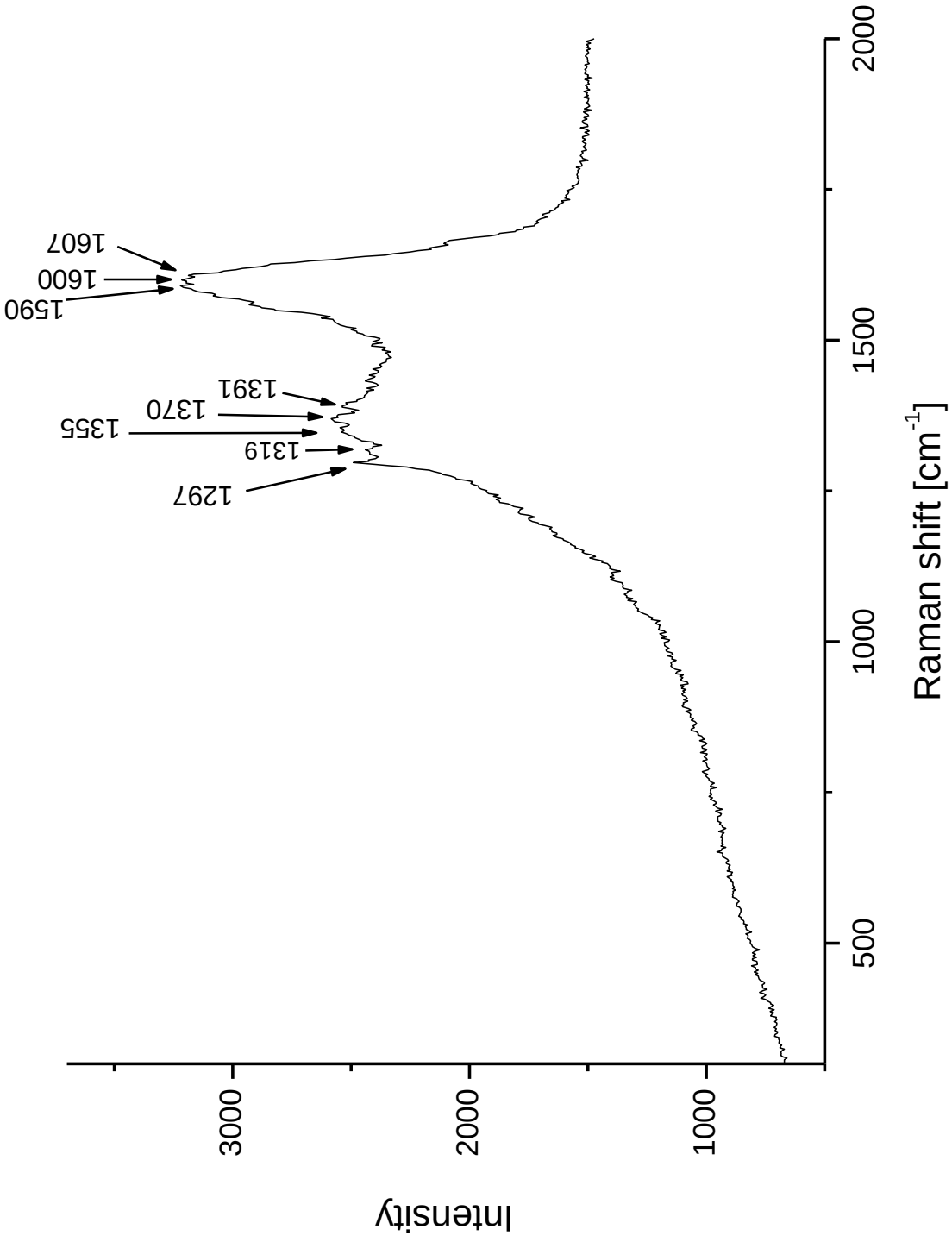

Fig. 4.5: Selected SERS spectrum from the SERS spectral set shown in Fig. 4.4

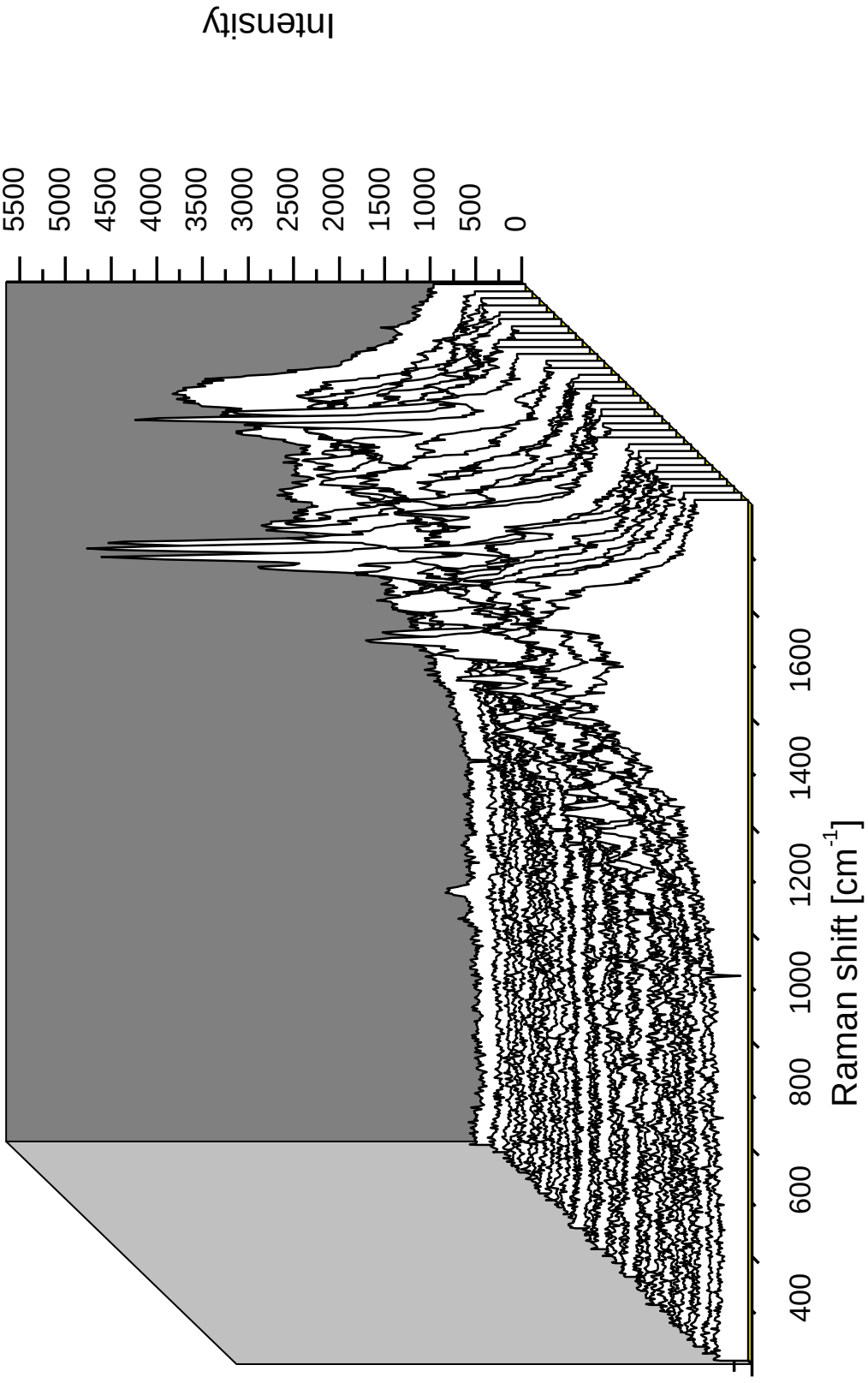

Fig. 4.6: Time-evolution of SERS spectra obtained from the samples shown in Fig. 4.3 B

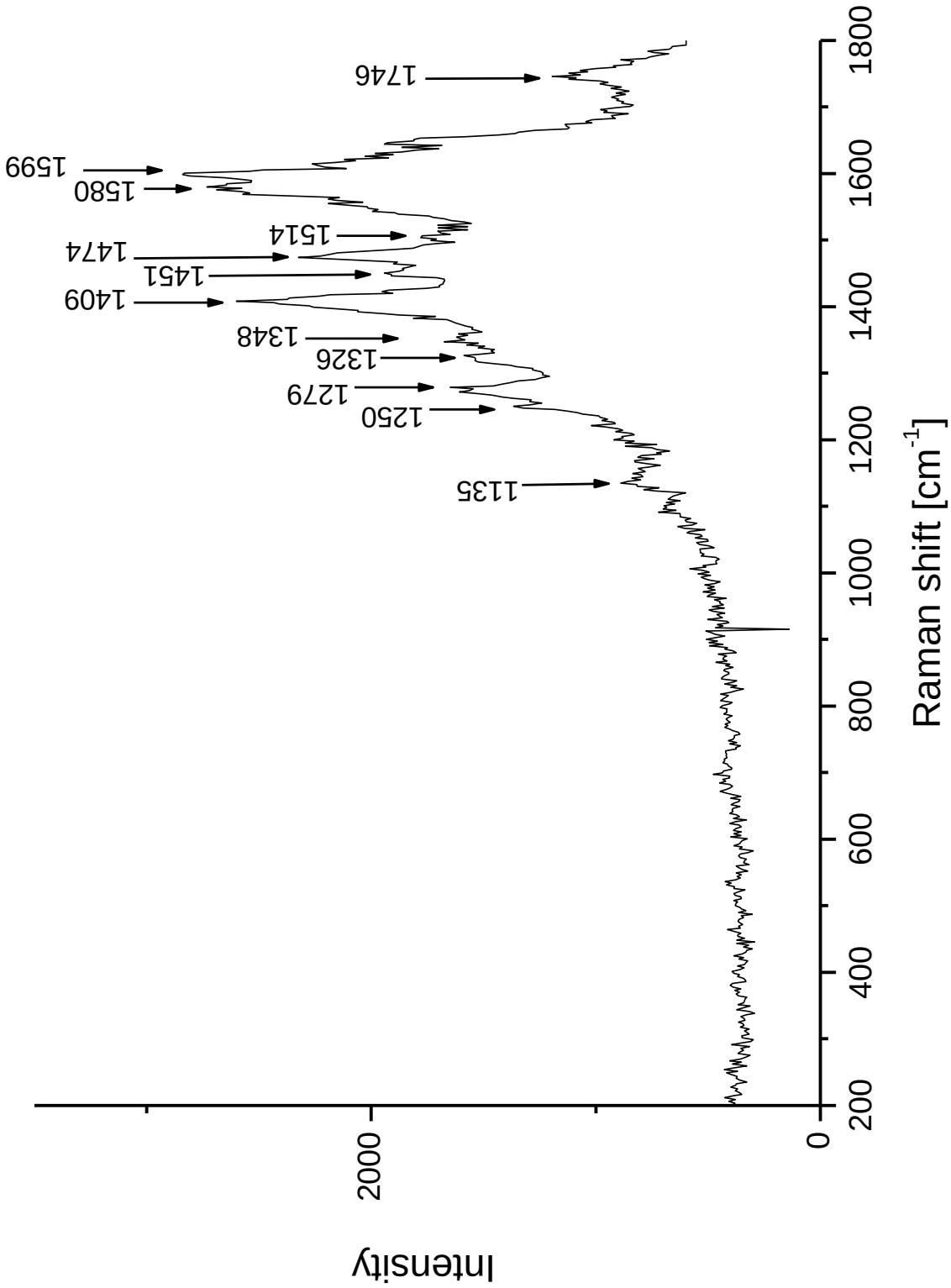

Figure 4.7: Selected SERS spectrum from the SERS spectral set shown in Fig. 4.5

fluctuations of the signal in which the characteristic spectral bands of the bridging TAPP molecules can clearly be distinguished (Figure 4.6). A typical such spectrum is shown in Figure 4.7. It should be noted that, in both cases, SERS signals were collected from several dimers and/or small aggregates, as witnessed by their rather dense packing in comparison to the size of the laser spot. SERS signals collected from both samples indicate that bridging TAPP molecules undergo photodecomposition under 514.5 nm laser irradiation. While for pentylamine capped dimers and small aggregates, this decomposition is very fast and actually prevents detection of a meaningful porphyrin signal, for citrate capped dimers and aggregates, the process is much slower and allows for TAPP detection. One of the possible explanations of this difference can be related to a low ordering of the capping pentylamine monolayer (which can further decrease at elevated temperatures under irradiation) which might be responsible for re-orientation of porphyrin molecules and for a direct contact between the porphyrin macrocycle and Ag NP surface, which in turn, may promote photodecomposition of TAPP molecules.

4.3. DATP-bridged Ag NP dimers and small aggregates

Ag NPs were assembled into dimers and small aggregates by a bifunctional, amine-terminated rigid aromatic linker 4,4'-diaminoterphenyl (DATP). The aggregates were assembled on the surfaces of SiO_x-coated TEM finder grids functionalized by APTMS using a three-step procedure described in Chapters 3.4.3 and 3.4.5.

A typical TEM image of DATP-bridged Ag nanoparticle aggregates and its statistical evaluation are presented in Figure 4.8. The statistics shows that dimers and trimers are the most abundant types of Ag nanoparticle aggregates, while larger aggregates are rarely encountered.

Furthermore, the TEM image in Figure 4.8 shows that the dimers and small aggregates are oriented parallel to the surface of the functionalized TEM grid. It appears that after its formation through the action of the DATP linker, a dimer and/or a small aggregate re-orients with respect to the surface in such a way that all the Ag nanoparticles in the aggregate are attached to the APTMS-functionalized TEM grid surface.

The intension in carrying out the SERS spectral measurements from a selected single dimer and/or aggregate was to obtain an unequivocal correspondence between the morphology of the aggregate and the SERS signal obtained from it. This

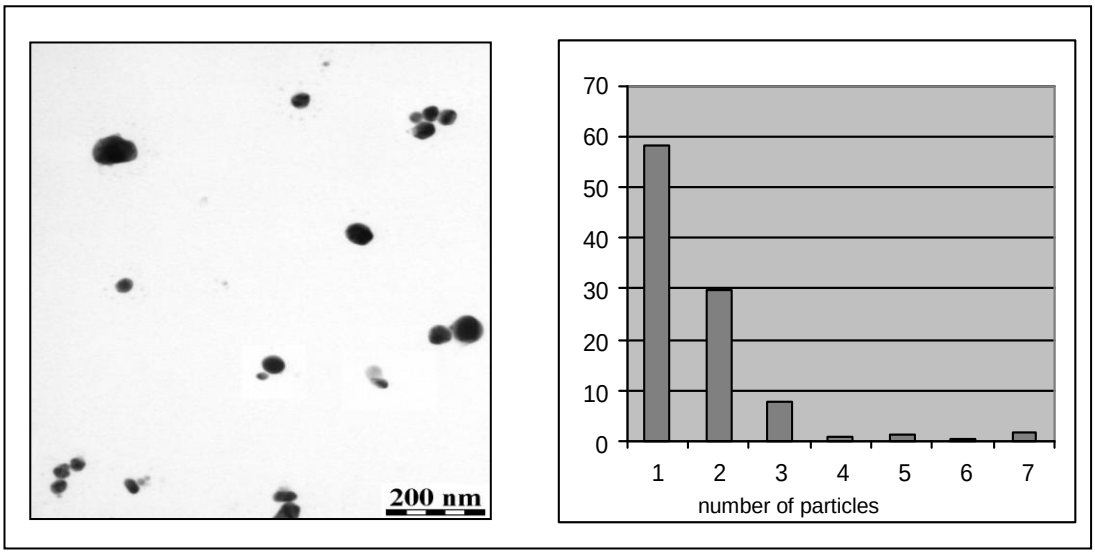

Figure 4.8: TEM image and size-distribution of DATP-bridged Ag nanoparticle aggregates (expressed in terms of number of particle per aggregate).

was accomplished by determination of the aggregate position with help of the markers on a finder grid. This exact aggregate position was located on both the optical image of the sample prior to the SERS measurement, and on the TEM image, which revealed the aggregate morphology in detail.

TEM image of a selected small aggregate of DATP-bridged Ag NPs consisting of a trimer of small particles located between two larger particles is shown in Figure 4.9. Time-evolution of SERS spectra measured from this particular aggregate (Figure 4.10) shows that the SERS signal fluctuates in time. In particular, the signal of DATP (Figure 4.11) alternates with that of graphitic carbon, represented by two distinct, rather broad bands (Figure 4.12). A possible scenario explaining the observed blinking pattern is decomposition of the bridging DATP molecule in at least one of the several hot spots within the aggregate into graphitic carbon. However, since the observed signal likely originates from more than one hot spot, the observed time evolution

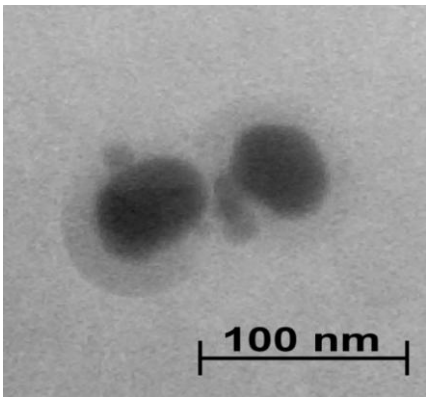

Figure 4.9: TEM image

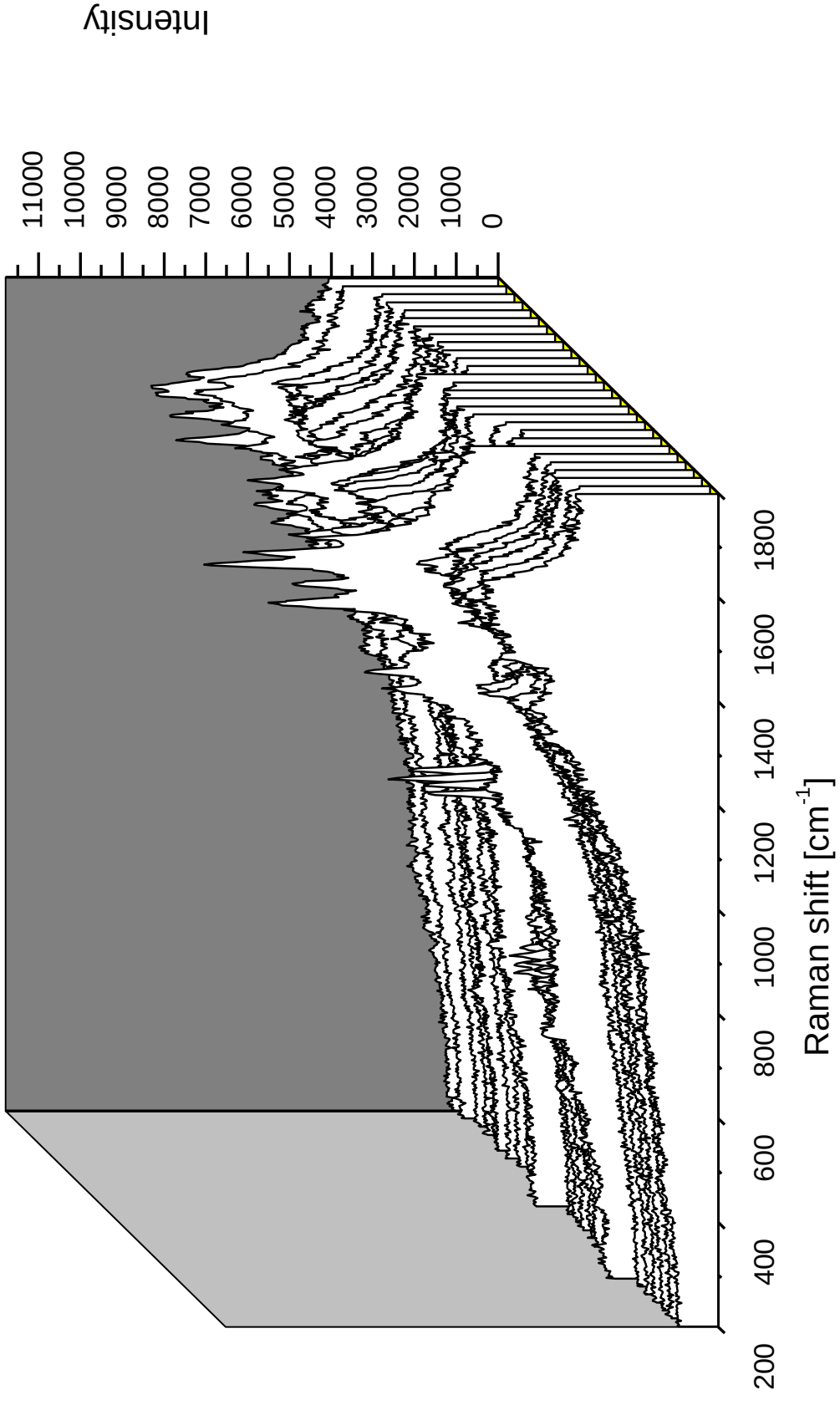

Figure 4.10: Time-evolution of SERS signal of a selected DATP-bridged Ag nanoparticle aggregate.

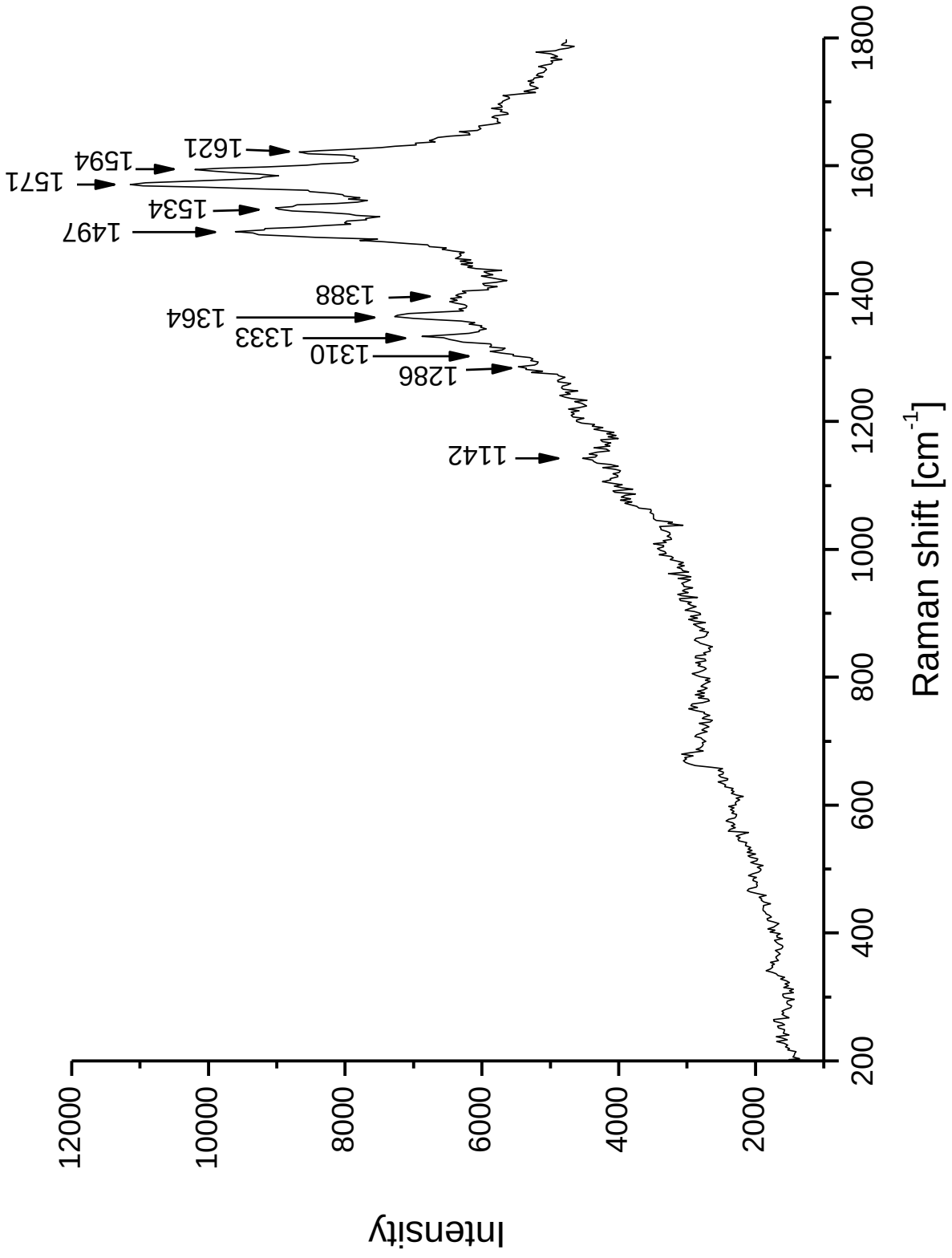

Figure 4.11: SERS signal of DATP from the SERS spectral set presented in Figure 4.10

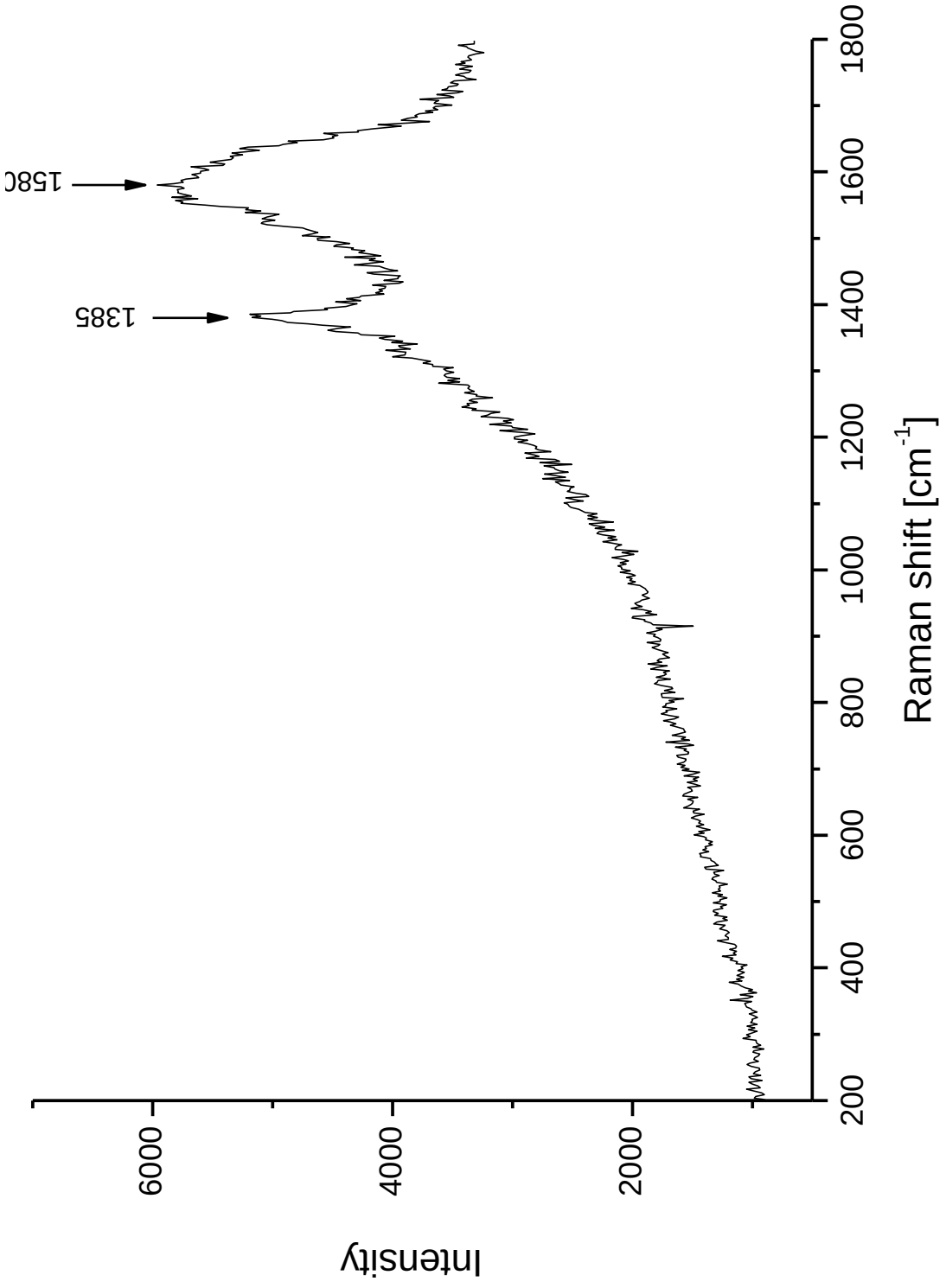

Figure 4.12: SERS signal of graphitic carbon from the SERS spectral set presented in Figure 4.10.

cannot be interpreted in terms of a single molecular dynamics event. Nevertheless, the observed results indicate that DATP molecules decompose in strong optical fields into graphitic carbon.

Furthermore, although the blinking pattern of alternating DATP and graphitic carbon signals observed under the conditions of our experiment cannot be unambiguously ascribed to a photochemical process (as opposed to a thermal decomposition), it should be noted that photodecomposition of substituted benzenes into graphitic carbon which proceeds on Ag NPs and is conditioned by their adsorption in a perpendicular orientation has been previously reported [66] and further supported by the results presented in ref [67]. On the basis of these results, we assume that DATP, which contains three interconnected benzene rings and is purposefully adsorbed in a perpendicular orientation with respect to the surface of Ag NPs (to perform its role as a linker), is prone to photodecomposition in the strong optical fields.

Our results thus provide experimental evidence for the presence of the theoretically predicted strong optical fields in small, molecularly-bridged Ag NP aggregates and for the localization of the bifunctional linking molecules in these hot spots. The nanocomposite systems: Ag NP-molecular bridge-Ag NP can be employed in studies of single molecule dynamics and in detection of species on a single molecule level.

4.4. DAAB-bridged Ag NP dimers and small aggregates

Ag NPs were assembled into dimers and small aggregates by a bifunctional, amine-terminated linker DAAB. The dimers and small aggregates were assembled on the surfaces of SiO_x-coated TEM finder grids functionalized by APTMS using a three-step procedure described in Chapters 3.4.3 and 3.4.6.

A TEM image of Ag nanoparticle aggregates assembled using DAAB and their size-distributions are shown in Figure 4.13. A high statistical frequency of

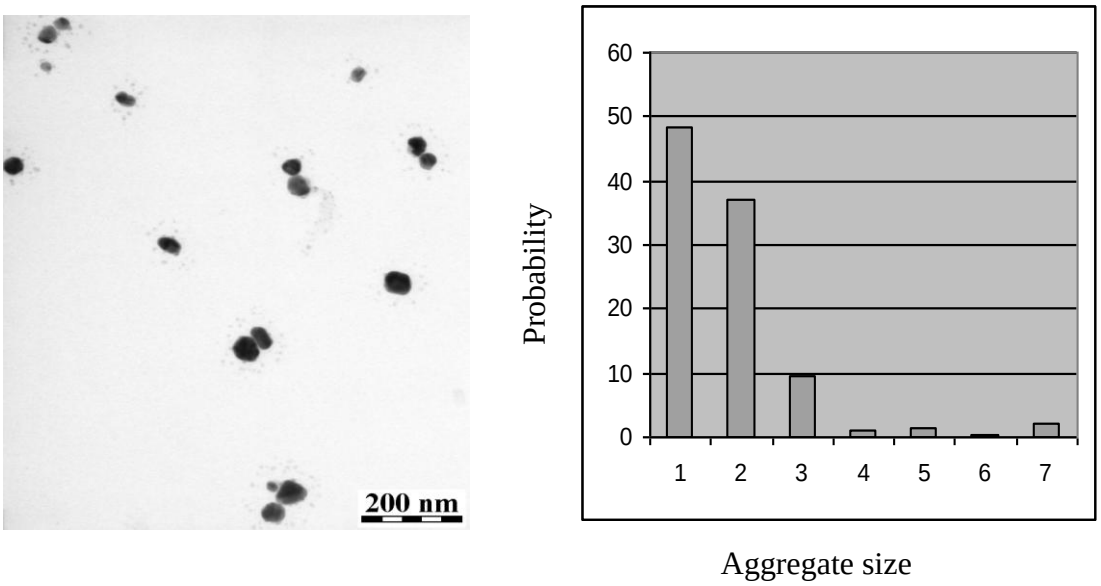

Fig. 4.13: TEM image and size-distribution of DAAB-linked Ag nanoparticle aggregates determined by TEM image analysis.

dimers and trimers, as opposed to that of the larger aggregates (tetramers to heptamers) indicates, that the aggregates were formed preferentially by linking of the NP by DAAB.

Furthermore, the TEM image in Figure 4.13 shows that the dimers are oriented parallel to the surface of the functionalized TEM grid. It appears that after formation of the dimer, i.e. after the attachment of a second Ag NP to the second (i.e. still free) amine-group of the DAAB linker, the dimer re-orients with respect to the surface in such a way that both Ag NPs in the dimer are attached to the APTMS-functionalized TEM grid surface.

In SERS spectral measurements from a selected single dimer and/or aggregate, our intension was to obtain an unequivocal correspondence between the morphology of the selected nanoobject (i.e. Ag NP dimer) and the SERS signal obtained from it. This was accomplished by determination of the dimer position with respect to the markers on a finder grid. This exact position of the dimer with respect to the markers was located on both the optical image of the sample prior to the SERS measurement, and on the TEM image, which revealed the details of its morphology.

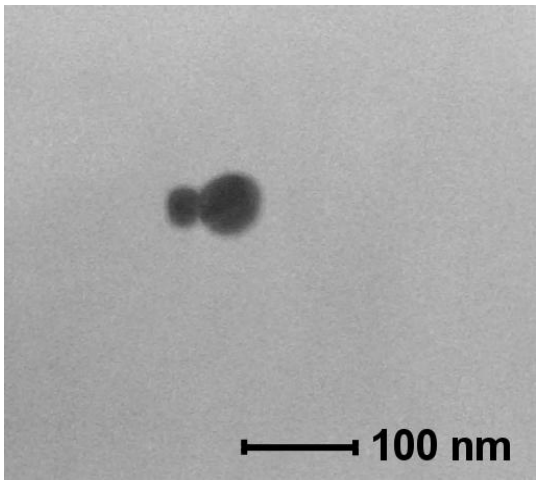

Figure 4.14: TEM image of a selected DAAB-linked Ag nanoparticle dimer

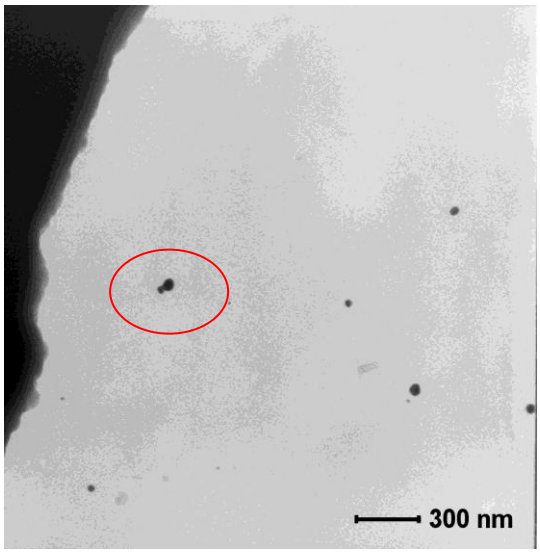

Figure 4.15: TEM image of a selected DAAB-linked Ag nanoparticle dimer – lower magnification

TEM images of a selected dimer of Ag nanoparticles bridged by DAAB are shown in Figure 4.14 and 4.15. The lower magnification image was used for determination of the dimer position, the higher magnification one reveals its morphology in detail. Time-evolution of SERS spectra measured from this particular dimer (Figure 4.16) shows that the SERS signal fluctuates, giving rise to an "in" and "off" signal pattern. The "in" signal observed in this particular time-evolution in the 8th and 14th spectrum of the series contains characteristic marker bands of DAAB, while the "off" signal consists of a broad background (Figure 4.16, details in Figure 4.17). Comparison of the two "in" spectra reveals that 9 of the 12 characteristic bands of DAAB observed in the 8th spectrum (Figure 4.17, spectrum A) were detected also in the 14th spectrum (Figure 4.17, spectrum C). A probable reason for the absence of the three weakest bands of DAAB in the 14th spectrum is the lower overall intensity of this spectrum than of the 8th spectrum. We can thus conclude that the majority of SERS spectral bands of DAAB were recovered in the second signal"in" spectrum. The broad background in Figure 4.17, spectrum B shows traces of graphitic carbon spectral bands.

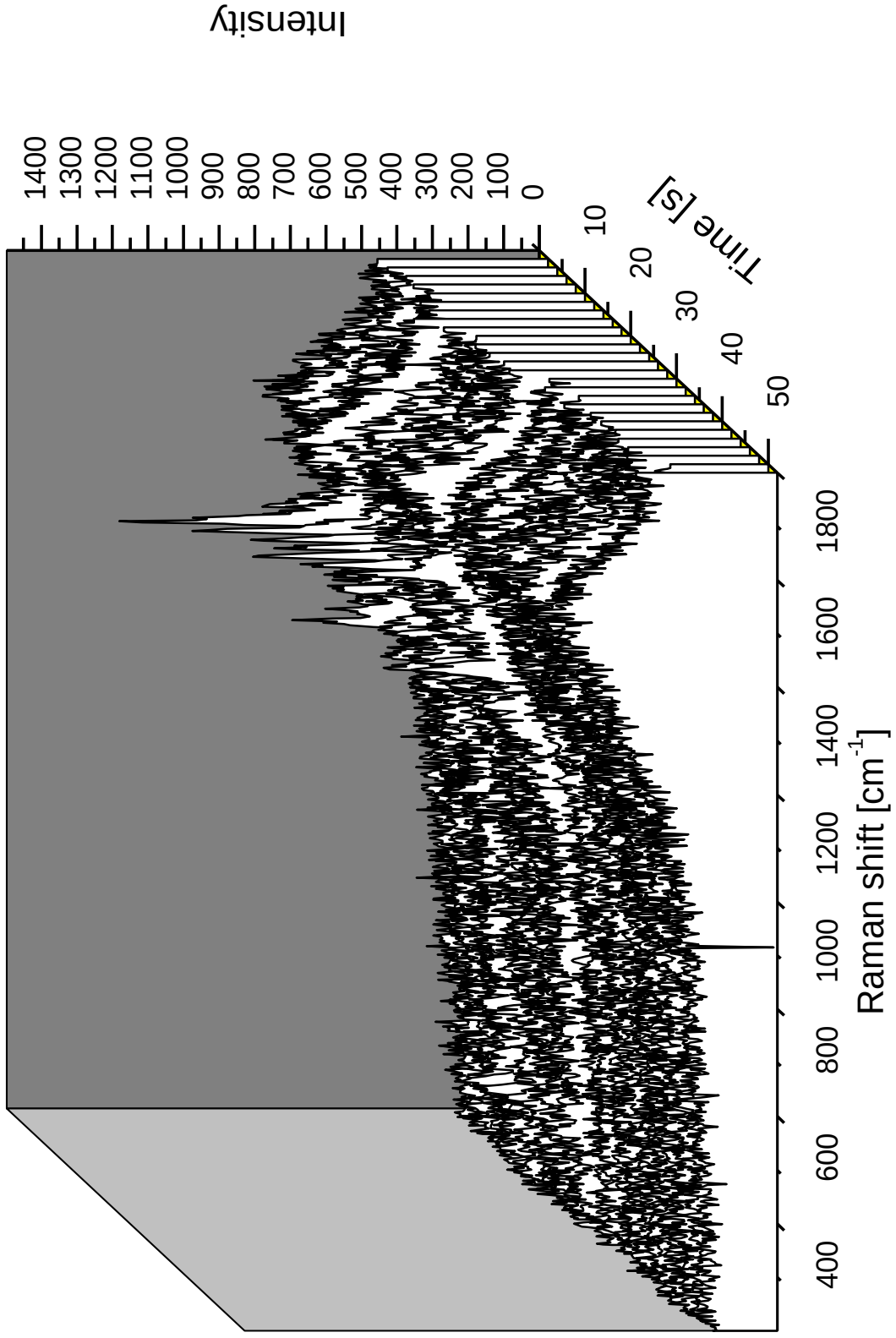

Figure 4.16: Time-evolution of SERS signal obtained from the dimer shown in Figure 4.15

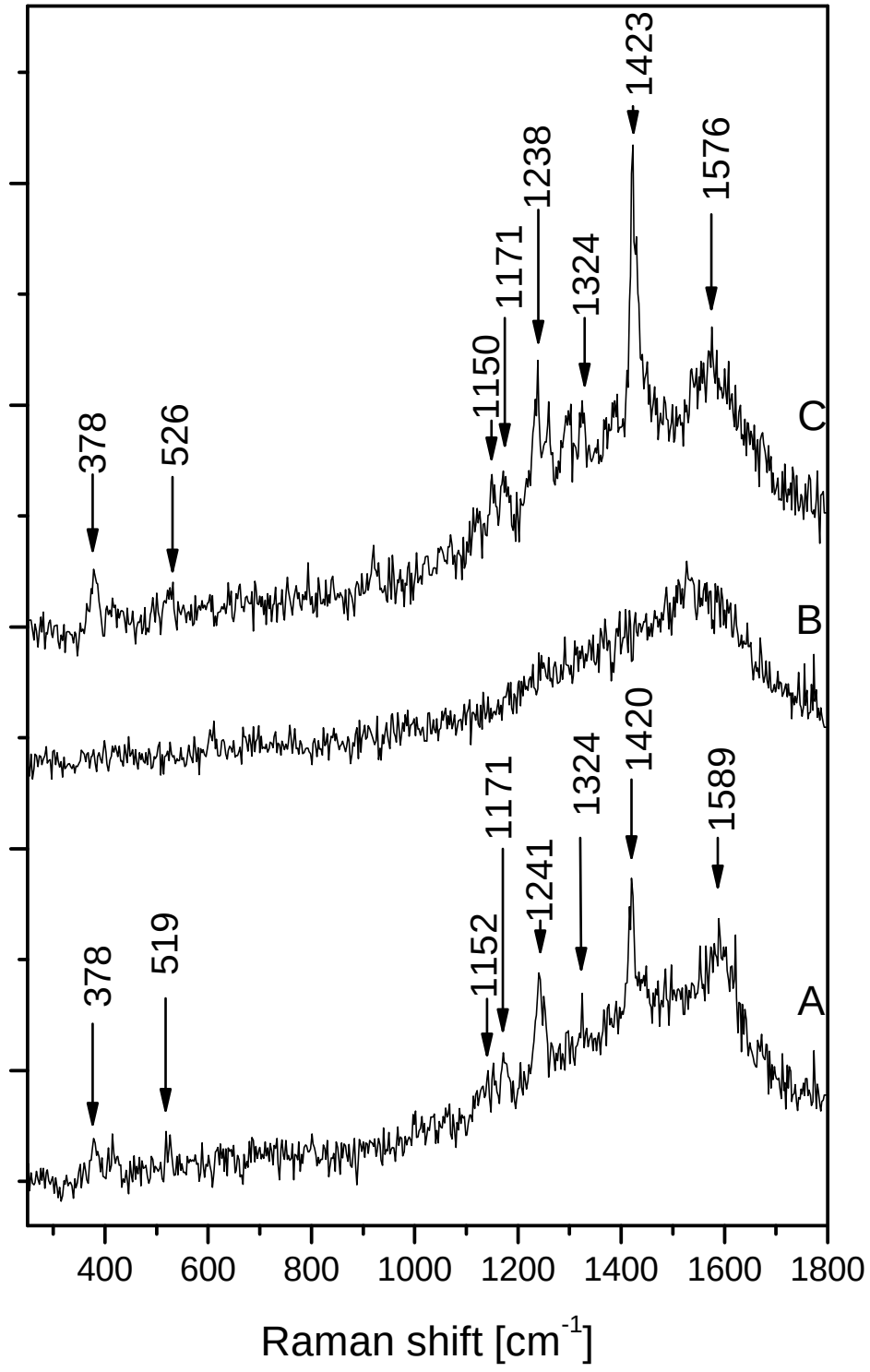

Figure 4.17: The "signal in" spectra, namely the 8th (A) and the 14th (C) spectrum, and the signal "off" spectrum (B) within the SERS spectral set depicted in Figure 4.16

It is generally agreed that blinking reflects the dynamics of a single, or very few molecules. A simple hypothesis which appears to be pertinent to the signal fluctuations pattern observed in our particular case is thus proposed. The "in" signals are assigned to Ag NP dimer bridged by DAAB (Figure 4.18 A), while the "off" signal periods are attributed to a temporally limited loss of the DAAB signal caused by breaking of one of the Ag-NH_2 bonds which leads to disconnection of the DAAB bridge (Figure 4.18B). The disconnected NPs are supposed to remain tethered to the grid by APTMS chains, however, the distance between them increases. Since the wavelength for resonance excitation of strong optical field in a Ag nanoparticle dimer is strongly dependent on interparticle distance [26], it is probable that the 514.5 nm excitation wavelength suitable for excitation of a strong optical field in the bridged dimer (Figure 4.18 A) is no longer "in resonance" with the disconnected (and hence elongated) dimer which is the reason why no SERS signal of DAAB is observed. After remaking of this Ag-NH_2 bond, the bridging of two Ag nanoparticles by DAAB is resumed, and the SERS signal of DAAB is recovered.

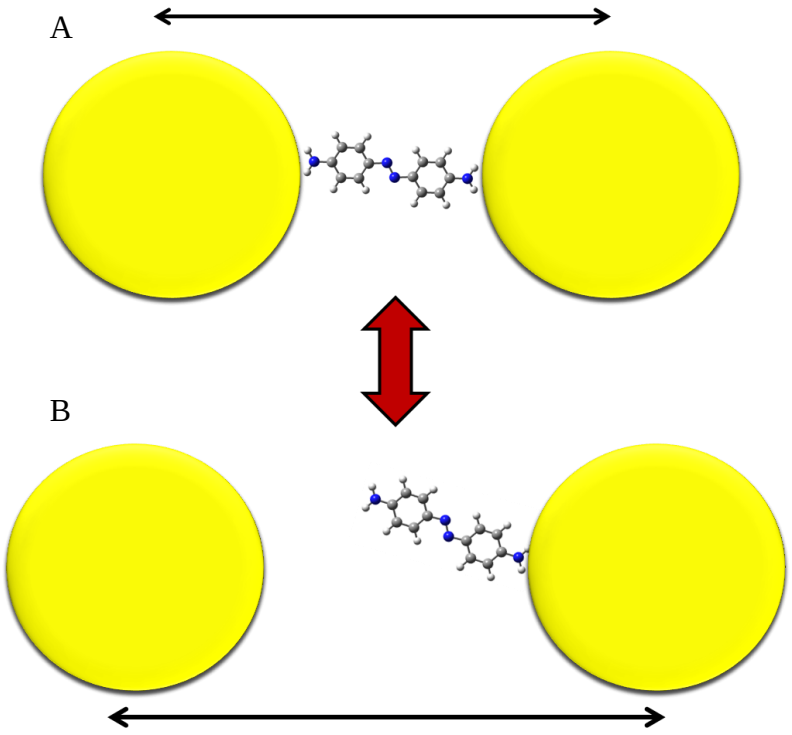

Figure 4.18: Ag NP dimer

A) bridged by DAAB (signal "in")
B) disconection of the DAAB bridge (signal "off")

4.5. Factors affecting stability of adsorbates and linkers in strong optical fields

SERS and SERRS signal from a single compact aggregate incorporating PPIX molecules shows rapid alternations of the porphyrin and of the graphitic C signal. The porphyrin signal is a superposition of the free-base and of the Ag metallated porphyrin spectral features, and indicates the presence of both H_2PPIX and Ag PPIX molecules in the aggregate. In a previously published study [68] dealing with the thermal stability of another free-base porphyrin, 5,10,15,20-tetrakis(N-methylpyridinium-4-yl) porphine (TMPyP), in strong optical fields, it has been demonstrated that Ag TMPyP surface species formed by Ag metallation of H_2TMPyP on Ag nanoparticle surface is prone to decomposition to graphitic C, in contrast to the native H_2TMPyP. On the basis of this result, we propose tentatively that the graphitic C signal probably originates from decomposition of Ag PPIX molecules formed by H_2PPIX metallation.

SERRS spectra obtained from several dimers and small aggregates bridged by TAPP molecules are markedly different for aggregates assembled from the citrate-capped Ag NPs in aqueous ambient and from the penthylamine-capped Ag NPs in organic ambient. In particular, in the former case, fluctuating SERRS signal of TAAP molecules has been detected. The porphyrin molecules are preserved in the free-base form, and they are most probably are attached to Ag NP surface by one or two amine groups of the peripheral aminophenyl substituents, adopting a perpendicular orientation to Ag NP surface and acting as molecular linkers of Ag NPs. On the other hand, in the latter case, only very strong, fluctuating signal of graphitic C is observed. A possible explanation stems from the difference in the quality of the pre-orienting matrices formed by the capping molecules: citrate and/or penthylamine. Citrate, bidentatelly coordinated by two carboxylate groups to Ag NP surface, forms a very efficient pre-orienting matrix (as demonstrated also in [56]) ensuring adsorption of the porphyrin in the perpendicular orientation with respect to Ag NP surface ("standing up"). By contrast, the aliphatic chains of pentylamine molecules are most probably twisted and randomly oriented, thus allowing for re-orientation of porphyrin molecules into a paralel orientation with Ag NPs surface, their metallation and decomposition to graphitic C. Finally, it should be emphasized

that citrate has been shown to act as an efficient pre-orienting matrix for other linkers, namely DATP and DAAB.

Time-evolution of SERS signal obtained from the DAAB-bridged Ag NP dimer shows alternation of "signal in" and "signal off" periods. The SERS signal is constituted by SERS spectral bands of DAAB, and its evolution indicates that DAAB molecules do not decompose in strong optical fields. On the other hand, time-evolution of SERS signal from DATP-bridged small aggregate shows alternations of DATP and of the graphitic C signal. Considering the differences between the time-evolutions of SERS signal from the DAAB-bridged Ag NP dimer and from DATP-bridged Ag NP aggregate, we have to take into account that, in the former case, the SERS signal originates from a single hot spot between the two Ag NPs, while, in the latter case, the SERS signal represents a superposition of signals obtained from several hot spots. Nevertheless, observation of strong graphitic carbon signal indicates decomposition of DATP molecule(s) in at least one of the several hot spots. Both the molecular structure of DAAB and DATP linkers and the actual structure of Ag NP assembly (dimer or aggregate) can contribute to their different propensity towards decomposition. In the case of the DAAB-bridged dimer, a trans-cis izomerization of DAAB could possibly play a positive role in the Ag NP-DAAB bond breaking which leads to increased distancing of the NPs in the dimer and to a temporal "switch off" of the strong field which, in turn, can be responsible for DAAB molecule(s) preservation. By contrast, none of these possibilities applies to the case of DATP-bridged small Ag NP aggregate, since (i) the DATP linker molecule is rigid and (ii) even in the case of a temporal single Ag NP-DATP bond breaking, the remaining hot spots in the aggregate will remain preserved.

5. CONCLUSIONS

I. Methodologies of assembling compact aggregates, dimers and small aggregates of Ag NPs and of their anchoring to supporting surfaces have been developed. The supporting surfaces were either glass slides or SiO_x – coated Cu or Au grids for TEM, both chemically functionalized by APTMS. Compact aggregates of Ag NPs were assembled and PPIX molecules were incorporated into them in a hydrosol system and subsequently, they were chemically attached to NH_2 terminal groups of APTMS – functionalized Cu grids for TEM. The basic methodology for preparation of a sample from which SERRS spectra of an adsorbate (PPIX) could be obtained by Raman microspectroscopy from a single compact aggregate after visualization of the sample by TEM has thus been developed. A similar strategy has been elaborated for attachment of Ag NP dimers and small aggregates assembled by a TAPP linker in a hydrosol system to chemically functionalized, SiO_2 coated TEM grids. Ag NP dimers and small aggregates bridged by TAPP and assembled and in a pentylamine – stabilized Ag NP organosol were attached to APTMS – functionalized glass slides and SEM has been employed for their visualization Finally, the strategy for obtaining SERS signal of molecular linker from a particular, selected single dimer and/or small aggregate of Ag NPs visualized by TEM has been developed by further substantial refinement of the procedures elaborated and tested in the previous studies. The key points of this refinement were:

1) assembling of dimers and small aggregates by a three – step procedure involving
   i) attachment of isolated Ag NPs to the NH_2 groups of APTMS functionalized Au finder TEM grid
   ii) attachment of molecular linker (with two functional NH_2 groups in para position) to Ag NPs by one terminal NH_2 group
   iii) attachment of Ag NPs to the second, free terminal NH_2 group of the linker
2) Control over the perpendicular orientation of the bifunctional linker and its attachment by one terminal group to Ag NP surface has been

accomplished by functionalization of Ag NPs by adsorbed citrate (in the course of the Ag NP hydrosol preparation by reduction $AgNO_3$ by $Na_3C_6H_5O_7 \cdot 2H_2O$) which acted as the adsorbate pre – orienting matrix. The evidence for the importance of the pre – orienting matrix for a successful function of a linker has been provided already in the study of TAPP bridged dimers and aggregates assembled in the sol systems, in which adsorbed citrate manifested itself to be a substantially better pre – orienting matrix than pentylamine.

3) Control over the resulting dimer (small aggregate) separation from other dimers and small aggregates by a sufficiently wide spacing of Ag NPs in the first step (i) of the three – step procedure, achieved by dilution and by very short time of exposure of the derivatized surface to Ag organosol.

4) An unequivocal correspondence between the TEM – imaged dimer (and/or small aggregate) and the SERS signal obtained from it has been accomplished by employment of SiO_2 coated Au finder grids for TEM. An accurate establishment positional coordinates of the nanoobject (dimer or aggregate) with respect to the marks (letter or number) on the finder grid enabled to find the same nanoobject both in TEM (for its visualisation) and in the optical microscope which focused exciting laser beam onto it and enabled to obtain SERS signal of the molecular linker from it.

II. The single molecularly – bridged Ag NP dimer represents an optimal system in which the single molecule dynamics can be followed via time – evolution of the SERS signal of the molecule linker obtained from it. The advantage of a dimer over a small aggregate is, that the SERS signal of the dimer originates from a single hot spot, while, in the case of a small aggregate, the SERS signal is a superposition of molecular dynamic events occurring in several hot spots. Furthermore, the molecularly – bridged Ag NP dimer is an exact experimental realization of a model system of Ag NP dimer with a single molecule located in a single hot spot at the interconnect between the two NPs. According to the theoretical model calculations, a dimer of Ag NPs with the molecule located between them is also the most efficient light amplification system providing largest enhancement of SERS by the EM mechanism. Importantly, evaluation of the temporal fluctuation of SERS

signal of DAAB linker obtained from the DAAB – bridged Ag NP dimer shows, that the DAAB linker “survives” in such extreme by strong optical field without decomposition.

6. REFERENCES

[1] R.S. Raman, K.S. Krishnan, *Nature* 121 (1921) 501

[2] A. Smekal, *Naturwissenschaften* 11 (1923) 873

[3] G. Landsberg, L. Mandelstam, *Naturwissenschaften* 16 (1928) 557

[4] M. Fleischmann, P.J. Hendra, A.J. McQuillan, *Chem. Phys. Lett.* 26 (1974) 163

[5] D.L. Jeanmaire, R.P.V. van Duyne, *J. Electroanal. Chem*. 84 (1977) 1

[6] M.G. Albrecht, J. A. Creighton, *J. Am. Chem. Soc.* 99 (1977) 5215

[7] M. Moskovits, *J. Chem.Phys*. 69 (1978) 4159

[8] M. Moskovits, *Rev. Mod. Phys.* 57 (1985) 783

[9] J.A. Creighton, *Spectroscopy of Surfaces*, R.J.H. Clark, R.E. Hester (Eds.), John Wiley & Sons, New York, 1988

[10] A. Otto, in: M. Cardona, G. Guntherodt (Eds.), *Light in Solids IV*, Springer-Verlag, Berlin, 1984

[11] T.M. Cotton, *Spectroscopy of Surfaces*, R.J.H. Clark, R.E. Hester (Eds.), John Wiley & Sons, New York, 1988

[12] D.A. Weitz, S. Garoff, J.I. Gersten, A. Nitzan, *J. Chem.Phys* 78 (1983) 5324

[13] A. Campion, P. Kambhampati, *Chem. Soc. Rev.* 27 (1998) 241

[14] K. Kneipp, H. Kneipp, I. Itzkan, R.R. Dasari, M.S. Feld, *Chem. Rev.* 99 (1999) 2957

[15] K. Kneipp, H. Kneipp, I. Itzkan, R.R. Dasari, M.S. Feld, *J. Phys. Condens. Matter* 14 (2002) R597

[16] M. Moskovits, L.L. Tay, J. Yang, T. Haslett, *Topics in Applied Physics* 82 (2002) 215

[17] M. Moskovits, *J. Raman Spectr*. 36 (2005) 485

[18] G.A. Baker, D.S. Moore, *Anal. Bioanal. Chem*. 382 (2005) 1751

[19] C. Y. Chen, I. Davoli, G. Ritchie, E. Burnstein, *Surf. Sci.* 101 (1980) 363

[20] A.M. Ahern, R.L. Garrell, *Anal. Chem*. 59 (1987) 2813

[21] B. Vlčková, P.Matějka, J. Šimonová, P. Pančoška, K.Čermáková, V. Bamruk, *J. Phys. Chem*. 97 (1993) 9719

[22] P. C. Lee, D. Meisel, *J. Phys. Chem*. 86 (1982) 3391

[23] C.F. Bohren, D.F. Hufman, *Absorption and Scattering of Light by Small Particles*, Wiley&Sons, New York, 1983

[24] M.I. Stockman, V.M. Shalaev, M. Moskovits, R. Botet, T. F. George, *Phys.Rev. B* 46 (1992) 2821

[25] P. Zhang, T.L. Haslett, C. Douketis, M. Moskovits, *Phys.Rev. B* 57 (1998) 15513

[26] H. Xu, J. Aizpurua, M. Kall, P. Apell, *Phys. Rev. E* 62 (2000) 4318

[27] P. Johansson, H. Xu, M. Käll, *Phys. Rev. B* 72 (2005) 035427

[28] M. Käll, H. Xu, P. Johansson, *J.Raman Spectr*. 36 (2005) 510

[29] H. Xu, E.J. Bjerneld, M. Kall, L. Borjenson, *Phys. Rev.Lett*. 83 (1999) 4357

[30] A.M. Michaels, J. Jiang, L. Brus, *J.Phys. Chem. B* 104 (2000) 11965

[31] M. Procházka, B. Vlčková, J. Štěpánek, P.Y. Turpin, *Langmuir* 21 (2005) 2956

[32] M. Sládková, B. Vlčková, P. Mojzeš, M. Šlouf, C. Naudin, G. Le Bourdon, *Faraday Discuss.* 132 (2006) 121

[33] I. Srnová, B. Vlčková, T.L. Snoeck, D.J. Stufkens, P. Matějka, *Inorg.Chem.* 39 (2000) 3551

[34] K. Kneipp, Y. Wang, H. Kneipp, L.T. Perelman, I. Itzkan, R.R. Dasari, M.S. Feld, *Phys. Rev. Lett*. 78 (1997) 1667

[35] S. Nie, S.R. Emory, *Science* 275 (1997) 1102

[36] K.A. Bosnick, J. Jiang, L. Brus, *J. Phys. Chem. B* 106 (2002) 8096

[37] W.E. Doering, S. Nie, *J. Phys. Chem. B* 106 (2002) 311

[38] P.C. Andersen, M.L. Jacobson, K.L. Rowlen, *J. Phys. Chem. B* 108 (2004) 2148

[39] A.R. Bizarri, S. Cannistraro, *Phys. Rev. Lett.* 94 (2005) 068303

[40] G. Schmid, *Nanoparticles: From Theory to Application*, Wiley-VCH, Weinheim, 2004

[41] S.A. Maier, *Plasmonics: Fundmentals and Applications*, Springer, New York, 2007

[42] M. Inoue, K. Ohtaka: *J. Phys. Soc*. 52 (1983) 3853

[43] L. Gunnarsson, T. Rindzevicius, J. Prikulis, B. Kasemo, M. Kall, S. L. Zou, G. C. Schatz, *J. Phys. Chem. B* 109 (2005) 1079

[44] E. Y. Poliakov, V. M. Shalaev, V. A. Markel, R. Botet, *Opt. Lett*. 21 (1996) 1628

[45] Y. Yamaguchi, M. K. Weldon, M. D. Morris, *Appl. Spectrosc*. 53 (1999) 127

[46] A. Otto, *J. Raman Spectrosc*. 36 (2005) 497

[47] M. Futamata, *Faraday Discuss.,* 132 (2006) 45

[48] D. J. Anderson, M. Moskovits, *J. Phys. Chem. B* 110 (2006) 13722

[49] S. J. Lee, A. R. Morrill, M. Moskovits, *J. Am. Chem. Soc*. 128 (2006) 2200

[50] M. A. Bryant, J. E. Pemberton, *J. Am. Chem. Soc*. 113 (1991) 8284

[51] M. Babjuk, R. Petřík, M. Jirsa, *Fluorescenčni diagnostika nádorů močového měchýře*, Triton, Praha 2001

[52] M. Sládková, *Master Thesis*, Charles University in Prague, 2004

[53] I. Inamura, K. Uchida, Bull., *Chem. Soc. Jpn*., 64 (1991) 2005

[54] L. M. Scolaro, M. Castriciano, A. Romeo, S. Patane, E. Cefali, and M. Allegrini, *J. Phys. Chem*., 106 (2002) 2453

[55] B. Vlčková, P. Šmejkal, M. Michl, M. Procházka, P. Mojzeš, F. Lednický, and J. Pfleger, *J. Inorg. Biochem*., 79 (2000) 295

[56] K. Šišková, B. Vlčková, P.-Y. Turpin, A. Thorel, A. Grosjean ,*Vib. Spec.*, 48 (2008) 44

[57] M.S. Hybertsen, L. Venkataraman, J.E. Klare, A.C. Whalley, M.L. Steigerwald, C. Nuckolls, *J. Phys. Condens. Matter* 20 (2008) 374115

[58] G. Zimmerman, L.-Y. Chow, U. J. Paik, *J. Am. Chem. Soc*., 80 (1958) 3528

[59] T. Schultz, J. Quenneville, B. Levine, A. Toniolo, T. J. Martinez, S. Lochbrunner, M. Schmitt, J. P. Shaffer, Z. Zgierski, A. Stolow, *J. Am. Chem. Soc.* 125 (2003) 8098

[60] S. D. Evans, S. R. Johnson, H. Ringsdorf, L. M. Williams, H. Wolf, *Langmuir*, 14 (1998) 6436

[61] M. Irie, Y. Hirano, S. Hashimoto, K. Hayashi, *Macromolecules*, 14 (1981), 262

[62]. M. Kamenjicki, I. K. Lednev, S. A. Asher, J. Phys. Chem. B, 2004, 108, 12637

[63] A. Archut, F. Vogtle, L. De Cola, G. C. Azzellini, V. Balzani, P. S. Ramanujam and R. H. Berg, *Chem.–Eur. J*., 4 (1998) 699

[64] D. S. Sidhaye, S. Kashyap, M. Sastry, S. Hotha, B. L. V. Prasad, *Langmuir* 21 (2005) 7979

[65] P. Šmejkal, K. Šišková, B. Vlčková, J. Pfleger, I. Šloufová, M. Šlouf, P. Mojzeš, *Spectrochim. Acta Part A* 59 (2003) 2321

[66] J. S. Suh, M. Moskovits, J. Shakhesemampour, *J. Phys. Chem*. 97 (1993) 1678

[67] E. J. Bjerneld, F. Svedberg, P. Johansson, M. Kall, *J. Phys. Chem. A* 108 (2004) 4187

[68] K. Šišková, B. Vlčková, P.-Y. Turpin, A. Thorel, M. Procházka, *J. Phys. Chem. C* 115 (2011) 5404

7. LIST OF ABBREVIATIONS AND SYMBOLS

APTMS	3-aminopropyltrimethoxysilane
BPY	2,2'-bipyridine
DAAB	4,4´-diaminoazobenzene
DAPT	4,4´- diaminoterphenyl
EM	electromagnetic
NP	nanoparticle
PPIX	protoporphyrin IX
SEM	Scanning electron microscopy
SERRS	Surface enhanced resonance Raman scattering
SERS	Surface enhanced Raman scattering
SM-SERS	Single-molecule surface-enhanced Raman spectroscopy
TAPP	5,10,15,20-tetrakis(4-aminophenyl)porphine
TEM	Transmision electron microscopy
TMPyP	5,10,15,20-tetrakis(N-methylpyridinium-4-yl) porphine

8. PUBLICATIONS

8.1. List of articles

Article I

M. Sládková, B. Vlčková, I. Pavel, K. Šišková, M. Šlouf

Surface-Enhanced Raman Scattering from a Single Molecularly-Bridged Silver Nanoparticle Aggregate

J.Mol. Structure, 924–926 (2009) 567

Article II

B. Vlčková, M. Moskovits, I. Pavel, K. Šišková, **M. Sládková**, M. Šlouf,:

Single-molecule surface-enhanced Raman spectroscopy from a molecularly-bridged silver nanoparticle dimer

Chem. Phys. Lett., 455 (2008) 131

Article III

B. Vlčková, I. Pavel, **M. Sládková**, K. Šišková, M. Šlouf

Single molecule SERS: Perspectives of analytical applications

J.Mol. Structure, 834–836 (2007) 42

Article IV

M. Sládková, B. Vlčková, P. Mojzeš, M. Šlouf, C. Naudin and G. Le Bourdond

Probing strong optical fields in compact aggregates of silver nanoparticles by SERRS of protoporphyrin IX

Faraday Discuss., 132 (2006) 121–134

8.2. List of conference contributions

1. **M. Sládková**, B. Vlčková, K. Šišková, I Pavel, M. Šlouf: "Surface-enhanced Raman scattering from a single molecularly bridged silver nanoparticle aggregate", *XXIX European Congress on Molecular Spectroscopy,* Rijeka, Croatia, 31.8 – 5.9. 2008, Book of Abstracts, p. 340

2. **M. Sládková**, B. Vlčková, I. Pavel, K Šišková, M. Moskovits, M. Šlouf: "Vývoj a optimalizace systému pro SERRS spektrální detekci na úrovni jedné molekuly", *13. spektroskopická konference*, Lednice, Česká Republika, 21-18.06.2007, Proceedings, p. 36

3. P. Šmejkal, B. Vlčková, I. Pavel, M. Moskovits, **M. Sládková**, K. Šišková, M. Šlouf: "Nanocomposites with strong optical resonances: Silver nanoparticles-organic molecules systems" *2nd Multifunctional Nanocomposites and Nanomaterials Conference,* Sharm El Sheikh, Egypt, 11–13.1. 2008, Proceedings of the ASME, p. 193

4. M. Dvořáková, **M. Sládková**, B. Vlčková: "Využití elektronové absorpční spektroskopie ke studiu agregace kationtového porfyritu ve vodném prostředí", *13. spektroskopická konference*, Lednice, Česká Republika, 21-18.06.2007, Proceeding, p. 92

5. **M. Sládková**, B. Vlčková, P. Šmejkal, P. Mojzeš, M. Šlouf: "SERRS spectral study of protoporphyrin IX in system with native Ag hydrosol modified by chlorides in acidic and neutral ambient", *12th European Conference on the Spectroscopy of Biological Molecules,* Paris, France, 1.-6.9. 2007, Book of Abstracts, p. 301

6. B. Vlčková, M. Moskovits, I. Pavel, **M. Sládková**, K. Šišková, M. Šlouf: "Single molekule SERS: perspectives of analytical applications" *28th European congress on molecular spectroscopy,* Istanbul, Turkey, 3. – 8. 9. 2006; Book of Abstracts,.p. 10

7. **M. Sládková**, B. Vlčková, M. Moskovits, I. Pavel: "Temporally fluctuating SERS signals from porphyrin-bridged silver nanoparticle dimers and small aggregates", *2nd International Conference on Bioengineering and Nanotechnology*, Santa Barbara, California, 5.–7.9. 2006, Abstracts SBE's, p. 30

8. **M. Sládková**, K. Šišková, T. Tombler, B. Vlčková, M. Moskovits: "Possibilities to control spacing of Ag nanoparticle dimers and aggregates attached to chemically functionalized supporting surfaces: AFM study" *International Conference NANO'06*, Brno, Czech Republic, November 13.–15. 2006, Abstract Booklet, p. 71 – ISBN: 80-214-3308-6.

9. P. Šmejkal, B. Vlčková, M. Moskovits, I. Pavel, **M. Sládková**, E. Pavlova: "SERS spectral probing of dimers of silver nanoparticles molecularly bridged by various molecules" *International Conference NANO'06*, Brno, Czech Republic, 13.–15.11. 2006, Abstract Booklet p.35 (ISBN: 80-214-3308-6)

10. B. Vlčková, **M. Sládková**, K. Šišková, P. Mojzeš, M. Šlouf: "Surface-enhanced Raman spectral probing of porphyrins: Towards single molecule detection" *ESF Research Conference Biological Surfaces and Interfaces*, San Feliu de Guixols, Spain, 18–23 6. 2005, Book of Abstracts p.172.

11. B. Vlčková, M. Moskovits, I. Pavel, **M. Sládková**, K. Šišková, P. Šmejkal, M. Šlouf, J. Hromádková: "Probing strong optical fields in molecularly bridged silver nanoparticle dimers and small aggregates by surface-enhanced Raman scattering" *Twelfth Annual International Conference on Composites- Nano Engineering (ICCE-12)*, August 1–6.8. 2005, Tenerife, Spain. Proceedings Session Nano 6, CD-file Vlckova.pdf

12. B. Vlčková, M. Moskovits, **M. Sládková**, I. Pavel, M. Šlouf, K. Šišková: "Comparing temporally fluctuating SERS signals from samples of porphyrin-bridged silver nanoparticle dimers and small aggregates prepared in the aqueous and in the organic ambient" *International Conference NANO'05*, Brno, Czech Republic, 8–10.11. 2005; Abstract Booklet p.90 (ISBN: 80-214-3044-3)

13. **M. Sládková**, B. Vlčková, P. Mojzeš, M. Šlouf, G. LeBourdon, C. Naudin: "Probing strong optical fields in compact aggregates of silver nanoparticles by SERRS of protoporphyrin IX"; *International Conference NANO´04*, Brno, Czech Republic, 13–15.11. 2004, Brno, Proceedings p. 224 (ISBN: 80-214-2793-0)

Article I

M. Sládková, B. Vlčková, I. Pavel, K. Šišková, M. Šlouf

Surface-Enhanced Raman Scattering from a Single Molecularly-Bridged Silver Nanoparticle Aggregate

J.Mol. Structure, 924–926 (2009) 567

Journal of Molecular Structure 924–926 (2009) 567–570

Contents lists available at ScienceDirect

Journal of Molecular Structure

journal homepage: www.elsevier.com/locate/molstruc

Surface-enhanced Raman scattering from a single molecularly bridged silver nanoparticle aggregate

M. Sládková [a], B. Vlčková [a,*], I. Pavel [b], K. Šišková [c], M. Šlouf [c]

[a] Department of Physical and Macromolecular Chemistry, Charles University, Hlavova 2030, 12840 Prague 2, Czech Republic
[b] Department of Chemistry, Wright State University, 3640 Colonel Glenn Hwy., Dayton, OH 45435, USA
[c] Institute of Macromolecular Chemistry ASCR, Heyrovsky Sq.2, 16206 Prague 6, Czech Republic

ARTICLE INFO

Article history:
Received 3 October 2008
Received in revised form 29 October 2008
Accepted 3 November 2008
Available online 9 November 2008

Keywords:
Single molecule SERS
4,4″-Diaminoterphenyl
Molecularly bridged Ag nanoparticle aggregates

ABSTRACT

Temporally fluctuating SERS signals originating from a single specific small aggregate of 4,4″-diaminoterphenyl (DATP)-bridged Ag nanoparticles are reported. Unequivocal correspondence between the aggregate and the SERS signal obtained from it was achieved by determination of the aggregate position with respect to markers on chemically functionalized, SiO_x coated finder grids and its TEM imaging. Since the temporally fluctuating (blinking) SERS signal originates from several hot spots within the aggregate, it cannot be interpreted in terms of a single molecular dynamic event. However, the time-evolution of SERS spectra indicates that the linker decomposes into the graphitic carbon in at least one of these hot spots.

1. Introduction

Optical responses of Ag nanoparticles and their assemblies are the subject of permanent interest stimulated further by their applications as sensors and light amplifiers. In Ag nanoparticle assemblies containing electromagnetic "hot spots", amplification of optical processes undergone by molecules, such as surface enhanced Raman scattering (SERS), is so efficient that single molecule sensitivity can be achieved [1–4]. "Hot spots" are strong, nanoscale-localized optical fields resonantly excited in Ag nanoparticle assemblies by external laser excitation.

The SERS signal of molecules located in hot spots frequently shows temporal fluctuations (blinking). The precise cause of blinking is not yet fully understood although several possible reasons have been proposed and widely discussed [2–8]. The common point of all these tentative explanations is that blinking reflects the dynamics of a single, or a very few molecules.

Theoretical calculations [9,10] have predicted that the largest enhancement of Raman scattering are achieved for molecules located in interstices between two Ag nanoparticles, i.e., in dimers or small aggregates of Ag nanoparticles. One of the strategies of localization of molecules directly into these "hot spots" is to make them to bridge two or several Ag nanoparticles.

Recently, we have successfully demonstrated this strategy by preparation of 4,4′-diaminoazobenzene (DAAB)-bridged Ag nanoparticle dimers and small aggregates. Evidence for formation of such dimers and small aggregates was obtained by TEM image analysis and temporally fluctuating SERS signals originating from a selected single DAAB-bridged dimer were measured and analysed [11]. In this contribution, we report fluctuating SERS signals collected from a single small aggregate of 4,4″-diaminoterphenyl-bridged Ag nanoparticles.

2. Experimental

The small, molecularly bridged Ag nanoparticle aggregates were assembled from citrate-capped Ag nanoparticles (prepared according to the Lee–Meisel procedure [12]) and 4,4″-diaminoterphenyl (DATP) molecules possessing two terminal amine groups in *para*-position. The capping citrate anions were expected to serve as an orienting matrix which would prevent a flat-on adsorption of the aromatic molecules thereby promoting their attachment to Ag nanoparticles via the terminal amine groups which, in turn, will allow them to assume the role of the nanoparticle linkers. To enable Raman spectral probing as well as TEM imaging of the same sample, the dimers and small aggregates were assembled on chemically derivatized SiO_x/formvar coated copper finder grids for TEM microscopy (pre-treated by vapor-depositing a thin carbon layer on their reverse sides and derivatized with 3-aminopropyl-trimethoxysilane by condensing the reagent vapor onto the grids and removing the excess reagent in vacuo), The three-step assembling procedure involved (1) tethering the Ag nanoparticles to the grids with 3-aminopropyltrimethoxysilane during floating of the

* Corresponding author.
E-mail address: vlc@natur.cuni.cz (B. Vlčková).

0022-2860/$ - see front matter © 2008 Elsevier B.V. All rights reserved.
doi:10.1016/j.molstruc.2008.11.006

grids on Ag colloid surface for 1.5 h, (2) attaching the linker molecules to the tethered Ag nanoparticles (by one amine group) during the immersion of the grids into a 1×10^{-7} M solution of DATP in ethanol for 4 h., and, finally, (3) linking of additional nanoparticles to those already tethered to the grid surfaces with help of the free amine groups of the linker, which was accomplished during exposure of the grids to Ag nanoparticle hydrosol for a second time (for 2 h). The procedure is schematically depicted in Fig. 1. The appropriately wide spacing of aggregates (allowing for a single aggregate selection) was accomplished by the optimization of the preparation steps duration.

TEM images were obtained with a JEOL JEM 200 CV transmission electron microscope.

SERS spectra were collected from the selected small Ag nanoparticle aggregates through a confocal optical microscope (with a 100× magnification objective) using a micro-Raman Labram spectrometer (Horiba Jobin Yvon). Spectra were excited by 514.5 nm Ar^+ laser line (Spectra Physics, model 164) using 100 μW power at the sample and a laser spot size of ca 1.5 μm. Time-evolution of the spectra was followed in 2 s intervals. For the sake of a relevant comparison, the conditions of the SERS spectra acquisition (namely the overall micro-Raman setup, the microscope objective, the excitation wavelength, the laser power at the sample, the laser spot size and the spectral acquisition time) were kept the same as in Ref. [11], in which fluctuating SERS signals from a DAAB-bridged dimer were reported.

3. Results and discussion

A typical TEM image of DATP-bridged Ag nanoparticles and its statistical evaluation are presented in Fig. 2. The statistics shows that dimers and trimers are the most abundant types of Ag nanoparticle aggregates, while larger aggregates are rarely encountered.

Our intension in carrying out the SERS spectral measurements from a selected single dimer and/or aggregate was to obtain an unequivocal correspondence between the morphology of the aggregate and the SERS signal obtained from it. This was accomplished by determination of the aggregate position with help of

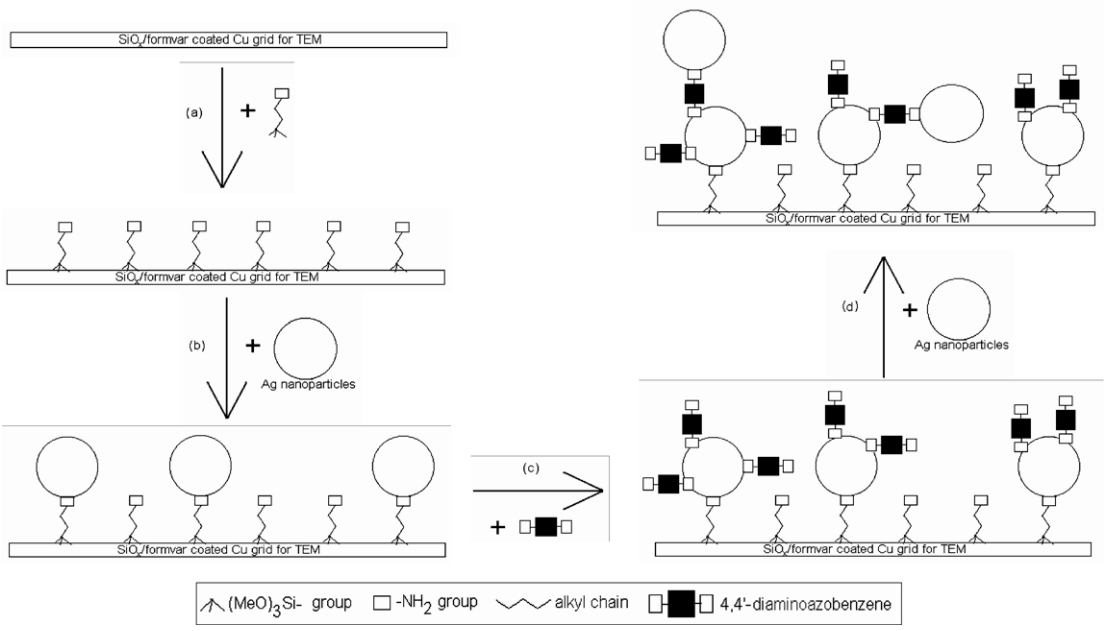

Fig. 1. Schematic depiction of molecularly bridged Ag nanoparticle dimers and small aggregates assembling.

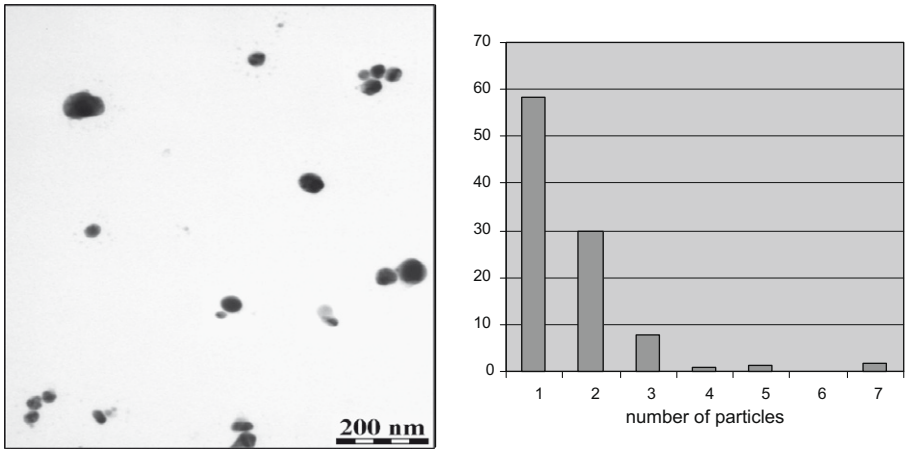

Fig. 2. TEM image and size-distribution of DATP-bridged Ag nanoparticle aggregates (expressed in terms of number of particle per aggregate).

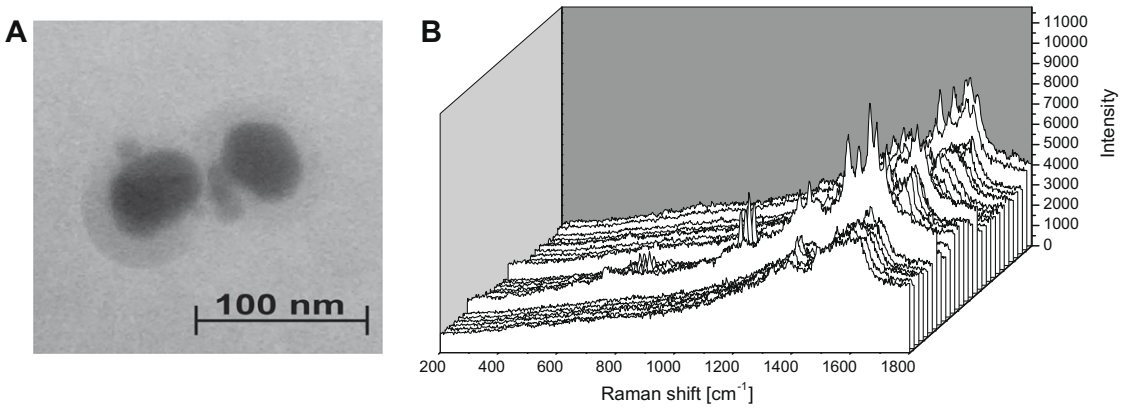

Fig. 3. (A) TEM image and (B) time-evolution of SERS signal of a selected DATP-bridged Ag nanoparticle aggregate.

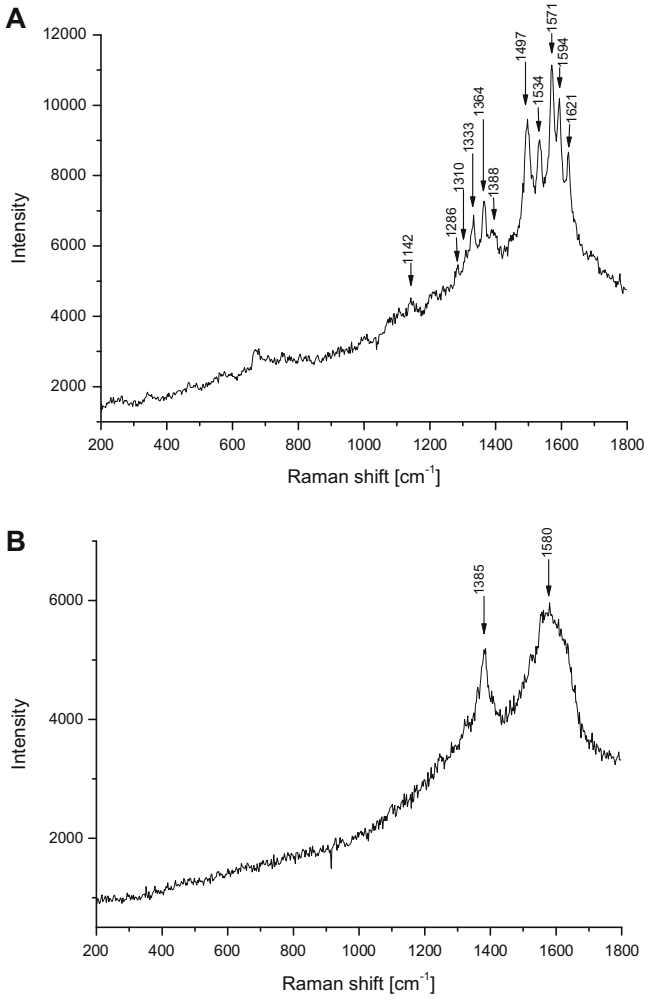

Fig. 4. SERS signal of (A) DATP and (B) graphitic carbon from the SERS spectral set presented in Fig. 3B.

the markers on a finder grid. This exact aggregate position was located on both the optical image of the sample prior to the SERS measurement, and on the TEM image, which revealed the aggregate morphology in detail.

TEM image of a selected small aggregate of DATP-bridged Ag nanoparticles consisting of a trimer of small particles located between two larger particles is shown in Fig. 3A. Time-evolution of SERS spectra measured from this particular aggregate (Fig. 3B) shows that the SERS signal fluctuates in time. In particular, the signal of DATP (Fig. 4A) alternates with that of graphitic carbon, represented by two distinct, rather broad bands (Fig. 4B). A possible scenario which can explain the observed blinking pattern is decomposition of the bridging DATP molecule in at least one of the several hot spots within the aggregate into graphitic carbon. However, since the observed signal likely originates from more than one hot spot, the observed time-evolution cannot be interpreted in terms of a single molecular dynamics event. Nevertheless, the observed results indicate that DATP molecules decompose in strong optical fields into graphitic carbon, in contrast to DAAB molecules previously investigated in Ag nanoparticle dimers [11] under the same experimental conditions.

Furthermore, although the blinking pattern of alternating DATP and graphitic carbon signals observed under the conditions of our experiment cannot be unambiguously ascribed to a photochemical process (as opposed to a thermal decomposition), it should be noted that photodecomposition of substituted benzenes into graphitic carbon which proceeds on Ag nanoparticles and is conditioned by their adsorption in a perpendicular orientation has been previously reported [13] and further supported by the results presented in Ref. [14]. On the basis of these results, we assume that DATP, which contains three interconnected benzene rings and is purposefully adsorbed in a perpendicular orientation with respect to the surface of Ag nanoparticles (to perform its role as a linker), is prone to photodecomposition in the strong optical fields.

4. Conclusions

The bifunctional, amine-substituted aromatic molecule DATP was proved to be a suitable mediator of assembling of Ag nanoparticles into small aggregates. SERS spectra obtained from a single, selected small aggregate of Ag nanoparticles show temporal fluctuations (“blinking”) associated with manifestations of the dynamics of the molecular linker. This, in turn, is the result of the localization of these molecules into strong optical fields. However, since the observed signal likely originates from more than one hot spot, the observed time-evolution cannot be unequivocally interpreted in terms of a single molecular dynamics event. Nevertheless, the observed results indicate that DATP molecules, in contrast to DAAB molecules previously investigated in Ag nanoparticle dimers, decompose in the strong optical fields into graphitic carbon.

Our results thus provide experimental evidence for the presence of the theoretically predicted strong optical fields in small,

molecularly bridged Ag nanoparticle aggregates and for the localization of the bifunctional linking molecules in these hot spots. The nanocomposite systems: Ag nanoparticle-molecular bridge-Ag nanoparticle can be employed in studies of single molecule dynamics and in detection of species on a single molecule level.

Acknowledgments

The authors thank Prof. Martin Moskovits, Univeristy of California at Santa Barbara, for valuable comments and discussion. Financial support by the 203/07/0717 and 203/05H001 Grants awarded by GACR, the 1P05ME790 Grant awarded by MSMT of Czech Republic, the KAN 100500652 Grant awarded by ASCR and by the MSM0021620857 long term research program are gratefully acknowledged.

References

[1] K. Kneipp, Y. Wang, H. Kneipp, L.T. Perelman, I. Itzkan, R.R. Dasari, M.S. Feld, Phys. Rev. Lett. 78 (1997) 1667.
[2] K. Kneipp, H. Kneipp, I. Itzkan, R.R. Dasari, M.S. Feld, Chem. Rev. 99 (1999) 2957.
[3] M. Moskovits, L.L. Tay, J. Yang, T. Haslett, Top. Appl. Phys. 82 (2002) 215.
[4] M. Moskovits, J. Raman Spectrosc. 36 (2005) 485.
[5] K.A. Bosnick, J. Jiang, L. Brus, J. Phys. Chem. B 106 (2002) 8096.
[6] P.C. Andersen, M.L. Jacobson, K.L. Rowlen, J. Phys. Chem. B 108 (2004) 2148.
[7] A.R. Bizarri, S. Cannistraro, Phys. Rev. Lett. 94 (2005) 068303.
[8] E.C. LeRu, P.G. Etchegoin, J. Chem. Phys. 125 (2006) 204701.
[9] H. Xu, J. Aizpurua, M. Kall, P. Apell, Phys. Rev. E 62 (2000) 4318.
[10] P. Johansson, H. Xu, M. Käll, Phys. Rev. B 72 (2005) 035427.
[11] B. Vlckova, M. Moskovits, I. Pavel, K. Siskova, M. Sladkova, M. Slouf, Chem. Phys. Lett. 455 (2008) 131.
[12] P.C. Lee, D. Meisel, J. Phys. Chem. 86 (1982) 3391.
[13] J.S. Suh, M. Moskovits, J. Shakhesemampour, J. Phys. Chem. 97 (1993) 1678.
[14] E.J. Bjerneld, F. Svedberg, P. Johansson, M. Kall, J. Phys. Chem. A 108 (2004) 4187.

Article II

B. Vlčková, M. Moskovits, I. Pavel, K. Šišková, **M. Sládková**, M. Šlouf,:

Single-molecule surface-enhanced Raman spectroscopy from a molecularly-bridged silver nanoparticle dimer

Chem. Phys. Lett., 455 (2008) 131

Chemical Physics Letters 455 (2008) 131–134

Contents lists available at ScienceDirect

Chemical Physics Letters

journal homepage: www.elsevier.com/locate/cplett

Single-molecule surface-enhanced Raman spectroscopy from a molecularly-bridged silver nanoparticle dimer

Blanka Vlčková [a,*], Martin Moskovits [b,*], Ioana Pavel [b,1], Karolina Šišková [a,2], Magdalena Sládková [a], Miroslav Šlouf [c]

[a] Department of Physical and Macromolecular Chemistry, Charles University in Prague, Hlavova 2030, 128 40 Prague 2, Czech Republic
[b] Department of Chemistry and Biochemistry, University of California at Santa Barbara, Santa Barbara, CA 93106, USA
[c] Institute of Macromolecular Chemistry Academy of Sciences of Czech Republic, Heyrovsky Sq. 2, 162 06 Prague 6, Czech Republic

ARTICLE INFO

Article history:
Received 7 December 2007
In final form 23 February 2008
Available online 29 February 2008

ABSTRACT

Silver nanoparticle dimers were produced and immobilized on a functionalized TEM finder grid, by sequential assembly using bifunctional molecular linker 4,4′-diaminoazobenzene. SERS spectra recorded were ascribed to the specific dimer by TEM-imaging. Temporal fluctuations (blinking) of SERS signal demonstrate observation of single-molecule Raman. By linker-mediated assembly at small linker to nanoparticle ratios, electromagnetic hot spots are created with one or very few molecular linkers localized in them. Observed recurrence times are consistent with known surface diffusion constants, suggesting that single molecule dynamics causing the blinking might arise from breaking of linker bond to one of the nanoparticles, linker diffusion over the other nanoparticle and return to the hot spot.

1. Introduction

Single-molecule surface-enhanced Raman spectroscopy (SM-SERS) is approximately a decade old [1,2]; however, the fact that SERS, as it normally manifests itself from most samples, is really an average over a broad range of local enhancements, some of which are very great, had already been proposed in the 1980 s [3]. Recent interest in SM-SERS [4–10] is part of a resurgence of interest in SERS generally which has occurred on account of a number of contributing causes, among them the unique physical and chemical properties of nanosystems [11] and the development of the field of plasmonics [12].

While it is now recognized that SM-SERS arises when molecules find themselves situated in special sites within the SERS-active nanostructures where the electromagnetic optical fields are greatly concentrated, a number of important issues in SM-SERS remains to be addressed including how to determine when an observation truly constitutes an instance of SM-SERS. Le Ru et al. [13], for example, challenged reports of SM-SERS based on observation of SERS intensities that appear to form a Poisson-Boltzmann distribution with discrete peaks attributed to signals arising from one, two etc. molecules, pointing out that the SERS intensity originating from a single-molecule system would be sufficiently diverse to wash out the discreteness in the Poisson distribution. Accordingly, other hallmarks of single-molecule spectroscopy, such as blinking, must be called upon to ensure that one is reporting a genuine case of SM-SERS. Likewise, SM-SERS is not easily attainable with all molecules. Calculations indicate that for molecules situated in the SERS 'hot spots', such as the interstice between two very closely-spaced silver nanoparticles [14,15], SERS enhancements greater than $\sim 10^{11}$ are hard to generate. For observation of intense SM-SERS, it is helpful if the molecule situated in the hot spot also has a large Raman cross-section, such as one that might result from a molecular resonance.

In this Letter, we describe observation of SM-SERS from silver nanoparticle dimers formed by the sequential assembly of small nanoparticle aggregates using bifunctional molecules that act as linkers which simultaneously hold the nanoparticles together and automatically place themselves in the SERS hot spot. By using a very low linker-to-nanoparticle ratio, one can limit the distribution of aggregates to very small ones dominated by dimers in which the number of linker molecules is on average only slightly greater than unity. A numerical simulation we performed shows that, under the conditions we use, the majority of the dimers formed in the linker-induced aggregation process are linked by a single bifunctional molecule. The entire aggregate-assembly process, as well as the Raman spectroscopy, were carried out on a TEM finder grid at a surface density small enough so that only a single dimer resides within the focal spot of the illuminating laser. The SERS spectra recorded almost always showed temporal fluctuations (blinking) with long

* Corresponding authors. Fax: +420 224919752 (B. Vlčková).
E-mail addresses: vlc@natur.cuni.cz (B. Vlčková), mmoskovits@ltsc.ucsb.edu (M. Moskovits).
[1] Present address: Marist College, Poughkeepsie, New York, NY 12 601, USA.
[2] Present address: Institute of Macromolecular Chemistry ASCR, Heyrovsky Sq. 2, 162 06 Prague 6, Czech Republic.

0009-2614/$ - see front matter © 2008 Elsevier B.V. All rights reserved.
doi:10.1016/j.cplett.2008.02.078

recurrence times – corroborating the proposition that most aggregates are linked by single molecules which are, in turn, responsible for the observed SERS spectra. Moreover, by carrying out the assembly directly on TEM finder grids, one can use the feducial marks on TEM finder grids to unequivocally locate and image the dimer that gave rise to the observed SERS spectra.

One should keep in mind the operational difference between mono- and bi-functional adsorbate in causing aggregation. To observe SERS, one needs to produce assemblies of strongly-interacting nanostructures [16]. For colloidal particles this means producing nanoparticle dimers or aggregates. Most molecules observed by SERS promote aggregation by displacing adsorbed ions from the surface of the isolated silver nanoparticle replacing it with an uncharged adsorbate and lowering the Coulomb barrier to aggregation [17]. For an adsorbed molecule to succeed in doing so it must normally possess some functionality such as amine that has a greater chemical affinity for silver than the displaced ion. For mono-functional adsorbate to cause aggregation, a sufficient number of them must adsorb on the nanoparticle to lower the Coulomb barrier sufficiently. This is highly improbable at very low adsorbate concentrations. By contrast, a bifunctional linker possessing two ends with affinity for silver can form nanoparticle dimers and small aggregates even at very low linker-to-nanoparticle ratios. In this study, 4,4′-diaminoazobenzene has been selected as such a bifunctional linker, which, additionally, provides some measure of molecular resonance enhancement under the conditions of our experiments.

2. Experimental

Citrate-capped Ag nanoparticles were prepared using the Lee-Meisel method [18]. 4,4′-Diaminoazobenzene (DAAB) was used as the bifunctional linker. The capping citrate anions are believed to serve as a molecule-orienting matrix, reducing the propensity of aromatic molecules to adsorb flat-on, thereby promoting their attachment to Ag nanoparticles via the terminal amine groups. The nanoparticle aggregates were assembled on chemically derivatized SiO_x/formvar-coated copper TEM finder grids pre-treated by vapor-depositing a thin carbon layer on their reverse sides and derivatized with 3-aminopropyltrimethoxysilane (APMS), by condensing the reagent vapor onto the grids and removing the excess reagent *in vacuo*. The assembling was accomplished in a three-step process: (1) Ag nanoparticles were tethered to APMS -derivatized grids by floating them on a Ag colloid surface for 1.5 h. (2) Linker molecules were attached to the Ag nanoparticles by immersing the grids into a 1×10^{-7} M ethanolic solution of DAAB for 4 h. (3) Finally, the grids were exposed to Ag nanoparticles for a second time (for 2 h), to allow additional nanoparticles to bind to DAAB linkers already present on the surfaces of the Ag nanoparticles already-tethered to the grid. The preparation steps were optimized to produce samples dominated by well-spaced dimers allowing the SERS of a single Ag nanoparticle dimer to be observed. Alternatively, by extending the deposition times twice, samples of more densely packed aggregates were produced for statistical evaluation of TEM images. Creating the samples directly on TEM grids enabled their TEM (JEOL JEM 200 CV) imaging.

SERS spectra were collected using a micro-Raman Labram spectrometer (Horiba Jobin Yvon) and excited by 100 μW of 514.5 nm Ar^+ laser light focused to ~1.5 μm spot. An acquisition time of 2 s and a 100× microscope objective were used to collect the SERS data.

3. Results and discussion

A TEM image of Ag-nanoparticle aggregates assembled using DAAB and their measured statistical frequencies are shown in Fig. 1. A simple statistical simulation assuming linker-mediated aggregation using nanoparticle-to-linker ratios more or less corresponding to those used experimentally, produces aggregate probabilities (Fig. 2) similar to those observed (Fig. 1), suggesting that a significant fraction of the observed aggregates are formed through the agency of the linker.

The calculation of the statistical distribution of Ag-nanoparticle aggregates was carried out by assuming a 1:1 ratio of linkers to Ag nanoparticles and presence of only isolated silver nanoparticles on the grid after the first Ag-nanoparticle deposition step. The silver monomers attached to the surface were assigned sequential numbers and linkers were randomly attached to them by selecting a nanoparticle number using a pseudo-random number generator. The simplifying assumption was then made that the size of the nanoparticle aggregate formed upon the second exposure to Ag nanoparticles was equal to the number of linkers attached to the first nanoparticle through the aforementioned procedure. Because we are in a regime where only very small aggregates form, these assumptions are not unreasonable, which accounts for the fact that the calculated aggregate size distribution (Fig. 2) is rather similar to those determined by particle counting in the TEM images of the experimentally produced samples (Fig. 1). One of the objectives of this study is to obtain an unequivocal correspondence between

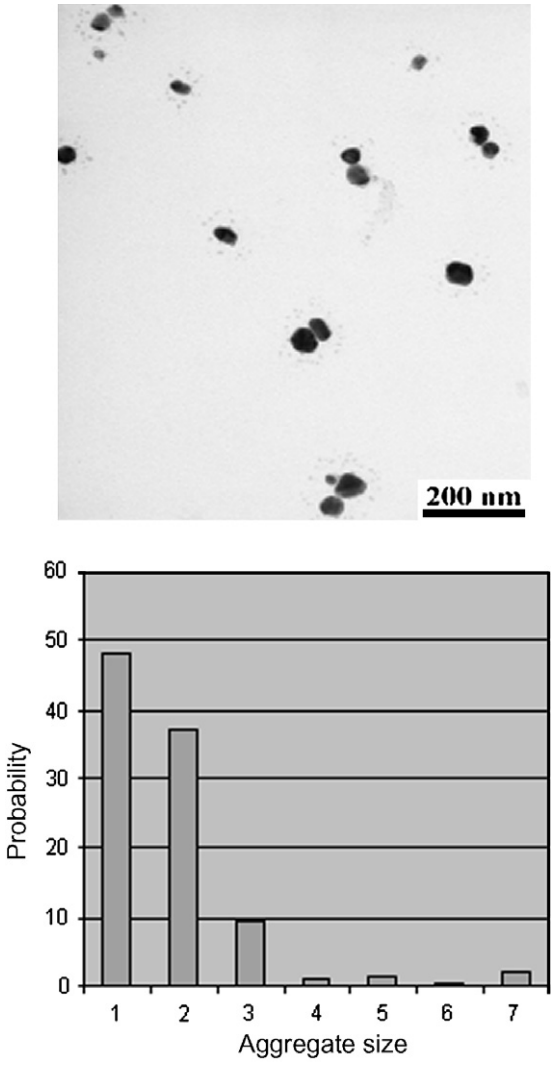

Fig. 1. TEM image and size-distribution of DAAB-linked Ag nanoparticle aggregates determined by TEM image analysis.

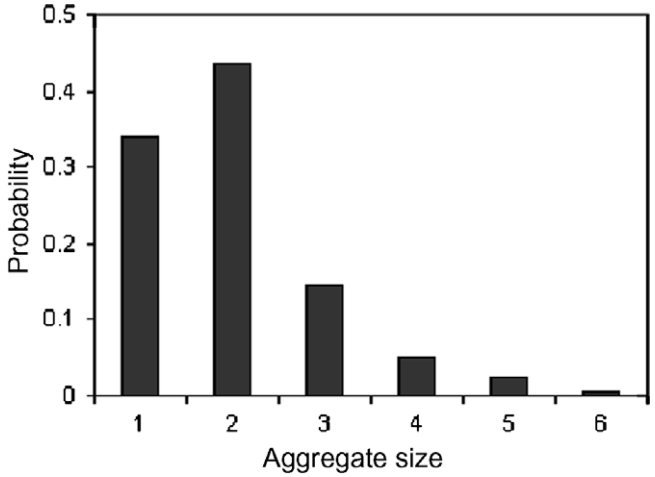

Fig. 2. Calculated size-distribution of molecularly-linked Ag nanoparticle aggregates.

the SERS signal and the dimer responsible for that spectrum. This was accomplished by determining the position of the nanoparticle aggregate with respect to markers on the finder grid using the confocal optical imaging function of the micro-Raman system during the SERS measurement, then imaging that small region by TEM. In almost every case only a single nanoparticle aggregate was found to reside at that location, unequivocally identifying the source of the observed SERS spectrum.

TEM images of a selected Ag nanoparticle dimer putatively bridged by DAAB are shown in Fig. 3A and B. The SERS signal (Fig. 3C) obtained from this dimer appears and disappears (blinks) with average recurrence times of tens of seconds. In the series of spectra shown in Fig. 3C, the SERS signal of DAAB appears in the 8th and 14th spectrum (Fig. 4A and C). The spectra are constituted by characteristic bands of di-substituted trans-azobenzene compounds [19–22]. During the 'off' episodes, the spectra consist of a broad background with weak traces of graphitic carbon (Fig. 4B).

The TEM image in Fig. 1 shows that almost all of the dimers and small aggregates lie flat on the surface of the grid. This suggests that, although the linkers were crucial in initially forming the

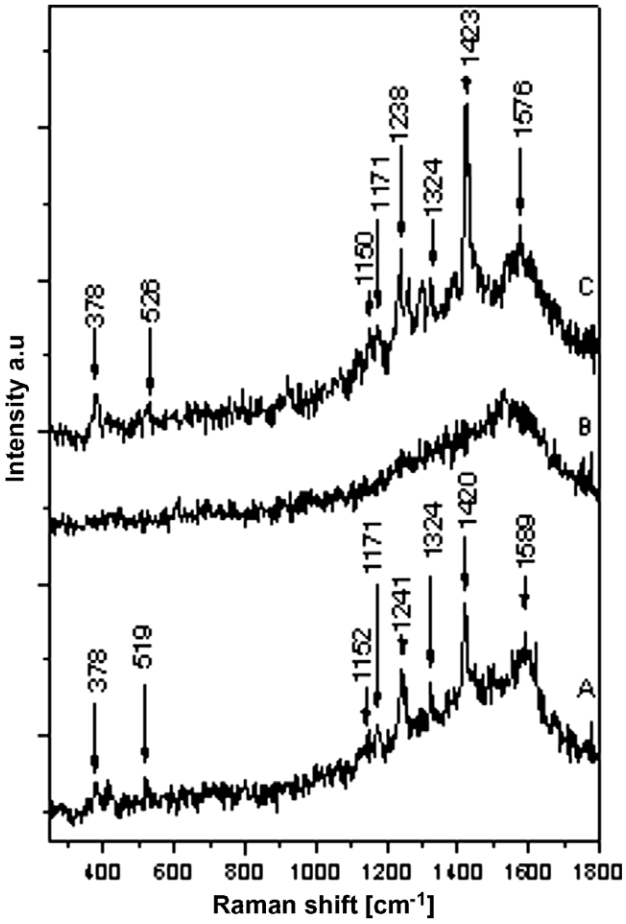

Fig. 4. The 'signal in' spectra, namely the 8th (A) and the 14th (C) spectrum, and the signal 'off' spectrum (B) within the SERS spectral set depicted in Fig. 3C.

nanoparticle aggregates, once formed, the aggregates could reorient to some extent eventually achieving stability when as many of the nanoparticles within a given aggregate as possible could interact with the APMS surface functionality. Because most of the

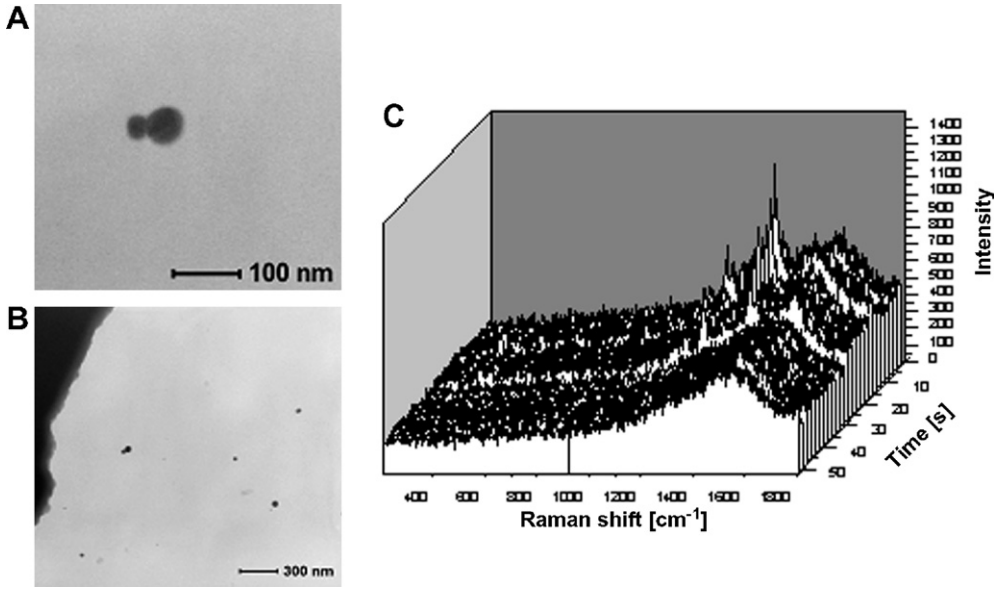

Fig. 3. (A) and (B): TEM images of a selected DAAB-linked Ag nanoparticle dimer and (C) time-evolution of SERS signal obtained from this dimer.

aggregates probed showed intense SERS activity, this reorientation process does not seem to have dislodged the linker from the hot spot.

The observed blinking is most likely due to dynamics of a single linker molecule. Because the dimer is securely bound to the TEM grid surface through multiple APMS moieties, a broad range of dynamics could be responsible for the observed blinking. For example, while retaining its bond to both nanoparticles of the dimer, the linker could diffuse into less-enhancing regions of the interstice between the two Ag nanopaticles then return to the most enhancing region. The rather long recurrence times are also consistent with a process in which one of the Ag-linker bonds breaks, allowing the linker to diffuse over the surface of one of the Ag nanoparticles before finding its way back to the hot spot. Because the Ag nanoparticles are held securely in place by the APMS it is unlikely that the two partners forming the dimer would diffuse away from each others proximity if the linker becomes detached. The observed recurrence times, averaging several tens to hundreds of seconds, are consistent with a random walk over the nanoparticle surface that occasionally revisits the origin. Assuming the average nanoparticle's diameter to be ~100 nm (Fig. 1), the average surface area of a nanoparticle is ~30 000 nm^2. Approximating the diffusion process of a molecule over the surface of the nanoparticle as a random walk over a finite lattice with 30 000 nodes (this assumes a ~1 nm^2 effective molecular area) the recurrence time, t, would be given approximately by the equation $\langle x^2 \rangle = 2Dt$, where $\langle x^2 \rangle$ is the mean square random walk length back to the origin and D is the diffusion constant. Surface diffusion constants for small atoms, molecules and atomic clusters on metal surfaces normally have values in the range $D = 1.0 \times 10^{-3}\ e^{-(0.3 \text{ to } 0.8 \text{ eV})/k_B T}\ cm^2/s$ [23]. Assuming the root mean squared value of a random walk trajectory back to the origin to be ~30,000 one-nm steps (i.e. on average every lattice node is visited before the molecule returns to the hot spot) one calculates room-temperature recurrence times ranging between 0.1 and 10^7 s. The observed recurrence time of the order of several tens of seconds corresponds to a diffusion barrier height ~0.5 eV, a commonly encountered surface diffusion barrier energy.

4. Conclusions

Ag nanoparticles were assembled into dimers and small aggregates using a bifunctional, amine-terminated aromatic molecule (DAAB) functioning as a linker. SERS spectra obtained from a single, specific Ag-nanoparticle dimer identified unequivocally using TEM, show temporal fluctuations (blinking) likely associated with single-molecule dynamics. The strong SERS signal from these small aggregates arises from the fact that in assembling the Ag-nanoparticle aggregates, the linkers automatically position themselves in the electromagnetic hot spot located in the small gap (or gaps) between the nanoparticles. Because the nanoparticle dimers were strongly bound to the surface of the TEM finder grid, the single-molecule dynamics giving rise to the blinking could involve bond breakage between the linker that assembled the dimer in the first place allowing the linker to diffuse over the surface of one of the nanoparticles before returning (stochastically) to the hot spot resulting in the recurrence of the SERS spectrum.

Acknowledgments

The authors thank Ms J. Hromadkova for her excellent technical assistance. Financial support by the 1P05ME790 grant awarded by MSMT of Czech Republic through the International Collaboration Programs project and by the NSF through International Science and Engineering grant OISE-0406665 are gratefully acknowledged. Funding from Grant Agency of Czech Republic by grant 203/07/0717, from MSMT CR by project MSM 0021620857, from the Institute of Collaborative Biotechnologies through grant DAAD19-03-D- 0004 from the US Army Research Office and from Lawrence Livermore National Laboratories through a UCDRD grant is gratefully acknowledged. M.M. gratefully acknowledges support from the Canadian Institute for Advanced Research.

References

[1] K. Kneipp, Y. Wang, H. Kneipp, L.T. Perelman, I. Itzkan, R.R. Dasari, M.S. Feld, Phys. Rev. Lett. 78 (1997) 1667.
[2] S. Nie, S.R. Emory, Science 275 (1997) 1102.
[3] P. Hildebrandt, M. Stockburger, J. Phys. Chem. 88 (1984) 5935.
[4] K. Kneipp, H. Kneipp, I. Itzkan, R.R. Dasari, M.S. Feld, Chem. Rev. 99 (1999) 2957.
[5] M. Moskovits, L.L. Tay, J. Yang, T. Haslett, Top. Appl. Phys. 82 (2002) 215.
[6] A.M. Michaels, J. Jiang, L. Brus, J. Phys. Chem. B 104 (2000) 11965.
[7] K.A. Bosnick, J. Jiang, L. Brus, J. Phys. Chem. B 106 (2002) 8096.
[8] W.E. Doering, S. Nie, J. Phys. Chem. B 106 (2002) 311.
[9] P.C. Andersen, M.L. Jacobson, K.L. Rowlen, J. Phys. Chem. B 108 (2004) 2148.
[10] A.R. Bizarri, S. Cannistraro, Phys. Rev. Lett. 94 (2005) 068303.
[11] G. Schmid, Nanoparticles: From Theory to Application, Wiley-VCH, Weinheim, 2004.
[12] S.A. Maier, Curr. Nanosci. 1 (2005) 17.
[13] E.C. Le Ru, P.G. Etchegoin, J. Chem. Phys. 125 (2006) 204701.
[14] H. Xu, J. Aizpurua, M. Kall, P. Apell, Phys. Rev. E 62 (2000) 4318.
[15] P. Johansson, H. Xu, M. Käll, Phys. Rev. B 72 (2005) 035427.
[16] M. Moskovits, Rev. Mod. Phys. 57 (1985) 783.
[17] M. Moskovits, B. Vlckova, J. Phys. Chem. B 109 (2005) 14755.
[18] P.C. Lee, D. Meisel, J. Phys. Chem. 86 (1982) 3391.
[19] D.R. Armstrong, J. Clarkson, W.E. Smith, J. Phys. Chem. 99 (1995) 17825.
[20] N. Kurita, S. Tanaka, S. Itoh, J. Phys. Chem. A 104 (2000) 8114.
[21] N. Biswas, S. Umapathy, J. Phys. Chem. A 104 (2000) 2734.
[22] N. Biswas, S. Umapathy, J. Phys. Chem. A 101 (1997) 5555.
[23] G.L. Kellogg, Surf. Sci. Rep. 21 (1994) 1.

Article III

B. Vlčková, I. Pavel, **M. Sládková**, K. Šišková, M. Šlouf

Single molecule SERS: Perspectives of analytical applications

J.Mol. Structure, 834–836 (2007) 42

Available online at www.sciencedirect.com
ScienceDirect
Journal of Molecular Structure 834–836 (2007) 42–47
Journal of MOLECULAR STRUCTURE
www.elsevier.com/locate/molstruc

Single molecule SERS: Perspectives of analytical applications

B. Vlckova [a,*], I. Pavel [b,1], M. Sladkova [a], K. Siskova [a], M. Slouf [c]

[a] Department of Physical and Macromolecular Chemistry, Charles University, Hlavova 2030, 12840 Prague 2, Czech Republic
[b] Department of Chemistry and Biochemistry, University of California at Santa Barbara, Santa Barbara, CA 93106, USA
[c] Institute of Macromolecular Chemistry ASCR, Heyrovsky Sq.2 16206 Prague 6, Czech Republic

Received 6 October 2006; accepted 18 November 2006
Available online 16 January 2007

Abstract

Recent developments in SERS (surface-enhanced Raman scattering) and SERRS (surface-enhanced resonance Raman scattering) spectroscopy are related to the discovery of its single molecule sensitivity. The achievement of single molecule level of SERS and/or SERRS spectral detection is understood to be conditioned by localization of detected molecules into unusually strong nanoscale-localized optical fields (dubbed hot spots). Recent calculations predict SERS enhancement factors as high as 1×10^{15} for certain chromophoric molecules located in the hot spot between two Ag nanoparticles [P. Johansson, H. Xu, M. Käll, Phys. Rev. B 72 (2005) 035427.]. Owing to a combination of single molecule sensitivity with the fingerprint selectivity inherent to vibrational spectroscopy, single molecule SERS spectroscopy can potentially offer unprecedented possibilities of analytical applications.

Keywords: Surface-enhanced Raman scattering (SERS); Surface-enhanced resonance Raman scattering (SERRS); Single molecule SERS; Ag nanoparticle dimers; Molecular linkers

1. Mechanisms of SERS

SERS originates from coupled optical responses of plasmonic metal (such as Ag and Au) nanostructures (nanoparticles, nanowires, etc.) and of molecules located on (or in a close proximity of) their surfaces (Fig. 1). In such coupled system, both the incident light and the light inelastically (Raman) scattered by adsorbed molecules are enhanced by resonance Mie scattering of light by the plasmonic metal nanostructures. This, in a nutshell, is the electromagnetic (EM) mechanism of SERS. The EM mechanism of SERS is the principal mechanism of SERS and operates independently on the nature of the target molecular species. Explanation of the phenomenon of SERS on the basis of the light amplification by free-electron-like (plasmonic) metal nanostructures has been published [1] just one year after its discovery [2]. Provided that the wavelength of incident light obeys simultaneously with the EM resonance condition also a molecular resonance condition, molecular resonances contribute to the overall enhancement of Raman scattering. The mechanisms and applications of SERS have been the subject of several seminal review and feature articles [3–12].

In this paper, we focus our attention on systems with Ag nanoparticles which are most frequently employed in single molecule SERS. Ag nanoparticles are usually polyhedral single crystals (such as dodecahedrons or icosaedrons), however, for simple theoretical treatments, they are approximated by spheres. Let us first briefly explain how and when a Ag nanoparticle operates as a light amplifier. When a small Ag nanoparticle (approximated by a sphere) is illuminated by light of a particular wavelength at which (or close to which) Mie resonance condition is fulfilled, the conduction electrons within the particle are caused to oscillate with the same frequency as that of the incident light, and an oscillating dipole is created. The resonance excitation of this dipole is also dubbed a dipolar surface plasmon

* Corresponding author. Tel.: +420 221951309; fax: +420 224919752.
E-mail address: vlc@natur.cuni.cz (B. Vlckova).
[1] Present address: Arkansas Nanotechnology Center, University of Arkansas at Little Rock, Little Rock, AR 72204, USA.

0022-2860/$ - see front matter © 2006 Elsevier B.V. All rights reserved.
doi:10.1016/j.molstruc.2006.11.053

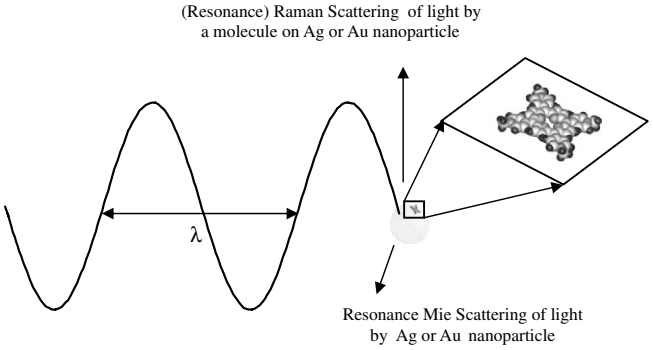

Fig. 1. Schematic depiction of surface-enhanced Raman scattering.

excitation. In a simple quasistatic approximation, the dipole is described by dipole moment P,

$$P = g \cdot r^3 \cdot E_0 \tag{1}$$

where E_0 is the intensity of the electric field of the incident light, r is the nanoparticle radius and g is a factor, in which the material (as well as the optical) characteristics of the system are interrelated:

$$g = \frac{\varepsilon(\lambda) - \varepsilon_m}{\varepsilon(\lambda) + 2\varepsilon_m} \tag{2}$$

where $\varepsilon(\lambda)$ is the relative complex permitivity (dielectric function) of a metal (which, in our case, is Ag) and ε_m is the relative permitivity (dielectric constant) of the medium (usually water or air) surrounding the Ag nanoparticles.

The material characteristics of the metal (Ag) and of the ambient are related to their optical characteristics, in particular to the complex refractive index of the metal $N(\lambda) = n + ik$ (where n is the refractive index and k is the index of absorption) and to the refractive index of the medium n_m (which is assumed to be non-absorbing throughout the visible spectral region and hence $k_m = 0$) by relations:

$$\varepsilon(\lambda) = N^2(\lambda) \quad \varepsilon_m = (n_m)^2 \tag{3}$$

The factor g and the dipole moment P maximize when the resonance condition is fulfilled, i.e. when

$$\mathrm{Re}\,\varepsilon(\lambda) = -2\varepsilon_m \tag{4}$$

and $\mathrm{Im}\,\varepsilon(\lambda)$ (which represents the resonance damping) is very small.

The resonance wavelength at which the resonance condition is fulfilled for isolated Ag spheres in water is ~390 nm, and the real system which fits this description is a Ag nanoparticle hydrosol.

The most important point is that the oscillating dipole re-radiates light, the intensity of which is proportional to the square modulus of the dipole moment:

$$I \approx \left(\frac{1}{\lambda}\right)^4 |P|^2 \tag{5}$$

Hence at (or close to) the resonance wavelength, Ag nanoparticles work as light amplifiers [13]. In the EM mechanism of SERS, both the incident and the Raman scattered light are enhanced, and the final enhancement of Raman scattering of a molecule adsorbed on an isolated Ag nanoparticle is about 4 orders of magnitude.

Nevertheless, assemblies of closely spaced Ag nanoparticles are far better amplifiers than those of the isolated ones. For closely spaced nanoparticles, the particles mutually interact by dipole–dipole interaction with several consequences. In most cases, a red shift and broadening of the resonance wavelength region is observed. In some of the assemblies, the strong optical fields excited by the incident laser light are non-uniformly distributed and spacially localized. The nanoscale regions in which the strong EM fields are localized are dubbed hot spots. Existence of hot spots has been predicted theoretically and proved experimentally both in large fractal aggregates of Ag nanoparticles and in dimers and very small aggregates of these nanoparticles [14–20]. The EM mechanism enhancement factors can range between 4 and 11 orders of magnitude, in dependence on the morphology of Ag nanoparticle assembly, localization of a molecule within the assembly and the excitation wavelength and light polarization selected for the SERS experiment. Theory of the EM mechanism of SERS has been explained in detail for example in [3,4,10].

Molecular resonances contribute to the overall enhancement of Raman scattering provided that their resonance condition is fulfilled simultaneously with the EM resonance. Molecular resonances are somewhat similar to resonance Raman scattering which occurs when the wavelength of the incident light matches that of an allowed electronic transition within a molecule. However, in SERS, one has always to evaluate possible alternations of the geometric as well as electronic structure of the target molecule caused by the molecule–Ag surface interaction. It became a custom in SERS literature to consider two types of molecular resonance contributions. In the case of SERRS, a molecule itself is a chromophore with respect to excitation wavelength used for SERS experiment. Nevertheless, when the molecular resonance contribution is evaluated for a given target molecule, its actual structure in the particular SERS-active system has to be considered. For example, free-base porphyrins adsorbed directly onto the Ag nanoparticle surface are frequently converted into Ag metalloporphyrins (Fig. 2). Such a conversion manifests itself

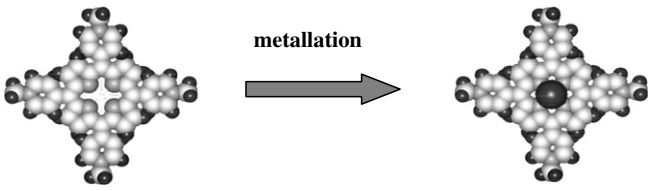

Fig. 2. Metallation of a free-base porphyrin directly adsorbed on Ag nanoparticle surface.

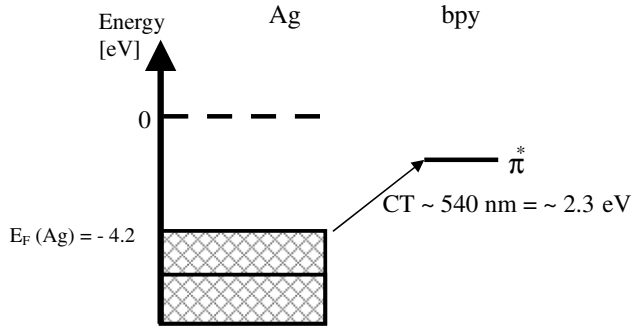

Fig. 3. Proposed electronic structure of Ag-2,2′-bipyridine surface complex.

clearly in the SERRS spectral pattern [21,22]. In that case, one has to evaluate the resonance contribution for a Ag metalloporhyrin. A theoretical treatment of SERRS has been published e.g. in Ref. [7]. Another possibility is that the molecule is non-chromophoric with respect to the excitation wavelength, but forms a chromophoric surface complex. An example of such molecule is 2,2′-bipyridine which, under specific conditions, forms a Ag-bpy surface complex [23]. In that case, molecular resonance contribution stems from the match between the excitation wavelength and the wavelength of a photo-induced charge transfer transition within the Ag-adsorbate (e.g. Ag-bpy) surface complex (Fig. 3), and is usually dubbed the chemical mechanism of SERS. Theoretical treatment and experimental evidence for the chemical mechanism of SERS can be found in Refs. [5] and [8].

While routine SERS spectral measurements of target molecules in systems with Ag nanoparticles can be performed with conventional Raman spectrometers, for single molecule SERS, the benefits of Raman microspectroscopy (stemming from coupling of a confocal optical microscope to a Raman spectrometer) are required.

2. SERS on a single molecule level: highlights and drawbacks

Single molecule SERS has been reported for the first time by Kneipp et al. [24]. In their Raman microspectroscopic measurements of very small volumes of a highly diluted hydrosol of small Ag nanoparticle aggregates containing cresyl violet in 10^{-14} M concentration, there was on average 0.6 molecules in the probed volume. SERS signal obtained from this system in 1 s intervals showed temporal fluctuations. A histogram of signal intensities for a particular Raman band showed, instead of a Gaussian profile obtained for more concentrated systems, a Poisson distribution of signal intensities, which was attributed to acquisition of the signal from 0, 1, 2 or 3 molecules.

Kneipp's results immediately evoked a question whether single molecule SERS and SERRS are explicable by a combination of the EM and molecular resonance mechanisms. The answer was provided chiefly through calculations of Kall and coworkers [16–18], which have shown that, indeed, for a molecule located in a hot spot between two Ag nanoparticles and excited by light polarized parallel to the dimer axis, the EM mechanism enhancement can be of 1×10^{11}, and when combined with another three orders of magnitude provided by a molecular resonance, it can achieve the 1×10^{14} enhancement [10,16–18] observed experimentally. In addition to that, observation of temporal fluctuations of the SERS signal (so called "blinking") has been interpreted as manifestation of a dynamic behavior of a single, or of very few molecules [10,11,19,20,22,24–27].

Localization of molecules into hot spots thus became an important task in single molecule SERS. Our research on this field has been driven by an idea that an efficient way how to localize molecules into hot spots is to make them to bridge two Ag nanoparticles. We explored the possibilities of molecularly-bridged dimers and small aggregates preparations and we have tested two approaches to their formation: a simple mixing of Ag nanoparticle sol with a prospective linker and, alternatively, a step-wise procedure in which dimers and small aggregates were assembled on a chemically functionalized supporting surface with help of the linker. As a prospective molecular linker, 5,10,15,20-tetrakis(4-aminophenyl)porphin (TAPP) was selected. This porphyrin species contains four strongly argentophilic terminal amine groups, however, it has been shown earlier [28] that, for steric reasons, a tetra-functional porphyrin can bridge only two Ag nanoparticles. The common point of both preparation strategies was stabilization of the parent Ag nanoparticles by a suitable molecular species which would direct the porphyrin towards adsorption in the perpendicular orientation with respect to Ag nanoparticle surface, that, in turn, is necessary for its functioning as a Ag nanoparticle linker. The first approach to TAPP-linked Ag nanoparticle dimers and small aggregates formation was based on preparation of an organosol of Ag nanoparticles stabilized by pentylamine (using chloroform as the organic solvent) and its subsequent mixing with a solution of TAPP in chloroform. Ag nanoparticles and their small aggregates were attached to glass slides functionalized by 3-aminopropyltrimethoxysilane and imaged by scanning electron microscopy (SEM). A typical SEM image shows

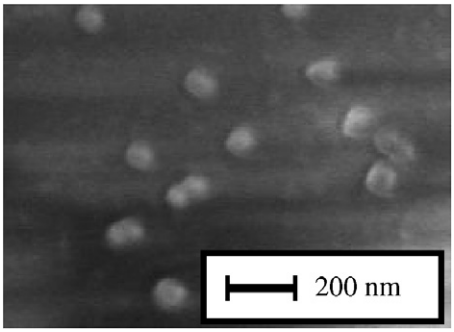

Fig. 4. SEM image of a sample of TAPP-bridged, pentylamine-capped Ag nanoparticles.

Ag nanoparticle dimers, in addition to the residual monomers (Fig. 4). SERS spectra obtained from the sample of TAPP-bridged, pentylamine-capped Ag nanoparticles at 514.5 nm excitation and in 1 s intervals are governed by the signal of graphitic carbon, which shows enormous temporal fluctuations of the signal intensity (Fig. 5). In some of the spectra, a few narrow bands of TAPP can be observed. The fluctuations of the graphitic carbon signal could possibly result from spacial oscillations of Ag nanoparticles, which, after TAPP decomposition, remain tethered to the supporting surface, but are no longer fixed by the rigid porphyrin bridge. These spacial oscillations can result into the interparticle distance fluctuations, which, in turn, can be responsible for Raman signal fluctuations.

Alternatively, TAPP-bridged dimers and small aggregates of citrate-capped Ag nanoparticles were assembled on a chemically functionalized, SiO_x-coated grid for transmission electron microscopy (TEM) using a three-step procedure analogous to that described in detail in Ref. [29]. TEM images (a typical example of which is shown in Fig. 6) and image analysis revealed a preferential formation of dimers and trimers of Ag nanoparticles, together with a small fraction of larger aggregates, and a substantial fraction of residual monomers. SERS spectra obtained from a sample of TAPP-bridged, citrate-capped Ag nanoparticles (514.5 nm excitation, 1 s intervals) show temporal fluctuations of the signal in which the characteristic spectral bands of the bridging TAPP molecules can clearly be distinguished (Fig. 7).

SERS signals collected from both samples indicate that the bridging TAPP molecules probably undergo a photodecomposition at 514.5 nm laser irradiation. While for pentylamine-capped dimers and small aggregates, this decomposition appears to be fast and actually prevents detection of a meaningful porphyrin signal, for citrate-capped dimers and aggregates, the process is much more limited and allows for TAPP detection. One of the possible explanations of this difference can be related to a low ordering of the capping pentylamine monolayer (which can further decrease at elevated temperatures under irradiation) which might be responsible for re-orientation of porphyrin molecules and for a direct contact between the porphyrin macrocycle and Ag nanoparticle surface, which in turn, may promote photodecomposition of TAPP molecules.

Finally, it should be noted that, in both cases, Raman signals were collected from several dimers and/or small aggregates, which was a consequence of their rather dense packing (Figs. 4 and 6) in comparison to the size of the laser spot. The fluctuating signals thus likely originate from several hot spots. A further elaboration of the three-step

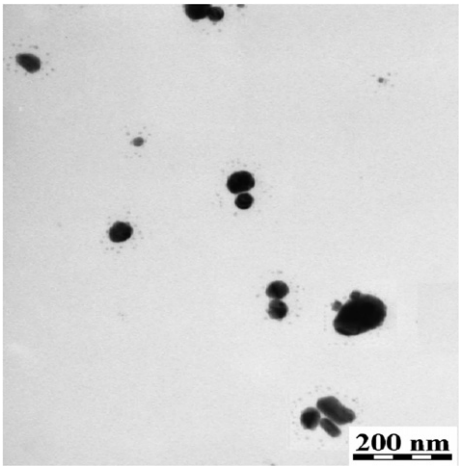

Fig. 6. TEM image of a sample of TAPP-bridged citrate-capped Ag nanoparticles.

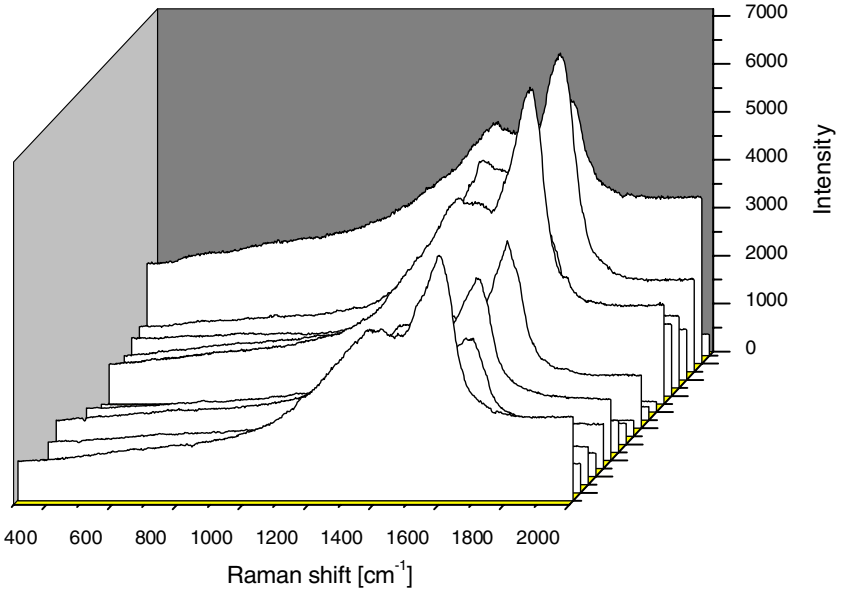

Fig. 5. Time-evolution of SERS signal obtained from the sample of TAPP-bridged, pentylamine-capped Ag nanoparticles (shown in Fig. 4).

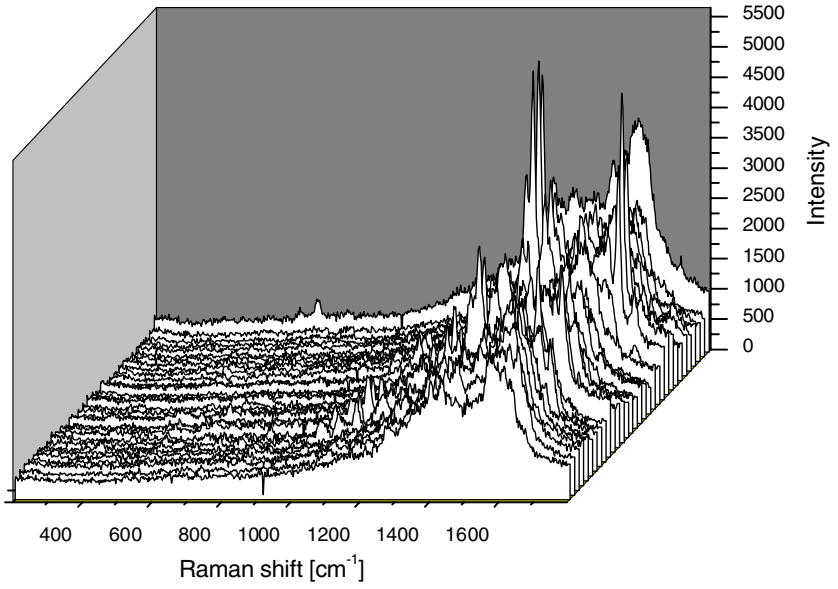

Fig. 7. Time-evolution of SERS signal obtained from the sample of TAPP-bridged citrate-capped Ag nanoparticles (shown in Fig. 6).

procedure of citrate-capped Ag nanoparticle assembling enabled us to prepare samples of widely spaced dimers and small aggregates and to obtain SERS signal from a selected single dimer of 4,4-diaminoazobenzene-bridged Ag nanoparticles, i.e. from a single hot spot [29].

Alternative approaches towards Ag nanoparticle dimer formation have also been explored by other investigators. For example, dimers formed by encapsulation of Ag nanoparticles by a protein, namely hemoglobin, were investigated, and temporally fluctuating SERS signals dominated by in-plane modes of heme were observed [19].

The interference of graphitic carbon signal in single molecule level SERS experiments has already been reported by several other research groups [26,28,30]. For example, Käll and coworkers observed that in small Ag nanoparticle aggregates excited at 514.5 nm, some aromatic aminoacids, e.g. tyrosin, degrade into graphitic carbon. While aromatic aminoacids, of course, do not absorb light in the visible spectral region, MO calculations have shown that in a Ag–tyrosin complex, a charge transfer transition can be excited by the 514.5 nm laser excitation. This CT transition can be responsible for a surface-induced and also surface-enhanced photochemical process, which, in turn, is responsible for aromatic acid photo-degradation [30].

3. Perspectives of analytical applications of single molecule SERS

What are the perspectives to use single molecule SERS as an analytical tool? In single molecule SERS, we have, on one hand, a tremendous sensitivity, while, on the other, very high demands on the selectivity of detection. The latter demands are reinforced by the fact that once we have achieved single molecule sensitivity, we can, in principle, have a single molecule impurity.

Another problem which has to be considered is that together with Raman scattering, other optical processes undergone by molecules are enhanced in strong optical fields, namely surface photochemistry. A photoproduct can thus act as a contaminant in these systems, together with a product of a possible thermal decomposition.

What are thus the prospective pathways and perspectives in single molecule SERS? It appears that the basic research will be the fast moving lane in single molecule SERS, since there are still many fundamental questions to be answered and drawbacks to be overcome. First of all, the origin of SERS signal fluctuations (so called ''blinking'') has to be elucidated in greater detail. Furthermore, some more advanced approaches to assembling of Ag nanoparticles into desired morphologies will probably be developed. For example, our current interest is employment of molecular spacers (originally designed for prevention of free based porphyrin metallation [21a]) in assembling of Ag nanoparticle dimers. Such a spacer is expected to localize target molecules into ''hot spots'' via specific spacer-adsorbate bonding and, simultaneously, prevent a direct surface–adsorbate interaction, i.e. prevent formation of new electronic states which, in turn, could be the pathways of an undesired photochemistry. Another point of interest is the efficient localization of target molecules into ''hot spots'', which can be accomplished by a chemical trapping (e.g. with help of a spacer), or, possibly, also by trapping through optical forces by the optical tweezers effect [31].

One of the possible pathways towards development of analytical applications of single molecule SERS can actually proceed first through improvement of the performance of the ensemble-averaged systems achieved by implementation of all these newly developed approaches mentioned above. It is probably still too early to predict if taking

the step from ensemble averaged to single molecule systems, i.e. from probing of an ensemble of e.g. 1000 dimers to a single one will actually be meaningful for practical spectro-analytical applications as we know them these days. Nevertheless, it is quite possible that once we fabricate single molecule devices, we will not only have to detect a single molecule, but also monitor its function.

Acknowledgements

The authors thank Prof. Martin Moskovits, University of California at Santa Barbara, for valuable discussions and advise. BV gratefully acknowledges the long-term collaboration with Prof. M. Moskovits and his research groups at the University of Toronto and University of California at Santa Barbara.

Financial support by the 203/04/0688 grant awarded by the Grant Agency of Czech Republic, by the 1P05ME790 grant awarded by MSMT of Czech Republic through the International Collaboration Programs project and by the NSF through International Science and Engineering grant OISE-0406665 are gratefully acknowledged.

References

[1] M. Moskovits, J. Chem. Phys. 69 (1978) 4159.
[2] D.L. Jeanmaire, R.P.V. van Duyne, J. Electroanal. Chem. 84 (1977) 1.
[3] M. Moskovits, Rev. Mod. Phys. 57 (1985) 783.
[4] J.A. Creighton, in: R.J.H. Clark, R.E. Hester (Eds.), Spectroscopy of Surfaces, John Wiley & Sons, New York, 1988, p. 37.
[5] A. Otto, in: M. Cardona, G. Guntherodt (Eds.), Light in Solids IV, Springer-Verlag, Berlin, 1984, p. 289.
[6] T.M. Cotton, in: R.J.H. Clark, R.E. Hester (Eds.), Spectroscopy of Surfaces, John Wiley & Sons, New York, 1988, p. 91.
[7] D.A. Weitz, S. Garoff, J.I. Gersten, A. Nitzan, J. Chem. Phys. 78 (1983) 5324.
[8] A. Campion, P. Kambhampati, Chem. Soc. Rev. 27 (1998) 241.
[9] (a) K. Kneipp, H. Kneipp, I. Itzkan, R.R. Dasari, M.S. Feld, Chem. Rev. 99 (1999) 2957;
(b) K. Kneipp, H. Kneipp, I. Itzkan, R.R. Dasari, M.S. Feld, J. Phys.: Condens. Matter 14 (2002) R597.
[10] M. Moskovits, L.L. Tay, J. Yang, T. Haslett, Top. Appl. Phys. 82 (2002) 215.
[11] M. Moskovits, J. Raman Spectrosc. 36 (2005) 485.
[12] G.A. Baker, D.S. Moore, Anal. Bioanal. Chem. 382 (2005) 1751.
[13] C.F. Bohren, D.F. Hufman, Absorption and Scattering of Light by Small Particles, Wiley & Sons, New York, 1983.
[14] M.I. Stockman, V.M. Shalaev, M. Moskovits, R. Botet, T.F. George, Phys. Rev. B 46 (1992) 2821.
[15] P. Zhang, T.L. Haslett, C. Douketis, M. Moskovits, Phys. Rev. B 57 (1998) 15513.
[16] H. Xu, J. Aizpurua, M. Käll, P. Apell, Phys. Rev. E 62 (2000) 4318.
[17] P. Johansson, H. Xu, M. Käll, Phys. Rev. B 72 (2005) 035427.
[18] M. Käll, H. Xu, P. Johansson, J. Raman Spectrosc. 36 (2005) 510.
[19] H. Xu, E.J. Bjerneld, M. Käll, L. Borjenson, Phys. Rev. Lett. 83 (1999) 4357.
[20] A.M. Michaels, J. Jiang, L. Brus, J. Phys. Chem. B 104 (2000) 11965.
[21] (a) B. Vlckova, P. Matejka, J. Simonová, P. Pancoska, K. Cermakova, V. Baumruk, J. Phys. Chem. 97 (1993) 9719;
(b) M. Prochazka, B. Vlckova, J. Stepanek, P.Y. Turpin, Langmuir 21 (2005) 2956.
[22] M. Sladkova, B. Vlckova, P. Mojzes, M. Slouf, C. Naudin, G. Le Bourdon, Faraday Discuss. 132 (2006) 121.
[23] I. Srnova, B. Vlckova, T.L. Snoeck, D.J. Stufkens, P. Matejka, Inorg. Chem. 39 (2000) 3551.
[24] K. Kneipp, Y. Wang, H. Kneipp, L.T. Perelman, I. Itzkan, R.R. Dasari, M.S. Feld, Phys. Rev. Lett. 78 (1997) 1667.
[25] K.A. Bosnick, J. Jiang, L. Brus, J. Phys. Chem. B 106 (2002) 8096.
[26] W.E. Doering, S. Nie, J. Phys. Chem. B 106 (2002) 311.
[27] A.R. Bizarri, S. Cannistraro, Phys. Rev. Lett. 94 (2005) 068303.
[28] I. Sloufova-Srnova, B. Vlckova, Nano Lett. 2 (2002) 121.
[29] B. Vlckova, M. Moskovits, I. Pavel, M. Sladkova, K. Siskova, M. Slouf, Chem. Phys. Lett., manuscript in preparation.
[30] E.J. Bjerneld, F. Svedberg, P. Johansson, M. Käll, J. Phys. Chem. 108 (2004) 4187.
[31] (a) H. Xu, M. Käll, Phys. Rev. Lett. 89 (2002) 246802;
(b) J. Prikulis, F. Svedberg, M. Käll, M.J. Enger, K. Ramser, M. Goksor, D. Hanstorp, Nano Lett. 4 (2004) 115.

Article IV

M. Sládková, B. Vlčková, P. Mojzeš, M. Šlouf, C. Naudin and G. Le Bourdond

Probing strong optical fields in compact aggregates of silver nanoparticles by SERRS of protoporphyrin IX

Faraday Discuss., 132 (2006) 121–134

Probing strong optical fields in compact aggregates of silver nanoparticles by SERRS of protoporphyrin IX

Magdalena Sládková,[a] Blanka Vlčková,*[a] Peter Mojzeš,[b] Miroslav Šlouf,[c] Coralie Naudin[d] and Gwenelle Le Bourdon[d]

Received 4th May 2005, Accepted 25th May 2005
First published as an Advance Article on the web 18th October 2005
DOI: 10.1039/b506247k

TEM images and measurements of SERRS (surface-enhanced resonance Raman scattering) spectra as a function of the porphyrin concentrations in systems with unmodified and chloride-modified Ag nanoparticles and protoporphyrin IX (PPIX) are reported. TEM images have shown formation of compact aggregates in systems with chloride modified Ag nanoparticles, as opposed to systems with the unmodified particles constituted by isolated particles. SERRS spectra of PPIX as a function of PPIX concentration were measured and subjected to factor analysis. Two spectral components were identified and tentatively attributed to unperturbed PPIX and to Ag^{+}–PPIX surface species. Concentration value of the SERRS spectral detection limit of the latter species was determined to be nearly three orders of magnitude lower in the system with the compact aggregates than in the system with separated nanoparticles and achieves the value of 1×10^{-10} M in a macrosampling Raman experiment. TEM images and SERRS-micro-Raman spectra of single compact aggregates of chloride-modified Ag nanoparticles incorporating PPIX molecules were acquired from a sample prepared by attachment of the aggregates to amine groups of derivatized, SiO_x/formvar coated copper grids for TEM. The SERRS signal has shown large temporal fluctuations as well as variations from one aggregate to another. Within the signal fluctuations, a SERRS spectrum showing the characteristic bands of both SERRS spectral forms of PPIX and originating most probably from a few PPIX molecules located in hot spots in the interstices between the Ag nanoparticles, was obtained.

Introduction

SERS (Surface-enhanced Raman scattering) and SERRS (surface-enhanced resonance Raman scattering) spectroscopy takes advantage of the simultaneous interaction of light with free-electron-like metal nanostructures and nanoparticle assemblies and with molecules located at their surfaces.[1,2] Recent developments in the field of SERS on one hand, and the pressing need for development of sensitive and a selective analytical tools for biomedical analysis on the other, offer unprecedented possibilities for the application of SERRS and SERRS spectroscopy towards these goals.[3]

Preparation of Ag nanoparticle assemblies in which strong nanoscale-localized optical fields can be generated by an external optical excitation are currently of interest due to numerous prospective applications. One of them is achievement of a single molecule level of SER(R)S spectral detection.[4–6] Current strongly supported opinion is that single molecule sensitivity in SER(R)S is conditioned

[a] *Department of Physical and Macromolecular Chemistry, Charles University in Prague, Hlavova 2030, 128 40 Prague 2, Czech Republic. E-mail: vlc@natur.cuni.cz*
[b] *Institute of Physics, Charles University in Prague, Ke Karlovu 5, 121 16 Prague 2, Czech Republic*
[c] *Institute of Macromolecular Chemistry , Academy of Sciences of Czech Republic, Heyrovsky Sq. 2 162 06 Prague 6, Czech Republic*
[d] *Jobin-Yvon S.A.S, 231, rue de Lille, 59650 Villeneuve d'Ascq, France*

by location of the molecules into such strong localized fields (hot spots).[7] Recent calculations show that the largest enhancement of Raman scattering will be achieved for molecules located in interstices between two particles. In addition to the most favorable cases of the nearly touching particles, dimers of interpenetrating particles were also shown to provide hot spots in the interstices between them.[8]

An interesting issue in SERS experiments on a single molecule level is the role of "incubation" of Ag colloids (hydrosols) by chlorides.[4,5,9–15] For example, Brus and coworkers[9] found a pronounced dependence of the SERS signal of rhodamine 6G on the concentration of chlorides added for incubation. Hildebrandt and Stockburger[16] reported formation of new adsorption sites on surfaces of Ag nanoparticles (prepared by reduction of silver nitrate by sodium citrate) in the presence of chloride, fluoride, bromide, iodide and sulfate anions. Adsorbates such as rhodamine 6G were found to be chemisorbed on these sites, which are present at very low coverages.[16] For the same type of Ag nanoparticle hydrosol, Doering and Nie reported no changes in the nanoparticle morphology after their treatment by these ions, and limited the SERS activating effect to chlorides, bromides and iodides only.[11]

It has recently been demonstrated that modification of Ag nanoparticles (prepared by reduction of silver nitrate by sodium borohydride) by adsorption of chlorides leads simultaneously to pronounced morphological changes which manifest themselves by formation of compact aggregates of interpenetrating Ag nanoparticles, and to generation of new, most probably Ag(0) adsorption sites, which can be stabilized by a suitable adsorbate, *e.g.* 2,2-bipyridine (bpy), yielding the Ag(0)–bpy surface complex.[17,18] Electronic structure, and, consequently, molecular resonances of Ag(0)–bpy were found to be distinctly different from those of Ag^+–bpy species encountered in systems with the unmodified Ag nanoparticles.[18] In that case, modification of Ag nanoparticles by adsorbed chlorides resulted into changes in both the electromagnetic (EM) and the chemical (molecular resonance) mechanism contributions to the overall SERS enhancement.[17,18] The specific contribution of each of the mechanisms to the large increase of the SERS enhancement factor observed thus could not be distinguished.

In this paper, we report the results based on an idea that for probing of the strong nanoscale localized optical fields generation in compact aggregates of interpenetrating Ag nanoparticles prepared by chloride-modifications, changes solely in the EM mechanism enhancement of the SERS signal of an adsorbate have to be evaluated. The success of such experiments was conditioned by finding of an adsorbate which does not stabilize Ag(0) adsorption sites and forms the same (most probably Ag^+–adsorbate) species in systems with both the unmodified and the chloride modified Ag nanoparticles. At that point, our above mentioned goal merged with an effort to optimize SERRS spectral detection (*i.e.* minimize the SERRS spectral detection limit) of protoporphyrin IX (PPIX, Fig. 1A), a porphyrin species recently found important for clinical diagnostics of early stages of cancer.[19] Regarding the previously mentioned experimental results[17,18] and calculations,[8] systems with compact aggregates of chloride modified Ag nanoparticles were selected as a prospective pathway to optimization of the SERRS spectral detection of the target porphyrin PPIX. In the course of this study, PPIX was shown to be a suitable adsorbate for evaluation of the effect of the morphological changes induced in Ag nanoparticles by adsorbed chlorides on the EM mechanism contribution to the SERRS enhancement.

Electronic absorption spectra of PPIX (free base) in aqueous ambient as a function of pH were thoroughly investigated and formation of porphyrin aggregates (both H- and J-type) at pH > 3 was reported, while monomeric PPIX was identified in some non-aqueous solvents.[20,21] Resonance Raman spectra (RRS) and SERRS spectra of PPIX (excited at 514.5 nm) in systems with Ag nanoparticle hydrosols were previously reported, however, an assignment of the RRS and SERRS spectral bands has not been provided.[22] We thus started our study by a thorough investigation of RR spectra of PPIX in both aqueous and non-aqueous ambient targeted on pinpointing of the differences between the monomeric and aggregated form of PPIX. The full details of this spectral study are reported elsewhere.[23] In this paper, we present only the results pertinent to the assignment of spectral forms of PPIX which have been identified by factor analysis (FA) of SERRS spectra measured as a function of PPIX concentration in Ag colloid/PPIX system (at 514.5 nm excitation). From this point, we proceed further by measurements of concentration dependence of the SERRS spectra of PPIX in Ag colloid/NaCl/PPIX system (at the same excitation wavelength) and by identification of the spectral forms contributing to the SERRS signal. These forms correspond to

those identified by FA in the previously mentioned system without chlorides. From the mutual comparison of SERRS spectral detection limits of PPIX in both systems, we deduce that the enhancement by the EM mechanism increases by about three orders of magnitude upon the compact aggregates formation. Finally, we provide evidence that by SERS-microRaman measurements of a single compact aggregate of chloride-modified Ag nanoparticles, SERRS signal of PPIX can be detected on a single molecule level.

Experimental

Materials and procedures

Materials. Protoporphyrin IX (disodium salt, Porphyrin Products, Inc.), sodium chloride (p.a., Lachema), 3-aminopropyltrimethoxysilane (97%, Aldrich), silver nitrate (p.a., Aldrich), sodium borohydride (p.a., Merck), and doubly distilled, deionized water were used for sample preparations.

Preparation of Ag nanoparticle hydrosol (Ag colloid). Ag colloid was prepared by reduction of silver nitrate by sodium borohydride according to procedure II in ref. 24.

Preparation of Ag colloid/PPIX and Ag colloid/NaCl/PPIX systems. In the latter case, Ag nanoparticles were modified by addition of 100 μl of 1 M NaCl to 2 ml of Ag colloid. To both types of systems, an appropriate amount of a stock aqueous solution of PPIX was added to yield systems with 10^{-7}–10^{-10} M PPIX concentrations.

Preparation of samples for TEM and micro-Raman measurements. SiO_x/formvar coated copper grids for TEM microscopy (Agar Scientific, Ltd.) were pre-treated by vapor-deposition of a thin carbon layer on their reverse sides. The outer SiO_x layer of the grids was derivatized by 3-aminopropyltrimethoxysilane through condensation of the reagent vapor onto the grids and removal of the excess reagent *in vacuo*. The derivatized grids were allowed to float on the surface of Ag colloid/NaCl/PPIX system for 3 h to enable the attachment of compact aggregates of Ag nanoparticles to the amine-groups on the surface of the derivatized grids. This procedure ensured a sufficient spacial separation of the aggregates required for acquisition of SERRS signal from a selected single aggregate.

Instrumentation

Electronic absorption spectra of PPIX as a function of PPIX concentration in both aqueous and non-aqueous ambient were measured with a Hewlett Packard HP 8462A diode array UV-Vis spectrometer and interpreted according to ref. 21. Electronic absorption spectra of 2.5×10^{-5} M solution of PPIX in dimethylsulfoxide and in aqueous solution of pH = 8.3 are compared in Fig. 1B. In the former case, observation of a single Soret band at 408 nm indicates the presence of PPIX monomers, while in the latter one, splitting of the Soret band into two maxima at 350 and 470 nm indicates the presence of both J- and H-type of PPIX aggregates.

TEM images of the samples were obtained with a JEOL JEM 200 CV transmission electron microscope. The instrumental magnification varied from 20 000 to 150 000.

SERRS spectra of Ag colloid/PPIX and Ag colloid/NaCl/PPIX systems were recorded with a multichannel Raman spectrometer equipped with a Monospec-600 monochromator and a liquid N_2-cooled CCD detector system (Princeton Instruments). A holographic notch-plus filter (Kaiser) was placed in front of the entrance slit of the monochromator to remove the Rayleigh line. Raman scattering was collected in a right-angle scattering geometry. Excitation was provided with the 514.5 nm line of an argon ion laser ILA-120 (Carl-Zeiss, Jena). The average laser power at the sample in a 10 mm quartz glass five-window cuvette was about 100 mW.

SERRS micro-Raman spectra of selected Ag nanoparticle aggregates attached to chemically derivatized TEM grids were collected through a confocal optical microscope using a micro-Raman Labram-HR spectrometer (Jobin-Yvon/Horiba) operating in either the spectral or the imaging mode. Measurements were performed with the 514.5 nm Ar^+ laser excitation line with incident laser

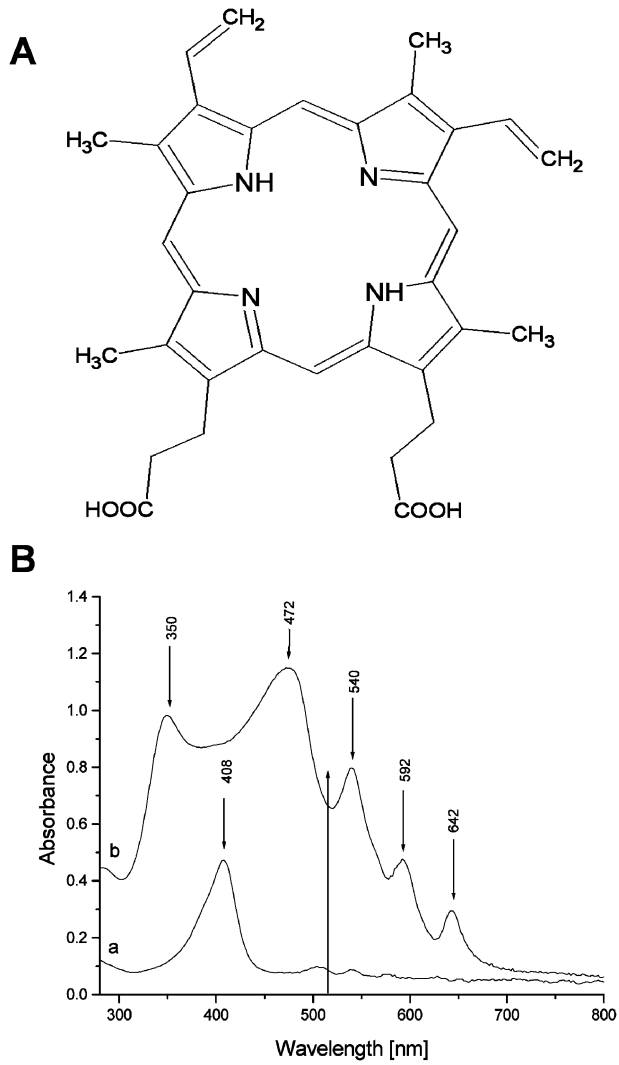

Fig. 1 (A) A schematic depiction of PPIX structure. (B) Electronic absorption spectra of 2.5×10^{-5} M solution of PPIX: (a) in dimethylsulfoxide (monomeric form), (b) in aqueous solution of pH = 8.3 (J- and H-type of aggregates).

power of 10 μW and a laser spot size of *ca.* 0.7 μm. In the control experiments Raman spectra of both parent and 3-aminopropyl-trimethoxysilane-derivatized SiO_x/formvar coated TEM grids (without any aggregates attached) showed only a single, very weak band at 1125 cm^{-1} attributed to SiO_x even with the laser power one order of magnitude higher than that actually used in the SERRS experiments.

Factor analysis of SERRS spectra

Sets of SERRS spectra measured as a function of PPIX concentration were treated by factor analysis (FA) procedure,[25] using a singular value decomposition algorithm.[26,27] The procedure provides a set of orthonormal subspectra $S_j(\nu)$, singular values W_j representing the statistical weight of each of the subspectrum, and a square matrix of virial coefficients V_{ij} which are related to the

experimental spectra $Y_i(\nu)$ by eqn. (1):

$$Y_i(\nu) = \sum_{j=1}^{N} W_j V_{ij} S_j(\nu) \; i,j = 1,2 \ldots N, \tag{1}$$

where N is the number of the experimental spectra.

The original dimension of the data set N is then reduced to a factor dimension $M < N$ by finding the minimal value of M for which difference between the right and the left hand side of the eqn. (2) will be within the experimental error.

$$Y_i(\nu) \approx \sum_{j=1}^{M} W_j V_{ij} S_j(\nu) \; i = 1,2 \ldots N; \;\; j = 1,2 \ldots M \tag{2}$$

The value of the factor dimension M can be determined from the plot of the singular values as a function of the subspectrum number and corresponds to the number of independent spectral components which can be resolved in the spectral set analyzed. Spectra of the pure spectral components (forms) P_n ($n = 1,2 \ldots M$) can be obtained as a linear combination of the statistically relevant subspectra S_j:

$$P_n(\nu) = \sum_{j=1}^{M} c_{nj} S_j(\nu) \text{ where } n = 1,2 \ldots M \text{ and } j = 1,2 \ldots M \tag{3}$$

The procedure by which the spectra of the pure spectral components were obtained has been described in detail in ref. 26. Prior to factor analysis, SERRS spectra in the set were normalized to an internal intensity standard, for which stretching vibrations of water in the 2800–3600 cm^{-1} region were employed. A baseline adjustment procedure (involving subtraction of the broad band of the bending mode of water at $\sim$1650 cm^{-1}) was applied to all spectra in order to avoid possible artifacts due to variations in the background signal.

Results

Morphologies of Ag nanoparticle assemblies in Ag colloid/PPIX and Ag colloid/NaCl/PPIX systems

TEM images of Ag colloid/PPIX and Ag colloid/NaCl/PPIX systems (deposited as drops on C-coated Cu grids and allowed to dry in the air) are compared in Fig. 2A and 2B. While the system with the unmodified Ag nanoparticles is constituted by separated nanoparticles (Fig. 2A), compact aggregates of interpenetrating Ag nanoparticles are observed on the TEM image of the system with the chloride-modified Ag nanoparticles (Fig. 2B).

SERRS spectra of PPIX in Ag colloid/PPIX system

SERRS spectra of Ag colloid/PPIX as a function of PPIX concentration were measured in the 7.5×10^{-5}–1×10^{-8} M range. The set of 16 experimental spectra was subjected to factor analysis (FA). The plot of the singular values *W versus* the subspectrum number for the first 10 subspectra (Fig. 3A) indicates, that only the first two subspectra S_1 and S_2 (shown in Fig. 3B and 3C) significantly contribute to the overall experimental spectral set, and hence the factor dimension of the problem is two. SERRS spectra of the two pure spectral forms of PPIX (denoted further as FI and FII) obtained as proper linear combinations of the first two subspectra are shown in Fig. 4. Comparison between the wavenumbers of the spectral bands of both SERRS spectral forms of PPIX and those found in the RRS spectra of PPIX in neutral aqueous ambient (Table 1) clearly indicates, that the spectral bands of SERRS spectral form FII are nearly identical with those observed in the RRS spectra (at the same excitation wavelength of 514.5 nm). SERRS spectral form FII is thus attributed to the free base form of PPIX, while FI is assigned to a surface species of PPIX. Furthermore, the plot of virial coefficients V_2 as a function of PPIX concentration (Fig. 3E) shows a distinct discontinuity at 1×10^{-5} M PPIX concentration. Evaluation of both the V_1 and V_2 concentration dependences (Fig. 3D and 3E) indicates that at PPIX concentrations in the 1×10^{-8}–1×10^{-5} M

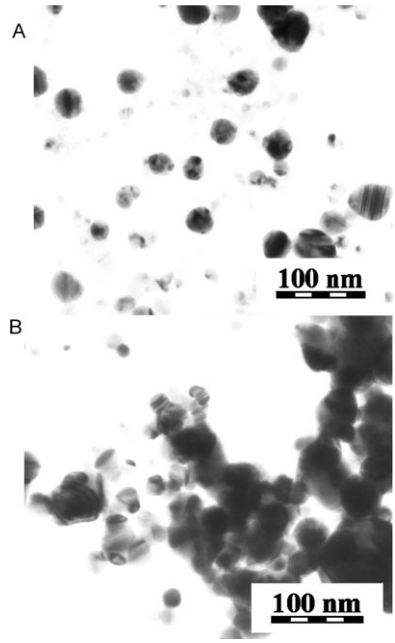

Fig. 2 TEM images of (A) Ag colloid/PPIX system, (B) Ag colloid/NaCl/PPIX system. Concentration of PPIX was 1×10^{-7} M in both systems.

range, only FI of PPIX meaningfully contributes to the SERRS signal obtained. At higher concentrations, the contribution of the FI signal is gradually replaced by that of FII. Since good quality RRS spectra of PPIX have been detected for concentrations 1×10^{-5} M and higher,[23] we cannot establish whether the signal of FII originates from an unperturbed surface, and/or a solution free-base PPIX species. On the other hand, FI represents the dominant contribution to the signal detected below the RRS detection limit of PPIX, and its SERRS origin is thus undisputable.

Tentative assignment of FI and FII spectral bands is provided in Table 1 and discussed in full detail elsewhere.[23] The assignment is based on that of the RRS spectra of Ni(II)PPIX[28–30] using the notation of porphyrin spectral bands adopted from refs. 31 and 32. Comparison of the RRS spectra of free base PPIX (Table 1) with those of the metallated PPIX species [28–30,33] indicates that distinguishing between the free-base and the Ag metallated form of the porphyrin may not be that straightforward as in the case of some other porphyrin species.[24,34,35] In particular, a doublet at 972 cm^{-1} and 990 cm^{-1}, usually typical for free-base porphyrins, is observed in RRS of Ni(II)PPIX,[30,33] as well as in SERRS of FI. Analogous doublet is observed in RRS and SERRS of FII, however, with the former band of the doublet somewhat shifted towards 960 cm^{-1} and 957 cm^{-1}, respectively. On the other hand, observation of only one single band (typical for metalloporhyrin species) located in the 1359–1380 cm^{-1} region in the RRS spectra of metallated PPIX species with a variety of central metal ions[33] as well as in SERRS of FI of PPIX (positioned at 1360 cm^{-1}, Table 1), in contrast to the presence of a doublet 1353, 1368 cm^{-1} in RRS of free base PPIX and SERRS of FII of PPIX (Table 1), indicates that the SERRS spectral form FI can be assigned to a Ag^{+}-metallated PPIX species. The concentration value of the SERRS spectral detection limit of PPIX (detected as FI) in Ag colloid/PPIX system was determined to be 8×10^{-8} M.

SERRS spectra of PPIX in Ag colloid/NaCl/PPIX systems

SERRS spectra of Ag colloid/NaCl/PPIX systems as a function of PPIX concentration were measured in the 1×10^{-7}–1×10^{-10} M range (Fig. 5). The overall range of PPIX concentrations in this set of experiments lies below the concentration value of the RRS spectral detection of PPIX, hence the signal detected belongs to SERRS of PPIX. The wavenumbers of SERRS spectral bands

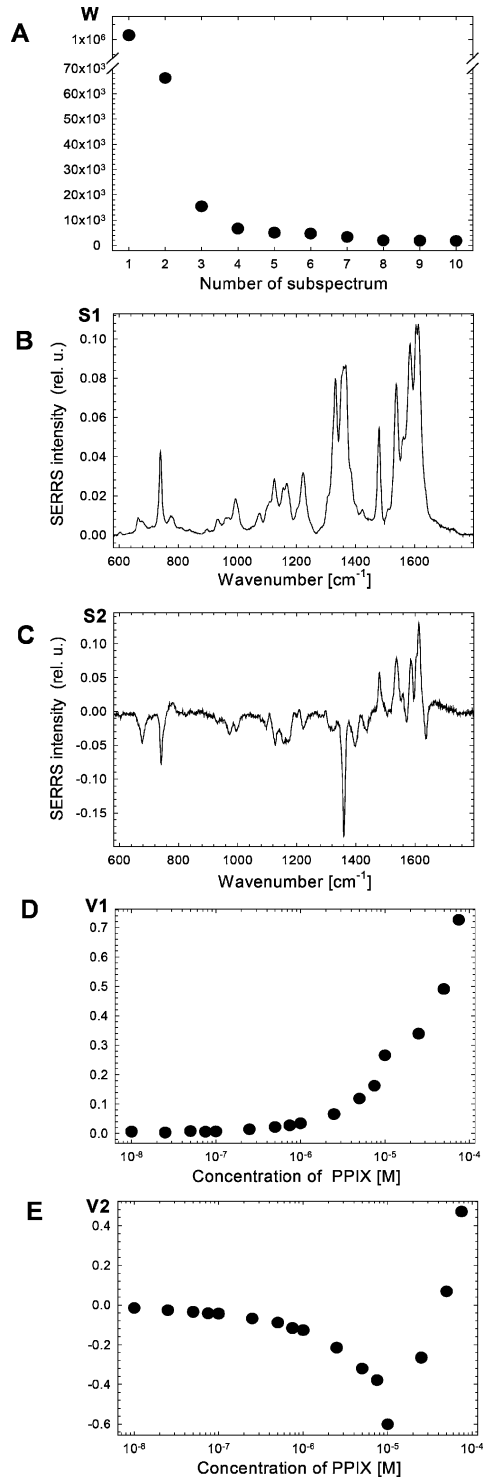

Fig. 3 Factor analysis of the set of SERRS spectra of Ag colloid/PPIX system measured as a function of PPIX concentration: (A) singular values W as a function of the subspectrum number, (B) 1st subspectrum, (C) 2nd subspectrum, (D) virial coefficient V_1 as a function of PPIX concentration, (E) virial coefficient V_2 as a function of PPIX concentration.

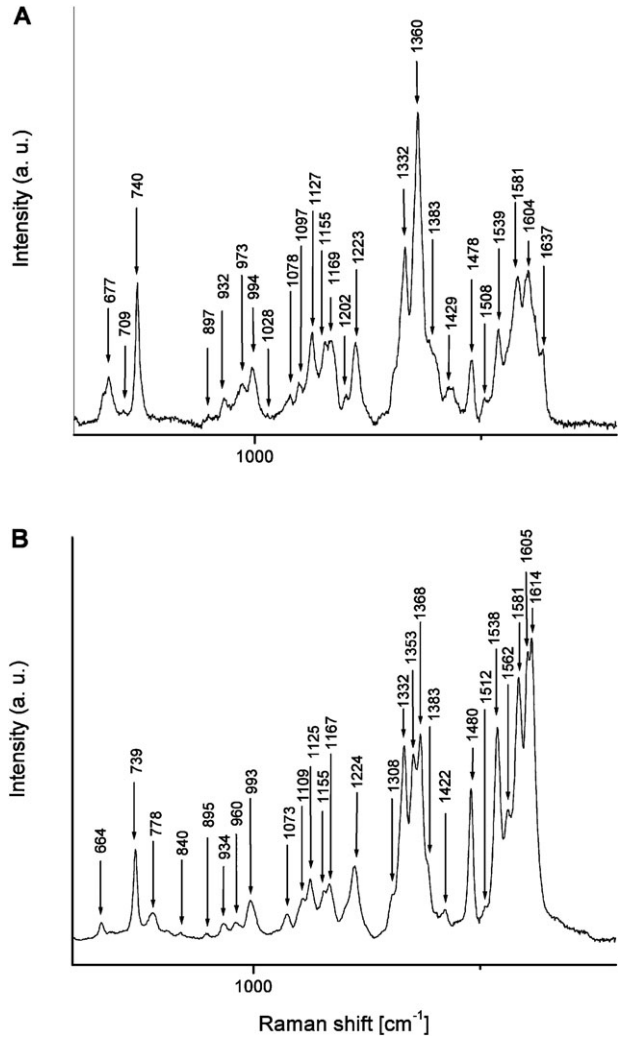

Fig. 4 SERRS spectra of pure spectral forms of PPIX in Ag colloid/PPIX system as determined by factor analysis: (A) form FI, (B) form FII.

detected for particular PPIX concentrations in the system are listed in Table 2. Comparing the wavenumbers of SERRS spectral bands of PPIX obtained from the Ag colloid/NaCl/PPIX system to those of FI and FII of PPIX (Table 1), we observe that the SERRS signal of FII dominates the spectra for concentrations 2.5×10^{-10} M and higher, while FI is detected in the system with 1×10^{-10} M PPIX. The latter concentration value represents the SERRS spectral detection limit of PPIX in Ag colloid/NaCl/PPIX system.

TEM images and SERRS-micro-Raman spectra of single compact aggregates of chloride-modified Ag nanoparticles incorporating PPIX

TEM images and SERRS-micro-Raman spectra of single compact aggregates of chloride-modified Ag nanoparticles incorporating PPIX molecules were acquired from the same sample of the aggregates attached to a chemically modified TEM grid. The TEM image of a typical single compact aggregate is shown in Fig. 6. SERRS spectra from several single compact aggregates were

Table 1 Wavenumbers (in cm^{-1}) of bands in SERRS spectra of two spectral forms F I and F II of PPIX and in RRS spectra PPIX in aqueous solution of pH = 7 measured at 514.5 nm excitation

SERRS FI	SERRS FII	RRS	Assignment
677	664	664	ν_7
740	739	738	ν_{16}
—	778	780	γ (CH_2) vinyl
932	934	931	ν_{32}
973	960	957	ν_{31}
994	993	990	ν_5
1028	—	—	
1078	1073	1073	ν_{23}
1097	1109	1109	ν (C_p–C_{vinyl})
1127	1125	1125	ν_{22}
1155	1155	1160	ν_{30}
1169	1167	1168	ν (C_p–C_{vinyl})
1202	—	—	
1223	1224	1223	ν_{13}
—	1308	—	
1332	1332	1332	ν_{21}
—	1353	1354	ν_{20}
1360	—	—	ν_4
—	1368	1368	ν_4
1383	1383	1383	ν_{40}
1429	1422	1424	ν_{29}
1478	1480	1480	δ $(CH_2)_2$
1508	1512	—	ν_{28}
1539	1538	1538	ν_3
—	1562	1563	ν_{11}
1581	1581	1586	ν_2
1604	1605	1604	ν_{19}
1637	1614	1614	ν (C═C) vinyl

acquired. The SERRS signal showed large temporal fluctuations as well as variations from one aggregate to another. Nevertheless, within the signal fluctuations, SERRS spectra showing the characteristic bands of PPIX were obtained. An example of such a spectrum is shown in Fig. 7. Interestingly, we observe in this SERRS spectrum some of the PPIX bands in the low wavenumbers region, which were missing in the SERRS spectra excited at 514.5 nm measured in a macrosampling setup. On the other hand, counterparts of these bands were detected in SERRS spectra of PPIX excited at 441.6 nm:[23] the 330 cm^{-1} band has its counterpart in the 329 cm^{-1} band of FII, while the 377 cm^{-1} band corresponds to the 381 cm^{-1} band of FI. Their observation indicates that both FI and FII probably contribute to the fluctuating SERRS signal. In addition to those, spectral contributions of graphitic carbon and 3-aminopropyl-trimethoxysilane to the fluctuating signals were also identified. The number of PPIX molecules per a single compact aggregate was estimated to be *ca.* 40 under the conditions of our experiment. Temporal fluctuations of SERRS signal obtained from single aggregates indicate achievement of single molecule level detection limit of PPIX. Acquisition of a larger statistical assembly of spectral data as well as achievement of an unequivocal correspondence between the TEM image of a particular aggregate and its SERRS signal with help of finder TEM grids in a manner similar to that reported in ref. 36, but modified by employment of the SiO_x-coated, chemically derivatized finder grids are planned to get a deeper insight into the origin of the SERRS signal fluctuations.

Discussion

Modification of Ag nanoparticles by adsorbed chlorides induces principal changes in the morphology of Ag nanoparticle assemblies, as witnessed in this paper by comparison of TEM images of Ag

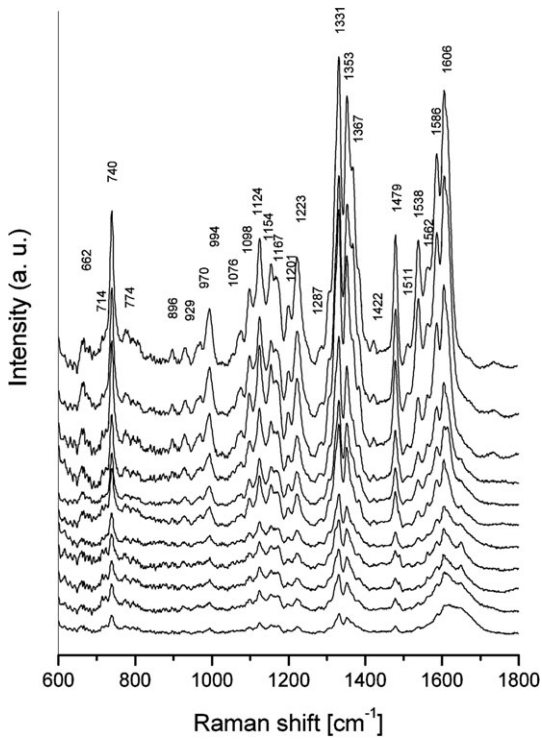

Fig. 5 SERRS spectra of Ag colloid/NaCl/PPIX systems measured as a function of PPIX concentration in the 1×10^{-7}–1×10^{-10} M range.

colloid/PPIX and Ag colloid/NaCl/PPIX (Fig. 2). The morphological changes can be described as formation of compact aggregates of several particles accompanied by an increase of the mean sizes of Ag nanoparticles in the aggregates (Fig. 6). Analogous types of aggregates were encountered earlier in systems with chloride and sulfate-modified Ag nanoparticle and other adsorbates in acidic[17,37] as well as in neutral[17] aqueous ambient. In all these cases, the parent Ag nanoparticles were prepared by reduction of silver nitrate by sodium borohydride. By contrast, no significant morphological changes were reported to result from treatment of immobilized citrate-reduced Ag nanoparticles by chlorides,[11] although formation of aggregates after the treatment of the citrate-reduced Ag nanoparticle hydrosol by HCl was observed.[38] The difference in the outcome of the chloride treatment can possibly be related not only to the chloride concentration and the ambient pH,[17] but also to the type and strengths of Ag nanoparticle stabilization in the parent hydrosol prior to the chloride treatment. While borohydride-reduced Ag nanoparticles in a freshly prepared hydrosol are stabilized by relatively weakly adsorbed borates[39] easily replaced by chlorides,[17] Ag nanoparticles in citrate-reduced hydrosols are chemically derivatized by strong bonding of citrate ions.[40,41] Further insight into the conditions and mechanism of chloride-induced morphological changes of Ag nanoparticles are expected to result from experiments with Ag nanoparticle hydrosols prepared by laser ablation and weakly stabilized most probably by hydroxide and carbonate ions,[42] which are currently in progress.

In systems with Ag nanoparticles and PPIX, the chloride-induced formation of compact aggregates was found to have a largely positive impact on the sensitivity of PPIX detection. In particular, the concentration values of the SERRS spectral detection limit of PPIX were determined to be 8×10^{-8} M in the system with unmodified, separated Ag nanoparticles and 1×10^{-10} M in the system with compact aggregates of chloride-modified Ag nanoparticles, respectively, which indicates that the limit of detection is nearly three orders of magnitude lower in the latter system than in the former one (under the same experimental conditions). Furthermore, the SERRS spectra of PPIX detected at the porphyrin concentrations corresponding to the limits of the SERRS spectral

Table 2 Wavenumbers (in cm^{-1}) of bands in SERRS spectra of Ag colloid/NaCl/ PPIX system with different concentrations of PPIX measured at 514.5 nm excitation

$c = 10^{-7}$ M	$c = 2.5 \times 10^{-10}$ M	$c = 10^{-10}$ M
666	—	—
739	738	737
897	896	—
928	922	—
970	—	—
994	995	—
1075	—	—
1098	1097	—
1125	1125	1124
1154	1154	—
1167	—	1173
1201	1196	—
1222	1223	1221
1331	1332	1332
1352	1352	
		1360
1367	1366	—
1422	1421	—
1479	1479	—
1511	1510	—
1538	1539	—
1564	—	—
1586	1588	—
1605	1605	1603

detection in both systems were found to show the same characteristic marker bands. Their comparison with the SERRS spectral bands of pure spectral forms FI and FII of PPIX determined by FA (Fig. 4) allows us to conclude that it is the spectral form FI (assigned to Ag^{+}-PPIX) which is detected in both systems. Hence, in both systems, the SERRS signal at the limit of detection originates from the porphyrin molecules which are in direct contact with the Ag nanoparticle surface. Assuming that all the porphyrin molecules administered to the system under these

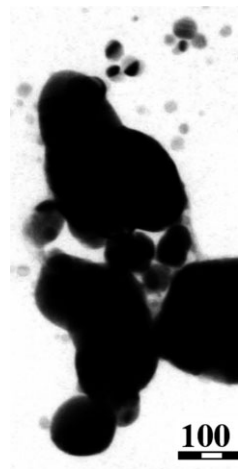

Fig. 6 TEM image of a typical compact aggregate of interpenetrating, chloride modified Ag nanoparticles incorporating PPIX molecules. The aggregate has been chemically attached to 3-aminopropyltrimethoxysilane derivatized, SiO_x coated TEM grid.

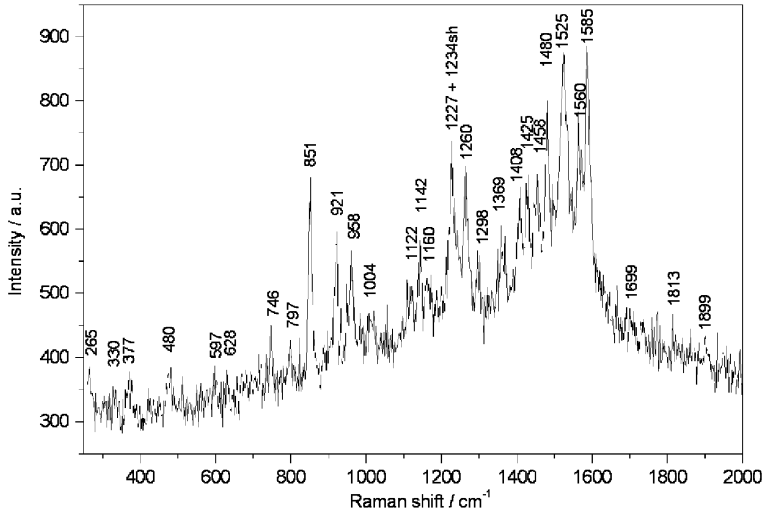

Fig. 7 SERRS spectrum of PPIX obtained from a single aggregate of chloride-modified Ag nanoparticles incorporating PPIX molecules.

conditions are located on the surface of Ag nanoparticles (which is feasible due to the very low concentrations at the detection limit) we can relate the decrease in detection limit to the increase of the average SERRS enhancement experienced by a porphyrin molecule. Moreover, since the molecular resonance contribution to the overall SERRS enhancement can be assumed to be the same for the same porphyrin surface species, the nearly three order of magnitude increase of the SERRS enhancement induced by formation of compact aggregates can most probably be attributed to the EM mechanism of SERRS. Nevertheless, one has to consider that the system with compact aggregates (in contrast to that with the separated Ag nanoparticles) is most probably largely heterogeneous with respect to localization of the strong optical fields after the external optical excitation, and consequently, with respect to the EM mechanism enhancement experienced by the individual adsorbed PPIX (*i.e.* Ag^{+}–PPIX) molecules. Recent calculations[8,43,44] have shown that the largest enhancement by the EM mechanism of SERS is experienced by molecules located in interstices between the touching and/or interpenetrating nanoparticles (*i.e.* in the hot spots). Therefore, in the system with the compact aggregates, only the fraction of the overall amount of adsorbed PPIX molecules, which is actually located in hot spots, most probably contributes to the SERRS signal detected. In accord with these considerations, we have observed temporal fluctuations of the SERRS signal from a single compact aggregate of chloride-modified Ag nanoparticles incorporating, on average, about 40 PPIX molecules. The temporal fluctuations indicate that the detected SERRS signal of the porphyrin is not ensemble averaged and thus, most probably, originates from a single, or only a few PPIX molecules actually located in the hot spots within the aggregate.

In addition to sensitivity, the selectivity of the SERRS spectral detection of PPIX is an important issue in the prospective biomedical analysis applications. Of particular interest is a possibility to distinguish the signal of free base PPIX from that of Fe–PPIX species, for which a single molecule level of detection has already been achieved.[13,14] Towards this goal, the free base form of PPIX (spectral form FII, Fig. 4B) rather than the silver metallated one (spectral form FI, Fig. 4A) should be detected. In the former case, the 1353 cm^{-1} band can be used as the marker band of the free base PPIX, since it lies outside the 1360–1373 cm^{-1} range in which the ν_4 bands of the Fe–PPIX species are located.[13,14,45] Therefore, detection of the spectral form F(II) (attributed to free-base PPIX) at concentrations above 2.5×10^{-10} M can be regarded as another advantage of Ag colloid/NaCl/PPIX systems. A possible explanation of free base PPIX detection in these systems stems from a large promoting effect of NaCl on PPIX aggregate formation.[21] This effect can be responsible for the presence and stabilization of PPIX aggregates even at rather low porphyrin concentrations and

their incorporation into the compact aggregates of Ag nanoparticles. Since a PPIX aggregate is constituted by several, or even several tens of PPIX molecules,[21] of which only one or two are in direct contact with the Ag nanoparticle surface, while the others remain in their native, free base form, the spectral form FII attributed to the free base PPIX represents the major contribution to the SERRS signal from PPIX aggregates incorporated into the compact aggregates of Ag nanoparticles.

Conclusions

A temporally fluctuating SERRS signal of PPIX has been detected from a single compact aggregate of chloride-modified Ag nanoparticles containing, on average, 40 (or less) PPIX molecules. Temporal fluctuations of the signal usually associated with a single molecule level of detection indicate, that only a few of the overall amount of molecules per aggregate actually contribute to the detected signal. Formation of compact aggregates of intergrown (interpenetrating) Ag nanoparticles has been accomplished by incubation of Ag nanoparticle hydrosol prepared by reduction of silver nitrate by sodium borohydride with 5×10^{-2} M NaCl prior to addition of a neutral aqueous solution of PPIX. The nearly three orders of magnitude decrease of the SERRS spectra detection limit of PPIX induced by chloride-modification of Ag nanoparticles and by their consequent morphological changes is attributed chiefly to the EM mechanism of SERS. Addition of chlorides was also found to increase the selectivity of SERRS spectral detection of PPIX.

Acknowledgements

Financial support by the 203/04/0688 grant awarded by Grant Agency of Czech Republic is gratefully acknowledged. The authors thank Dr Pavel Matějka, Prague Institute of Chemical Technology, for control micro-Raman measurements of the formvar/SiO_x coated grids for TEM, and Ms Jiřina Hromádková, Institute of Macromolecular Chemistry, for excellent technical assistance.

References

1 M. Moskovits, *J. Chem. Phys.*, 1979, **69**, 4159.
2 M. Moskovits, *Rev. Mod. Phys.*, 1985, **57**, 783.
3 K. Kneipp, H. Kneipp, I. Itzkan, R. R. Dasari and M. S. Feld, *J. Phys.: Condens. Matter*, 2002, **14**, R597.
4 K. Kneipp, Y. Wang, R. R. Dasari and M. S. Feld, *Appl. Spectrosc.*, 1995, **49**, 780.
5 K. Kneipp, Y. Wang, H. Kneipp, L. T. Perelman, I. Itzkan, R. R. Dasari and M. S. Feld, *Phys. Rev. Lett.*, 1997, **78**, 1667.
6 S. Nie and R. S. Emory, *Science*, 1997, **275**, 1102.
7 M. Moskovits, L. L. Tay, J. Yang and T. Haslett, *Top. Appl. Phys.*, 2002, **82**, 215.
8 H. Xu, J. Aizpurua, M. Kall and P. Apell, *Phys. Rev. E*, 2000, **62**, 4318.
9 A. M. Michaels, M. Nirmal and L. E. Brus, *J. Am. Chem. Soc.*, 1999, **121**, 9932.
10 A. M. Michaels, J. Jiang and L. Brus, *J. Phys. Chem. B*, 2000, **104**, 11965.
11 W. E. Doering and S. Nie, *J. Phys. Chem. B*, 2001, **106**, 311.
12 C. Eggeling, J. Schaffer, C. A. M. Seidel, J. Korte, G. Brehm, S. Schneider and W. Schrof, *J. Phys. Chem. A*, 2001, **105**, 3673.
13 A. R. Bizzarri and S. Cannistraro, *Chem. Phys.*, 2003, **290**, 297.
14 A. R. Bizzarri and S. Cannistraro, *Chem. Phys. Lett.*, 2004, **395**, 222.
15 M. Ishikawa, Y. Maruyama, J. Y. Ye and M. Futamata, *J. Lumin.*, 2002, **98**, 81.
16 P. Hildebrandt and M. Stockburger, *J. Phys. Chem.*, 1984, **88**, 5935.
17 (*a*) I. Srnová-Šloufová, K. Šišková, B. Vlčková and J. Štěpánek, in *Proceedings of the XVIII th International Conference on Raman Spectroscopy (ICORS 2002) 25–30 August Budapest Hungary*, ed. J. Mink, G. Jalsovsky and G. Keresztury, John Wiley and Sons, Ltd., Chichester, UK, 2002, p. 277–278; (*b*) I. Srnová-Šloufová, K. Šišková, B. Vlčková and J. Štěpánek, manuscript in preparation.
18 I. Srnová-Šloufová, B. Vlčková, T. L. Snoeck, D. J. Stufkens and P. Matějka, *Inorg. Chem.*, 2000, **39**, 3551.
19 R. C. Kreig, S. Fickweiler, O. S. Wolfbeis, M. Kongshuang and R. Knuechel, *Photochem. Photobiol.*, 2000, **72**, 226.
20 I. Inamura and K. Uchida, *Bull. Chem. Soc. Jpn.*, 1991, **64**, 2005.
21 L. M. Scolaro, M. Castriciano, A. Romeo, S. Patane, E. Cefali and M. Allegrini, *J. Phys. Chem. B*, 2002, **106**, 2453.
22 B. Vlčková, P. Šmejkal, M. Michl, M. Procházka, P. Mojzeš, F. Lednický and J. Pfleger, *J. Inorg. Biochem.*, 2000, **79**, 295.

23 M. Sládková, B. Vlčková and P. Mojzeš, manuscript in preparation.
24 B. Vlčková, P. Matějka, J. Šimonová, P. Pančoška, K. Čermáková and V. Baumruk, *J. Phys. Chem.*, 1993, **97**, 9719.
25 E. R. Malinowski, *Factor Analysis in Chemistry*, Wiley, New York, 1991.
26 J. Hanzlíková, M. Procházka, J. Štěpánek, V. Baumruk, J. Bok and P. Anzenbacher, *J. Raman Spectrosc.*, 1998, **29**, 575.
27 J. Hanuš, K. Chmelová, J. Štěpánek, P.-Y. Turpin, J. Bok, I. Rosenberg and Z. Točík, *J. Raman Spectrosc.*, 1999, **30**, 669.
28 S. Choi, T. G. Spiro, K. C. Langry and K. M. Smith, *J. Am. Chem. Soc.*, 1982, **104**, 4346.
29 S. Choi, T. G. Spiro, K. C. Langry, E. V. Smith, D. L. Budd and G. N. La Mar, *J. Am. Chem. Soc.*, 1982, **104**, 4346.
30 H. Lee, T. Kitagawa, M. Abe, R. K. Pandey, H.-K. Leung and K. M. Smith, *J. Mol. Struct.*, 1986, **146**, 337.
31 X.-Y. Li, R. S. Czernuszewicz, J. R. Kincaid, Y. O. Su and T. G. Spiro, *J. Phys. Chem.*, 1990, **94**, 31.
32 X.-Y. Li, R. S. Czernuszewicz, J. R. Kincaid, P. Stein and T. G. Spiro, *J. Phys. Chem.*, 1990, **94**, 47.
33 L. T. He, T. Q. Lie and T. L. Jiang, *J. Chem. Soc., Perkin Trans. 2*, 1990, **1**, 7.
34 M. Procházka, P.-Y. Turpin, J. Štěpánek and B. Vlčková, *J. Raman Spectrosc.*, 2002, **33**, 758.
35 T. M. Cotton, S. G. Schultz and R. P. van Duyne, *J. Am. Chem. Soc.*, 1982, **104**, 6528.
36 I. Khan, D. Cunningham, W. D. McComb and W. E. Smith, *J. Phys. Chem. B*, 2005, **109**, 3454.
37 M. Michl, B. Vlčková, I. Srnová-Šloufová and P. Mojzeš, *Can. J. Anal. Sci. Spectrosc.*, 2003, **48**, 46.
38 S. Sanchéz-Cortés, J. V. García-Ramos, G. Morcillo and A. Tinti, *J. Colloid Interface Sci.*, 1995, **175**, 358.
39 K. Čermáková, O. Šesták, P. Matějka, V. Baumruk and B. Vlčková, *Collect. Czech. Chem. Commun.*, 1993, **58**, 2682.
40 C. H. Munro, W. E. Smith, M. Garner, J. Clarkson and P. C. White, *Langmuir*, 1995, **11**, 3712.
41 Z. S. Pillai and P. V. Kamat, *J. Phys. Chem. B*, 2004, **108**, 945.
42 J. Pfleger, P. Šmejkal, B. Vlčková and M. Šlouf, *Proc. SPIE-Int. Soc. Opt. Eng.*, 2003, **5122**, 201.
43 S. Corni and J. Tomasi, *Chem. Phys. Lett.*, 2001, **342**, 135.
44 F. J. García-Vidal and J. B. Pendry, *Phys. Rev. Lett.*, 1996, **77**, 1163.
45 J. Reglinski, M. D. Spicer, J. F. Ojo, G. D. McAnally, A. Skórska, S. J. Smith and W. E. Smith, *Langmuir*, 2003, **19**, 6336.

